

**Environmental Programs**  
 P.O. Box 1663, MS M991  
 Los Alamos, New Mexico 87545  
 (505) 606-2337/FAX (505) 665-1812



TA16



**National Nuclear Security Administration**  
 Los Alamos Site Office, MS A316  
 Environmental Restoration Program  
 Los Alamos, New Mexico 87544  
 (505) 667-4255/FAX (505) 606-2132

Date: **FEB 23 2010**  
 Refer To: EP2010-0010

James Bearzi, Bureau Chief  
 Hazardous Waste Bureau  
 New Mexico Environment Department  
 2905 Rodeo Park Drive East, Building 1  
 Santa Fe, NM 87505-6303

**Subject: Submittal of the Completion Report for Regional Aquifer Well R-48**

Dear Mr. Bearzi:

Enclosed please find two hard copies with electronic files of the Completion Report for Regional Aquifer Well R-48.

If you have any questions, please contact Mark Everett at (505) 667-5931 (meverett@lanl.gov) or Woody Woodworth at (505) 665-5820 (lwoodworth@doel.gov).

Sincerely,

Michael J. Graham, Associate Director  
 Environmental Programs  
 Los Alamos National Laboratory

Sincerely,

David R. Gregory, Project Director  
 Environmental Operations  
 Los Alamos Site Office

MG/DG/TB/ME:sm

Enclosures: Two hard copies with electronic files – Completion Report for Regional Aquifer Well R-48 (LA-UR-10-0864)

Cy: (w/enc.)  
Neil Weber, San Ildefonso Pueblo  
Woody Woodworth, DOE-LASO, MS A316  
Mark Everett, EP-ET-DO, MS M992  
RPF, MS M707 (with two CDs)  
Public Reading Room, MS M992

Cy: (Letter and CD only)  
Laurie King, EPA Region 6, Dallas, TX  
Steve Yanicak, NMED-DOE-OB, MS M894  
Hai Shen, DOE-LASO, MS A316  
Tom Whitacre, DOE-LASO, MS  
Heather Smith, North Wind, Los Alamos, NM (including MS Word file on CD)  
Kristine Smeltz, EP-WES, MS M992

Cy: (w/o enc.)  
Tom Skibitski, NMED-OB, Santa Fe, NM  
Annette Russell, DOE-LASO (date-stamped letter emailed)  
Ted Ball, EP-ARRA Project, MS C348  
IRM-RMMSO, MS A150 (date-stamped letter emailed)

LA-UR-10-0864  
February 2010  
EP2010-0010

# Completion Report for Regional Aquifer Well R-48

Prepared by the Environmental Programs Directorate

Los Alamos National Laboratory, operated by Los Alamos National Security, LLC, for the U.S. Department of Energy under Contract No. DE-AC52-06NA25396, has prepared this document pursuant to the Compliance Order on Consent, signed March 1, 2005. The Compliance Order on Consent contains requirements for the investigation and cleanup, including corrective action, of contamination at Los Alamos National Laboratory. The U.S. government has rights to use, reproduce, and distribute this document. The public may copy and use this document without charge, provided that this notice and any statement of authorship are reproduced on all copies.

# Completion Report for Regional Aquifer Well R-48

February 2010

Responsible project leader:

Mark Everett		Project Leader	Environmental Programs	2-23-10
Printed Name	Signature	Title	Organization	Date

Responsible LANS representative:

Michael J. Graham		Associate Director	Environmental Programs	2-23-10
Printed Name	Signature	Title	Organization	Date

Responsible DOE representative:

David R. Gregory		Project Director	DOE-LASO	2/23/10
Printed Name	Signature	Title	Organization	Date

## EXECUTIVE SUMMARY

This completion report summarizes the drilling, well construction, well development, and aquifer testing for well R-48 performed from June 11 to October 20, 2009. Well R-48 was installed in the existing CdV-16-3(i) borehole, approximately 1800 ft southeast of existing well R-25, in Technical Area 16 (TA-16), at Los Alamos National Laboratory (the Laboratory) in Los Alamos County, New Mexico. The well was installed at the direction of the New Mexico Environment Department (NMED) to enhance the TA-16 monitoring well network by providing a regional aquifer well to the southeast of the TA-16 260 Outfall in Consolidated Unit 16-021(c)-99 and north of S-Site Canyon.

The CdV-16-3(i) borehole was originally drilled in 2004 to a total depth (TD) of 1405 ft below ground surface (bgs) by Kleinfelder, Inc., and WDC Exploration and Wells. The borehole was thought to have entered the regional aquifer around 1350 ft bgs in massive Tschicoma dacitic lavas. Because of the well's poor production in the saturated interval, it was determined that the borehole would be advanced farther in an attempt to encounter more permeable strata, and the well designation was changed to R-48. The R-48 borehole was drilled using dual-rotary fluid-assisted air-drilling methods. Drilling fluid additives included potable water. Although it was initially anticipated that a 10-in. casing would be used to control borehole instability, the R-48 borehole was successfully advanced to a TD of 1705 ft bgs using open-hole drilling methods. The entire interval, from 1405 ft to 1705 ft bgs, was drilled in dacite lava flows of the Tschicoma Formation.

R-48 was completed with a single screened interval from 1500 to 1520.6 ft bgs. The depth to water after well installation and well development was 1352.52 ft bgs, as measured on October 16, 2009.

The well was completed in accordance with the NMED-approved well design. Hydrogeologic testing indicated the well is productive, albeit with fracture-dominated flow, and will perform effectively to meet planned objectives. Groundwater sampling at R-48 will be performed as part of the Laboratory's interim facility-wide groundwater monitoring program.

## CONTENTS

<b>1.0</b>	<b>INTRODUCTION .....</b>	<b>1</b>
<b>2.0</b>	<b>PRELIMINARY ACTIVITIES.....</b>	<b>1</b>
2.1	Administrative Preparation .....	1
2.2	Site Preparation .....	2
<b>3.0</b>	<b>DRILLING ACTIVITIES.....</b>	<b>2</b>
3.1	Drilling Approach .....	2
3.2	Chronology of Drilling Activities .....	3
<b>4.0</b>	<b>SAMPLING ACTIVITIES.....</b>	<b>5</b>
4.1	Cuttings Sampling.....	5
4.2	Water Sampling .....	5
<b>5.0</b>	<b>GEOLOGY AND HYDROGEOLOGY .....</b>	<b>5</b>
5.1	Stratigraphy .....	6
5.1.1	Tschicoma Formation, Tt (1405 to 1705 ft bgs) .....	6
5.2	Groundwater .....	6
<b>6.0</b>	<b>BOREHOLE LOGGING .....</b>	<b>6</b>
6.1	Video Logging.....	6
6.2	Geophysical Logging .....	7
<b>7.0</b>	<b>WELL INSTALLATION.....</b>	<b>7</b>
7.1	Well Design.....	7
7.2	Well Construction.....	7
<b>8.0</b>	<b>POSTINSTALLATION ACTIVITIES .....</b>	<b>8</b>
8.1	Well Development.....	8
8.1.1	Well Development Field Parameters.....	8
8.2	Aquifer Testing.....	9
8.3	Dedicated Sampling System Installation .....	9
8.4	Wellhead Completion.....	9
8.5	Geodetic Survey .....	9
8.6	Waste Management and Site Restoration.....	10
<b>9.0</b>	<b>DEVIATIONS FROM PLANNED ACTIVITIES .....</b>	<b>10</b>
<b>10.0</b>	<b>ACKNOWLEDGMENTS .....</b>	<b>11</b>
<b>11.0</b>	<b>REFERENCES AND MAP DATA SOURCES.....</b>	<b>11</b>
11.1	References .....	11
11.2	Map Data Sources .....	11

**Figures**

Figure 1.0-1 Regional aquifer well R-48 with respect to surrounding regional wells ..... 13  
Figure 5.1-1 R-48 borehole stratigraphy ..... 14  
Figure 7.2-1 R-48 as-built well construction diagram ..... 15  
Figure 8.3-1a As-built schematic for regional well R-48 ..... 17  
Figure 8.3-1b Technical notes for regional well R-48 ..... 18

**Tables**

Table 3.1-1 Fluid Quantities Used during Drilling and Well Construction ..... 19  
Table 3.1-2 Fluids Recovered during Drilling and Well Construction ..... 19  
Table 4.2-1 Summary of Groundwater Screening Samples Collected during Drilling, Well Development, and Aquifer Testing of Well R-48 ..... 20  
Table 6.0-1 R-48 Geophysical Logging Runs ..... 20  
Table 7.2-1 R-48 Annular Fill Materials ..... 21  
Table 8.5-1 R-48 Survey Coordinates ..... 21  
Table 8.6-1 Summary of Waste Samples Collected during Drilling and Development of R-48 ..... 22

**Appendixes**

Appendix A Well R-48 Lithologic Log  
Appendix B Groundwater Analytical Results  
Appendix C Aquifer Testing Report  
Appendix D Geophysical Logs and Schlumberger Geophysical Logging Report (on CD included with this document)

**Acronyms and Abbreviations**

amsl	above mean sea level
APS	accelerator porosity sonde
AIT	array induction tool
bgs	below ground surface
BHA	bottom hole assembly
CMR	combinable magnetic resonance
Consent Order	Compliance Order on Consent
cu	capture unit
DO	dissolved oxygen
DTHH	down-the-hole hammer

DTW	depth to water
ECS	Elemental Capture Sonde
EES	Earth and Environmental Sciences Division
EPA	Environmental Protection Agency (U.S.)
FMI	fullbore formation microimager
gAPI	American Petroleum Institute gamma standard units
gpd	gallons per day
gpm	gallons per minute
HNGS	Hostile Natural Gamma Spectroscopy
IC	ion chromatography
ICPMS	inductively coupled (argon) plasma mass spectrometry
ICPOES	inductively coupled plasma optical emission spectroscopy
I.D.	inside diameter
LANL	Los Alamos National Laboratory
MCFL	microcylindrically focused log
MDA	material disposal area
MDL	method detection limit
mV	millivolt
NMED	New Mexico Environment Department
NTU	nephelometric turbidity unit
O.D.	outside diameter
ORP	oxidation-reduction potential
PCS	petroleum-contaminated soil
ppm	parts per million
QC	quality control
RPF	Records Processing Facility
SOP	standard operating procedure
SVOA	semivolatile organic analyte
TA	technical area
TD	total depth
TDS	total dissolved solids
TLD	Triple Litho-Density Detector
TOC	total organic carbon
TPH	total petroleum hydrocarbons

VFD	variable frequency drive
VOA	volatile organic analyte
WES-EDA	Waste and Environmental Services Division–Environmental Data and Analysis
wt%	weight percent

## 1.0 INTRODUCTION

This completion report summarizes the drilling, well construction, well development, and aquifer testing for well R-48. Well R-48 was drilled, constructed, and tested from June 11 to October 20, 2009, by Los Alamos National Laboratory (the Laboratory). It was installed in the existing CdV-16-3(i) borehole, approximately 1800 ft southeast of existing well R-25, in Technical Area 16 (TA-16) by North Wind, Inc., and Layne Christensen (see Figure 1.0-1). The purpose of well R-48 is to enhance the TA-16 monitoring well network by providing a regional aquifer well to the southeast of the TA-16 260 Outfall and north of S-Site Canyon.

The CdV-16-3(i) borehole was originally drilled in 2004 to a total depth (TD) of 1405 ft below ground surface (bgs) by Kleinfelder, Inc., and WDC Exploration and Wells. The borehole entered the regional aquifer at around 1350 ft bgs in massive Tschicoma dacitic lavas. Because of the well's poor production in the saturated interval, it was determined that the borehole would be advanced farther to encounter more permeable strata, and the well designation was changed to R-48. The borehole was advanced to a TD of 1705 ft bgs and was completed with a single screened interval from 1500 to 1520.63 ft bgs. The depth to water (DTW) after well installation and well development was 1352.52 ft bgs, as measured on October 16. Cuttings samples were collected at 5-ft intervals in the borehole from 1450 ft bgs to TD. Postinstallation activities included well development, aquifer testing, sampling system installation, surface completion, and geodetic surveying. Future construction activities include site restoration and waste management.

The information presented in this report was compiled from field reports and daily activity summaries. Records, including field reports, field logs, and survey information, are on file at the Laboratory's Records Processing Facility (RPF). This report contains brief descriptions of activities and supporting figures, tables, and appendixes completed to date associated with the R-48 project. Information on radioactive materials and radionuclides, including the results of sampling and analysis of radioactive constituents, is voluntarily provided to the New Mexico Environment Department (NMED) in accordance with U.S. Department of Energy policy.

## 2.0 PRELIMINARY ACTIVITIES

Preliminary activities included preparing administrative planning documents and preparing the drill site and drill pad. All preparatory activities were completed in accordance with Laboratory policies, procedures, and regulatory requirements.

### 2.1 Administrative Preparation

The following documents helped guide the implementation of the scope of work for well R-48:

- Final CdV-16-3(i) Drill Plan;
- Integrated Work Document for Regional and Intermediate Aquifer Well Drilling;
- Task Order #2: Request for Proposal (RFP) No. 74829-RFP-09: Exhibit D, Scope of Work and Technical Specifications, Drilling and Installation of Wells CdV-16-3(i) and R-47 at LANL; and
- Site-Specific Environmental Health and Safety Plan, Drilling and Installation of Wells CdV-16-3(i) and R-47.

## 2.2 Site Preparation

Laboratory personnel prepared the drill pad several weeks before mobilization. The drill rig, air compressors, trailers, and support vehicles were initially mobilized to the drill site between May 20 and 29, 2008. Alternative drilling tools and construction materials were staged at a Laboratory-approved staging area close to the drill site.

The office trailer, generators, and general field equipment were moved on-site after mobilization of the drilling equipment. Potable water was obtained from fire hydrant 592 on the 340 Loop near the drill site. Safety barriers and signs were installed around the cuttings containment pit and along the perimeter of the work area.

## 3.0 DRILLING ACTIVITIES

This section describes the drilling strategy and approach and provides a chronological summary of field activities conducted at monitoring well R-48.

### 3.1 Drilling Approach

The drilling method, the equipment selected, and the drill-casing sizes for R-48 were originally designed to stabilize the existing borehole to TD as well as to mitigate stability problems while drilling. It was anticipated that if more permeable strata were encountered at R-48, they would consist of fractured to brecciated dacitic lavas or, alternatively, weakly consolidated to unconsolidated Puye sediments. In addition, the casing size originally selected ensured that the 2-in.-minimum annular thickness of the filter pack around a 5.56-in.-outside diameter (O.D.) well required by Section X.C.3 of the Compliance Order on Consent (the Consent Order) was met.

Dual-rotary air-drilling methods using a Schramm T130XD drill rig were initially employed to drill the R-48 borehole. Dual-rotary drilling has the advantage of simultaneously advancing and casing the borehole. The Schramm T130XD drill rig was equipped with conventional 4-in. drill pipe, tricone bits, downhole hammer bits, and general drilling equipment. Auxiliary equipment included two Ingersoll Rand 1170-ft<sup>3</sup>/min trailer-mounted air compressors and one Ingersoll Rand 1070-ft<sup>3</sup>/min trailer-mounted air compressor. However, because of existing borehole deviations, casing could not be placed to the 1405-ft-bgs start depth. In addition, subsequent attempts to use the Schramm T130XD drill rig to drill open hole with conventional air-rotary techniques did not return drill cuttings. Therefore, an Atlas Copco RD-20 drill rig and associated equipment were mobilized to the site. The new drill rig provided the ability to drill using standard air-rotary drilling methods as well as the ability to convert to a dual-tube reverse-circulation drilling method should air rotary fail to achieve cuttings returns. Equipment associated with the Atlas Copco RD-20 included two Ingersoll Rand 1170-ft<sup>3</sup>/min compressors and one booster. TD was ultimately achieved using the Atlas Copco RD-20 drill rig using the dual-tube reverse-circulation methodology.

In the saturated zone, only air and municipal water were used to cool the bit and help lift cuttings from the borehole. Use of drilling fluid additives was not approved because the borehole had already intercepted the regional aquifer at 1350 ft. Total amounts of drilling fluids introduced into the borehole and those recovered are presented in Tables 3.1-1 and 3.1-2.

### 3.2 Chronology of Drilling Activities

Mobilization of necessary drilling equipment and supplies to the R-48 site originally began on May 20 and continued through May 29. Site set-up, final rig inspection, and construction of a 100-ft-long, 10-in. casing “dummy” occurred between May 29 and June 2. Downhole activities at R-48 began at 1024 h on June 2. During drilling activities, field crews worked one 12-h shift per day, 7 d/wk. The casing dummy was tripped into the open borehole on drill pipe to determine the feasibility of running 10-in. casing to the TD of 1405 ft bgs. At roughly 910 ft bgs, the casing dummy began to drag in the hole. At 928.35 ft bgs, the casing dummy could not be advanced further, and the decision was made to trip it out of the hole.

At 0753 h on June 3, the drill string was tripped into the borehole to conduct a borehole magnetic survey to determine borehole deviation. The bit landed at 1401.4 ft bgs at 0955 h. The crew was placed on standby because of lightning, and the survey began at 1452 h and was completed at 1647 h. The drill crew then tripped the drill string out of the borehole. The survey was conducted from the ground surface to TD and, other than the magnetic survey to determine borehole deviation, did not include additional geophysical parameters.

On June 4, the decision was made to trip-in with a 9 7/8-in. bit and down-the-hole-hammer (DTHH) to attempt to drill using open-hole, standard air-rotary drilling methods. This decision was made because the borehole deviated from vertical during drilling (Appendix D). The drill crew went on days-off after the June 4 shift and resumed work on June 9. At 0753 h, the drill crew began tripping-in their bottom hole assembly (BHA) consisting of the bit, DTHH, and four 7-in.-O.D. heavy-wall drill collars. The bit reached 1400 ft bgs at 1045 h but had to be tripped back out of the hole to measure depth-to-water before drilling. On June 10, the BHA was tripped back into the hole and attempts to drill started at 1049 h. With only one 1170 ft<sup>3</sup>/min compressor operating, circulation could not be established. In addition, the compressor system was building excessive pressure, indicating plugged jets in the bit. At 1118 h, the drill crew began tripping out of the hole. Attempts to clear the bit during the trip were unsuccessful, and the bit reached the surface at 1353 h. The bit and DTHH were disassembled and cleaned using a high-pressure steam cleaner. The bit and DTHH were then reassembled and tripped back into the borehole starting at 1523 h.

The bit reached the bottom of the borehole at 0826 h on June 11, and attempts to advance the borehole past 1405 ft bgs began. During the trip in, circulation was established with the bit at roughly 1336 ft bgs and was maintained to TD to prevent re-plugging the jets and air passages. With the bit on bottom, the initial discharge from the cyclone was observed to be dry and dusty with no water and only a trace of very fine fragments of Tschicoma dacite. The borehole was advanced to the end of the joint, with a resulting TD of roughly 1410 ft bgs. Cuttings returns were never established, and the decision was made to trip out of the hole. At 1255 h on June 11, the Laboratory directed the crew to temporarily suspend operations at R-48 and move to another well site while a path forward was decided. Demobilization of the Schramm T130XD and auxiliary equipment from R-48 began that afternoon and concluded on June 14.

Between June 14 and August 25 drilling was stopped. During this time, the decision was made to attempt to advance R-48 past 1410 ft bgs using open-hole standard air-rotary drilling methods. Approval was also given to convert to dual-tube reverse-circulation drilling methods if standard air rotary failed to achieve cuttings returns. An Atlas Copco RD-20 drill rig and associated equipment, including two Ingersoll Rand 1170 ft<sup>3</sup>/min compressors and one booster, were mobilized. Mobilization to the drill site, as well as site set-up, was conducted between August 25 and August 28. At 1340 h on August 28, the drillers assembled the BHA, which consisted of an 11 5/8-in. button-tooth tricone bit and two 7-in. heavy-wall drill collars, and began tripping into the borehole.

The drillers reached TD with the bit at 0811 h on August 29, and began advancing past 1410 ft bgs at 0831 h. Though circulation of air was established, only trace Tschicoma dacite cuttings and minor water

were returned. By 1537 h, a new TD of 1445 ft bgs had been reached and the drill crew began tripping-out of the hole to swap the tricone bit for a DTHH.

In the morning on August 30, the drill crew completed tripping the tricone bit out of the hole, and the new BHA (consisting of an 11 5/8-in. hammer bit, DTHH, interchange sub, and two 7-in. heavy wall drill collars) was assembled, tested, and tripped into the borehole to drill using dual-tube reverse-circulation methods. The bit was on bottom at 1321 h, and the drillers began attempts to establish circulation. By 1507 h, circulation had not been established and the DTHH would not fire. The decision was made to trip the drill string out of the borehole. The trip was completed at 0802 h on August 31. Although the DTHH was intact, the bit and retaining rings had come out and had been left downhole, which explained why the DTHH would not fire.

An attempt was made on the afternoon of August 31 to trip-in the DTHH after thick beads were welded inside the splined recesses to attempt to get over the bit and capture it using a tight friction fit. The drill string was tripped to bottom, rotated multiple turns while it was raised and lowered, and then tripped out of the hole. The trip-out was completed at 0850 h on September 1; however, the bit was not captured. Later that morning an overshot tool was tripped into the borehole. At 1600 h, the overshot was out of the hole with the bit, but the retaining rings remained in the hole. On the morning of September 2, a magnet was tripped into the borehole to capture the retaining rings. At 1350 h, the magnet was out of the hole with one retaining ring. A second trip was made with the magnet starting that afternoon. At 0938 h on September 3, the magnet was again out of the hole with the remainder of the missing parts.

At 1345 h on September 3, another 11 5/8-in. bit was tripped into the borehole with the same BHA as before, and the borehole was advanced from 1445 ft bgs to 1460 ft bgs. Circulation was established and cuttings were returned past 1450 ft bgs. Cuttings indicated the borehole was still being advanced into Tschicoma lavas.

The borehole was advanced from 1460 ft bgs to 1508 ft bgs on September 4. At 1307 h, the drill supervisor reported that the DTHH was not firing and it was tripped out of the hole. The trip out was completed at 1644 h; the DTHH and bit were intact and functional. The decision was made to replace the DTHH and bit with a 9 7/8-in. tricone bit and to trip-in with the same BHA used previously. The new bit was tripped-in starting at 1044 h on September 5 and reached bottom at 1236 h. Based on direction from the Laboratory, the crew air-lifted the hole until it was dry and monitored recharge before drilling resumed. The DTW was observed to rise 2.52 ft in 15 min, at which time direction was given to resume advancing the borehole past 1508 ft bgs. By 1730 h on September 5, the borehole had been advanced to 1533 ft bgs. The borehole was advanced to 1625 ft bgs on September 6, still in Tschicoma dacite. At 1157 h on September 7, minor metal shavings were noted in the cuttings being returned at 1648 ft bgs, and the decision was made to trip the bit out of the hole. The bit was removed from the hole at 1539 h with only minor wear on the shanks. A new 9 7/8-in. tricone bit was tripped-in on the morning of September 8, and the borehole reached its final TD of 1705 ft bgs at 1339 h, still in Tschicoma dacite. The drill crew cleaned the hole from 1339 h to 1601 h, at which time they began tripping out of the hole in preparation for geophysical logging by Schlumberger.

Schlumberger arrived on-site at 1015 h on September 9 and began to run tools into the hole. Open-hole geophysical logging commenced soon after their arrival. Array induction tool (AIT), combined magnetic resonance (CMR), natural and spectral gamma, accelerator porosity sonde (APS), caliper, and formation microimager (FMI) logs were run (Appendix D). No problems were encountered while logging, and Schlumberger left the drill site at 1830 h.

## 4.0 SAMPLING ACTIVITIES

This section describes the cuttings and groundwater sampling activities at well R-48. All sampling activities were conducted in accordance with applicable quality procedures.

### 4.1 Cuttings Sampling

Cuttings samples were collected from the R-48 borehole at 5-ft intervals from 1450 ft bgs to the TD of 1705 ft bgs. At each interval, approximately 500 mL of bulk cuttings was collected by the site geologist from the discharge cyclone, placed in resealable plastic bags, labeled, and archived in core boxes. Sieved fractions (>#10 and >#35 mesh) were also collected from 1450 ft bgs to TD and placed in chip trays along with unsieved (whole rock) cuttings. Recovery of the cuttings samples was fair; total recovery was 83% of the borehole. Intervals with no recovery included 1405 to 1450 ft bgs and 1620 to 1625 ft bgs. Radiation control technicians screened cuttings before removal from the site. The core boxes and chip trays were delivered to the Laboratory's archive at the conclusion of drilling activities. All screening measurements were within the range of background values.

The borehole lithologic log for R-48 is presented in Appendix A and summarized in section 5.1.

### 4.2 Water Sampling

An initial regional groundwater screening sample was bailed from the open borehole on August 20. Additional regional groundwater screening samples were collected from the cyclone discharge during drilling at 1625 ft bgs and 1705 ft bgs. In both cases, the driller stopped water circulation and circulated air to clean out the borehole. As the discharge cleared, a water sample was collected directly from the cyclone discharge. Drilling screening samples were analyzed for metals and perchlorate. The analytical samples collected at R-48 are summarized in Table 4.2-1, and the complete analytical results are provided as Appendix B.

Four regional groundwater screening samples were collected at the end of each day during development pumping. All four samples were collected from the lower-most portion of the screened interval (approximately 1520 ft bgs). The groundwater samples were collected at the surface from the discharge line of the submersible development pump. Groundwater screening samples collected during well development at R-48 were analyzed for total organic carbon (TOC) only.

Groundwater characterization samples will be collected from the completed well in accordance with the Consent Order (Section IX.B.2.i). Samples will be analyzed for the full suite of constituents, including radionuclides, anions/cations, general inorganic chemicals, volatile and semivolatile organic compounds, and stable isotopes of hydrogen, nitrogen, and oxygen. The groundwater analytical results will be reported in the annual update to the Interim Facility-Wide Groundwater Monitoring Plan.

## 5.0 GEOLOGY AND HYDROGEOLOGY

A brief description of the geologic and hydrogeologic features encountered from 1405 to 1705 ft bgs at R-48 is presented below. The original borehole, designated CdV-16-3(i), was drilled by Kleinfelder, Inc., and WDC Exploration and Wells in 2004. The stratigraphy encountered between ground surface and 1405 ft bgs is described in the "Final Borehole CdV-16-3(i) Status Report" (Kleinfelder 2004, 087845) and is shown in Figure 5.1-1.

## 5.1 Stratigraphy

The stratigraphy for the R-48 borehole is presented below. Lithologic descriptions are based on cuttings samples collected from the discharge cyclone. Cuttings and borehole geophysical logs were used to identify geologic contacts. Figure 5.1-1 illustrates the stratigraphy at R-48. A detailed lithologic log based on analysis of drill cuttings is presented in Appendix A.

### 5.1.1 Tschicoma Formation, Tt (1405 to 1705 ft bgs)

Dacite lava flows were drilled from 1405 ft bgs to the TD of 1705 ft bgs. Although cuttings were not returned in the interval between 1405 ft bgs and 1450 ft bgs, no evidence is available to support a change in lithology in that interval. In addition, Schlumberger density logs across this interval show no deviation from dense dacitic lava above and below.

Between 1450 ft bgs and 1500 ft bgs, the Tschicoma dacite consists of massive dacite lava similar to that described by Kleinfelder in the interval from 1206 ft bgs to 1405 ft bgs (Kleinfelder 2004, 087845). The cuttings are largely “monolithologic, consisting of coarsely porphyritic dacite with dark green pyroxene. Aphanitic groundmass is generally fresh to weakly altered” (Kleinfelder 2004, 087845). Trace to minor percentages of hornblende and biotite are present as well, and phenocrysts typically occur as cumuloxyric clusters. The percentage of plagioclase phenocrysts decreased slightly below 1535 ft bgs. Below 1500 ft bgs, evidence of fracturing increases. Cuttings contain oxidized and weathered fragments of dacite as well as clay nodules indicative of fracture fill.

## 5.2 Groundwater

Potential regional groundwater was first encountered in the CdV-16-3(i) borehole on January 16, 2004, at 1400.5 ft bgs, during the original phase of drilling. Between January 16 and March 26, 2004, the DTW stabilized at 1350.50 ft bgs. DTW was first tagged by drilling personnel on June 10, 2009, at 1351.02 ft bgs in the CdV-16-3(i) borehole. On October 16, following well R-48 construction and development, but before aquifer testing began, DTW was recorded at 1352.52 ft bgs.

The estimated water-flow rate from the cyclone discharge at TD on September 8 was 15 to 20 gallons per minute (gpm). During pump development, flow rates of 4.92 to 5.20 gpm were observed. During the 24-h constant-rate pump test, flow rates continuously declined, ending at 1.58 gpm at the conclusion of the test.

Groundwater screening samples collected during drilling, well development, and aquifer performance testing are discussed in section 4.2. Groundwater chemistry and field water-quality parameters are discussed in Appendix B. Aquifer testing data and analysis are discussed in Appendix C.

## 6.0 BOREHOLE LOGGING

Jet West Geophysical Services, LLC, ran a downhole magnetic deviation survey in the R-48 open borehole before drilling activities began. Schlumberger recorded a final suite of open-hole geophysical logs. Geophysical logging results are shown in Table 6.0-1.

### 6.1 Video Logging

No video logging was performed at R-48, either in the open borehole or following well construction.

## 6.2 Geophysical Logging

A suite of Schlumberger geophysical logs was run inside the open borehole on September 9. At the time of logging, only the preexisting 13 3/8-in.-O.D. conductor casing was in place to roughly 12 ft bgs. The open-hole geophysical suite included AIT, CMR, natural and spectral gamma, APS, caliper, and FMI logs. Interpretation and details of the logging are presented in Appendix D and are included on CD.

## 7.0 WELL INSTALLATION

R-48 well casing and annular fill were installed between September 11 and 25.

### 7.1 Well Design

The R-48 well was designed in accordance with the Consent Order. NMED approved the well design before the well was installed.

### 7.2 Well Construction

The R-48 monitoring well was constructed of 5.047-in.-inside diameter (I.D.)/5.563-in.-O.D. type A304 stainless-steel casing, threaded and coupled, and fabricated to American Society for Testing and Materials A312 standards. The screened section used two nominal 10-ft lengths of 5.047-in.-I.D. rod-based 0.020-in. wire-wrapped well screen. All casing and screens were steam-pressure washed on-site before installation. A 2.2-in.-O.D. (Rock Quality Designation core-size) steel, flush-threaded tremie pipe string was also decontaminated before it was used to deliver annular fill materials downhole during well construction (Table 7.2-1). Figure 7.2-1 shows the as-built well construction diagram for R-48.

One screened interval was specified in the R-48 well design. The top of the screened interval was set at 1500 ft bgs, with a resulting bottom depth of 1520.63 ft bgs. A 21.82-ft stainless-steel sump was placed below the bottom of the screen. The Atlas Copco RD-20 drill rig used to advance the borehole to TD was also used for all geophysical logging and well construction activities. Decontamination of the stainless-steel casing, screens, and tremie pipe along with mobilization of initial well-construction materials to the site took place September 11, while the borehole water level was being monitored and the final well design was considered.

On September 13, the borehole TD was tagged at 1701 ft bgs. Between September 13 and September 14, a lower seal of 0.375-in. bentonite chips (107.87 ft<sup>3</sup>) was placed from 1701 ft bgs to 1525 ft bgs. On September 15 at 1303 h, the 5-in. well casing was started into the borehole. Each joint of well casing and screen was threaded together using couplers and installed in the borehole. After the 284.26 ft of well casing was installed, on-site activities were suspended as a result of a safety incident at another well site. Work resumed September 19 after approval was received from the Laboratory. The well casing reached its TD of 1542.42 ft bgs at 0935 h on September 20.

On September 20, the primary filter pack was emplaced from 1495 ft bgs to 1525 ft bgs using 10/20 silica sand (14.50 ft<sup>3</sup>) and was swabbed to promote settlement. A fine sand collar was emplaced from 1493 ft bgs to 1495 ft bgs using 20/40 silica sand (0.73 ft<sup>3</sup>). Between September 20 and September 23, an upper seal of 0.375-in. bentonite chips was placed from 66 ft bgs to 1493 ft bgs (1007.01 ft<sup>3</sup>). The bentonite was hydrated with potable water during placement. The final surface seal was placed from 5 ft bgs to 66 ft bgs using a 98 weight percent (wt%) Portland cement/2 wt% IDP-381 mixture (51 ft<sup>3</sup>). This marked well construction completion at 0810 h on September 25.

Operationally, well construction proceeded smoothly and according to plan. Work was typically conducted in 12-h/d daylight shifts, 7 d/wk from September 13 to September 25. Work was interrupted only between September 15 and September 19 as a result of a safety incident at another site.

## **8.0 POSTINSTALLATION ACTIVITIES**

Following well installation, the well's screened interval was developed, and an aquifer test was conducted on October 19 and 20. Total water volume removed during development and aquifer testing was 12,908 gal. The wellhead and surface pad were completed between October 23 and October 24. A geodetic survey was completed on November 12.

### **8.1 Well Development**

Well development of the screened interval was conducted between October 3 and October 8 using a Semco S15000 pulling unit. Initially the screened interval was swabbed and bailed to remove formation fines from the filter pack and sump. Bailing and swabbing continued until the water clarity visibly improved. The swabbing tool was a 4.5-in.-O.D., 1-in.-thick rubber disc attached to a weighted-steel rod. The swabbing tool was lowered by wireline and drawn repeatedly in both directions across the screened interval. Swabbing was followed by 8 h and 48 min of bailing to remove fines. Final development was then performed using a 10-hp, 4-in.-diameter Grundfos submersible pump. In total, 9664 gal. of groundwater was pumped from the well during development.

During the pumping stage of well development, turbidity, temperature, pH, dissolved oxygen (DO), oxidation-reduction potential (ORP), and specific conductance parameters were measured (Appendix B). In addition, water samples for TOC analysis were collected. The required values for TOC and turbidity to determine adequate well development are less than 2.0 parts per million and less than 5 nephelometric turbidity units (NTUs), respectively.

#### **8.1.1 Well Development Field Parameters**

Field parameters, including pH, temperature, DO, ORP, specific conductance, and turbidity, were measured at regular time intervals during well development. The results are presented in Appendix B. Field parameters were measured at well R-48 by collecting aliquots of groundwater from the discharge pipe without the use of a flow-through cell, allowing the samples to be exposed to the atmosphere. This condition probably resulted in a slight variation of field parameters during well development and during the pumping test, most notably, temperature, pH, and DO.

During development, measurements of pH ranged from 6.48 to 8.87 in well R-48. Measurements of temperature varied from 11.43°C to 23.63°C. Measurements for DO varied from 2.67 to 10.31 mg/L and for ORP ranged from 62.0 to 156.9 millivolts. Specific conductance varied from 128 to 939 microsiemens per centimeter. Turbidity measurements of nonfiltered samples ranged from 19.9 to 94.7 NTUs. Field water-quality measurements collected during well development are summarized in Appendix B, Table B-1.2-1.

The removal of suspended sediment from the groundwater until turbidity reached less than 5 NTUs was not achieved during well development. However, in accordance with the Consent Order, the stabilization of pH, temperature, and conductivity measurements on October 8 was considered to be adequate for determining that the well was suitably developed. The low concentrations of TOC (0.45 to 0.58 mgC/L) detected in groundwater samples collected from the well also indicate that residual drilling fluids were removed from the well during development. Data about these samples are presented in Tables 4.2-1 and

B-1.3-2. Periodic groundwater sampling of the well will provide additional data on groundwater chemistry within the well.

## 8.2 Aquifer Testing

Aquifer pumping tests of R-48 were conducted by David Schafer and Associates between October 16 and 17 and October 19 and 20. Several short-duration pumping intervals with short-duration recovery intervals were performed on October 16 and 17 to test the system and determine the optimal pumping rate for the 24-h test. A 24-h pumping test was conducted on October 19 and 20. A 10-hp, 4-in.-diameter Grundfos submersible pump was used to perform the aquifer tests. A total of 3238.9 gal. of groundwater was purged during aquifer testing activities. The results of the R-48 aquifer tests are presented in Appendix C.

## 8.3 Dedicated Sampling System Installation

The dedicated sampling system was installed between November 18 and 22. A 4-in. Grundfos pump with a Franklin Electric motor with 1-in. stainless-steel Baski pipe was installed to a TD of 1476.86 ft bgs with a pump intake depth of 1470.10 ft bgs. Two 1-in. polyvinyl chloride sounder tubes with 2-ft screens were also installed along with the pump assembly: one to allow access for water-level elevations and one to install a transducer to collect water-level data points over time. Both sounder tubes were installed to a depth of 1470.10 ft bgs. A check valve and bleeder valve were installed at depths of 1469.14 ft bgs and 18.65 ft bgs, respectively. Details of the dedicated sampling system are presented in Figure 8.3-1a, and technical notes for R-48 are presented in Figure 8.3-1b.

## 8.4 Wellhead Completion

A 10-ft-long × 10-ft-wide × 6-in.-thick reinforced concrete pad was installed at R-48. The pad provides long-term structural integrity for the well. A brass survey monument imprinted with well identification information was placed in the northwest corner of the pad. A 10.75-in.-O.D. steel protective casing with a mushroom cap and locking bar lid was installed around the stainless-steel well riser. A weep hole was drilled near the base of the protective casing to prevent water buildup inside the casing. In addition, the concrete pad was sloped slightly outward to promote water runoff. In total, four removable bollards, painted yellow for visibility, were set approximately 1 ft from each of the pad edges to protect the well from traffic. Details of the wellhead completion are presented in Figure 8.3-1a.

## 8.5 Geodetic Survey

A New Mexico licensed professional land surveyor conducted a geodetic survey on November 17 (Table 8.5-1). The survey data collected conforms to Laboratory Information Architecture project standards IA-CB02, "GIS Horizontal Spatial Reference System," and IA-D802, "Geospatial Positioning Accuracy Standard for A/E/C and Facility Management." All coordinates are expressed as NAD 83 New Mexico State Plane Coordinate System Central Zone Feet; elevation is expressed in feet above mean sea level using the National Geodetic Vertical Datum of 1929. Survey points include ground-surface elevation near the concrete pad, the top of the brass pin in the concrete pad, the top of the well casing, and the top of the protective casing.

## 8.6 Waste Management and Site Restoration

Waste generated from the R-48 project includes contact waste, drill cuttings, drilling fluids, petroleum-contaminated soil, and purged groundwater. A summary of the waste characterization samples collected from R-48 is presented in Table 8.6-1.

Waste streams produced during drilling and development activities were sampled in accordance with "Exhibit D, Scope of Work and Technical Specifications, Drilling and Installation of Wells CdV-16-3(i) [R-48] and R-47 at LANL."

Drill cuttings are anticipated to be land-applied after a review of associated analytical results per the waste characterization strategy form and standard operating procedure (SOP) ENV-RCRA-SOP-011.0, Land Application of Drill Cuttings. If it is determined that the drill cuttings cannot be land applied, the drill cuttings will be excavated, containerized, placed in an accumulation area appropriate to the waste type, and managed accordingly.

Analytical results for fluids produced during drilling and well development, including drilling fluids and development and purge water, indicated these materials are "nonhazardous". However, a review of ENV-RCRA-SOP-010.0, Land Application of Groundwater, determined these materials cannot be land-applied. Currently, a review is underway to determine whether these materials can be disposed of at the Laboratory's sanitary wastewater system. Drilling fluids are presently contained within the cuttings pit; development and purge water is presently containerized in a 21,000-gal. frac tank.

Site restoration activities will include removing drilling fluids and cuttings from the pit and managing the fluids and cuttings in accordance with the waste characterization strategy form and ENV-RCRA SOPs. In addition, site restoration activities will include removing the polyethylene liner, removing the containment area berms, and backfilling and regrading the containment area, as appropriate.

## 9.0 DEVIATIONS FROM PLANNED ACTIVITIES

Before drilling, sampling, and well construction activities began at R-48, a site-specific drill plan, "Drilling Work Plan for Well CdV-16-3(i)" (LANL 2008, 101875.19), was prepared and was approved by NMED (2008, 101114). Deviations from the above referenced drill plan occurred during the course of field activities and are listed below.

- On June 2, it was determined through the use of a 100-ft-long, 10-in.-diameter casing "dummy" that installing a 10-in. casing to 1405 ft bgs was not feasible. On June 4, Laboratory personnel decided to drill using an open hole with a 9 7/8-in. tricone drill bit.
- On June 11, the Schramm T130XD drill rig and auxiliary equipment were demobilized from the drill site. On August 25, an Atlas Copco RD-20 drill rig and associated equipment (two Ingersoll Rand 1170-ft<sup>3</sup>/min compressors and one booster) were mobilized to the site, and the Laboratory approved the use of dual-tube reverse-circulation drilling methods should standard air rotary fail to achieve cuttings returns.

## 10.0 ACKNOWLEDGMENTS

Layne Christensen drilled the R-48 borehole (beginning at 1405 ft bgs) and installed the well.

David Schafer and Associates performed the aquifer testing and authored Appendix C, Aquifer Testing Report.

Schlumberger Water Services performed geophysical logging of the borehole, and Ned Clayton authored Appendix D.

North Wind, Inc., provided oversight on all preparatory and field-related activities.

## 11.0 REFERENCES AND MAP DATA SOURCES

### 11.1 References

*The following list includes all documents cited in this report. Parenthetical information following each reference provides the author(s), publication date, and ER ID. The information is also included in text citations. ER IDs are assigned by the Environmental Programs Directorate's RPF and are used to locate the document at the RPF and, where applicable, in the master reference set.*

*Copies of the master reference set are maintained at the NMED Hazardous Waste Bureau and the Directorate. The set was developed to ensure that the administrative authority has all material needed to review this document, and it is updated with every document submitted to the administrative authority. Documents previously submitted to the administrative authority are not included.*

Kleinfelder, May 18, 2004. "Final Borehole CdV-16-3(i) Status Report," report prepared for Los Alamos National Laboratory, Project No. 37151/11.12, Albuquerque, New Mexico. (Kleinfelder 2004, 087845)

LANL (Los Alamos National Laboratory), March 2008. "Drilling Work Plan for Well CdV-16-3(i)," Los Alamos National Laboratory document LA-UR-08-1534, Los Alamos, New Mexico. (LANL 2008, 101875.19)

NMED (New Mexico Environment Department), March 28, 2008. "Approval with Direction, Drilling Work Plans for Well CdV-16-3(i) and CdV-R-15-1," New Mexico Environment Department letter to D. Gregory (DOE-LASO) and D. McInroy (LANL) from J.P. Bearzi (NMED-HWB), Santa Fe, New Mexico. (NMED 2008, 101114)

### 11.2 Map Data Sources

Point feature locations of the Environmental Restoration Project Database; Los Alamos National Laboratory, Waste and Environmental Services Division, EP2008-0109; 28 February 2008.

Hypsography, 10-Foot Contour Interval; Los Alamos National Laboratory, ENV Environmental Remediation and Surveillance Program; 1991.

Paved Road Arcs; Los Alamos National Laboratory, KSL Site Support Services, Planning, Locating and Mapping Section; 06 January 2004; as published 04 January 2008.

Dirt Road Arcs; Los Alamos National Laboratory, KSL Site Support Services, Planning, Locating and Mapping Section; 06 January 2004; as published 04 January 2008.

Structures; Los Alamos National Laboratory, KSL Site Support Services, Planning, Locating and Mapping Section; 06 January 2004; as published 04 January 2008.

Technical Area Boundaries; Los Alamos National Laboratory, Site Planning & Project Initiation Group, Infrastructure Planning Division; 19 September 2007.

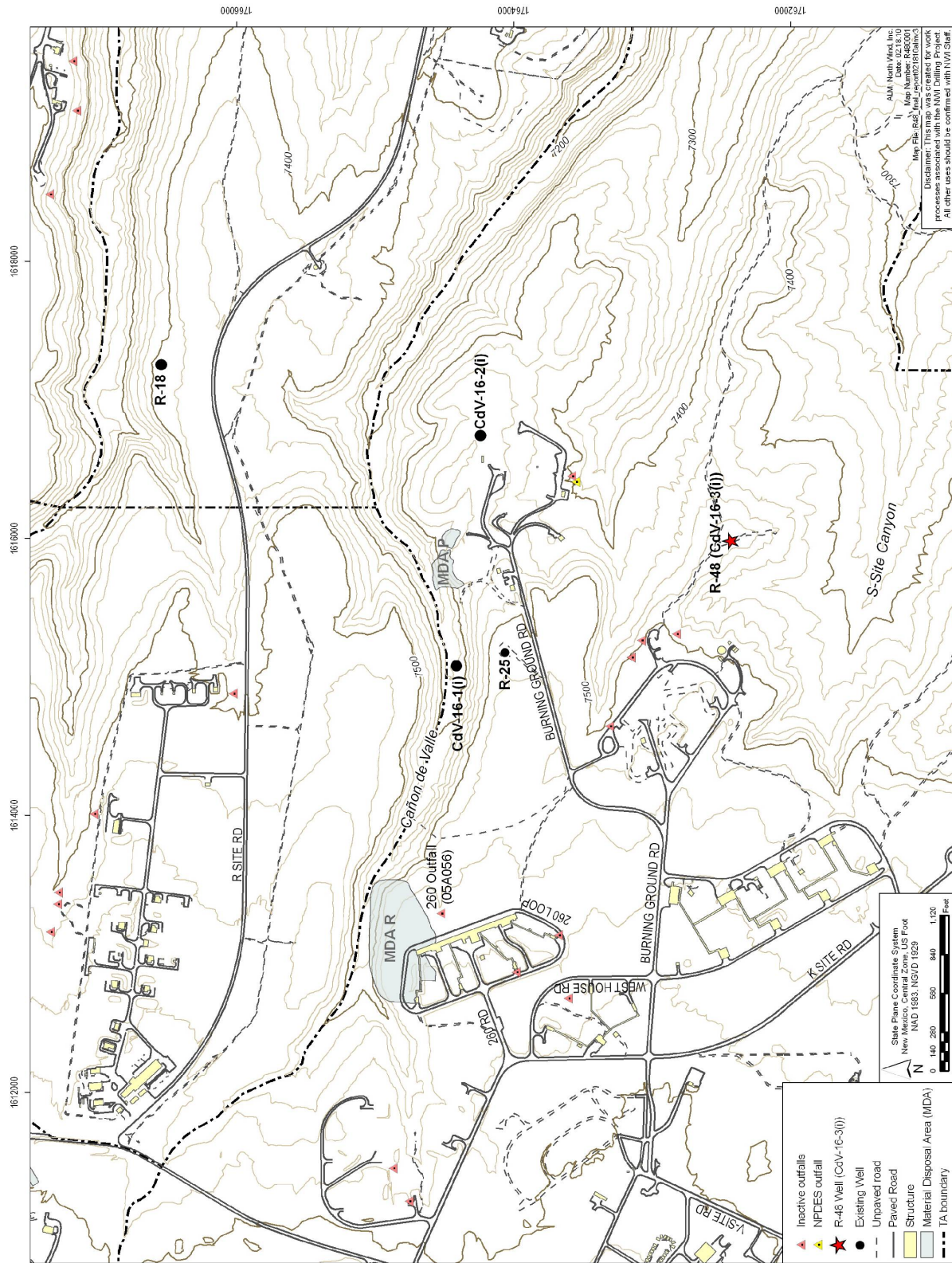


Figure 1.0-1 Regional aquifer well R-48 with respect to surrounding regional wells



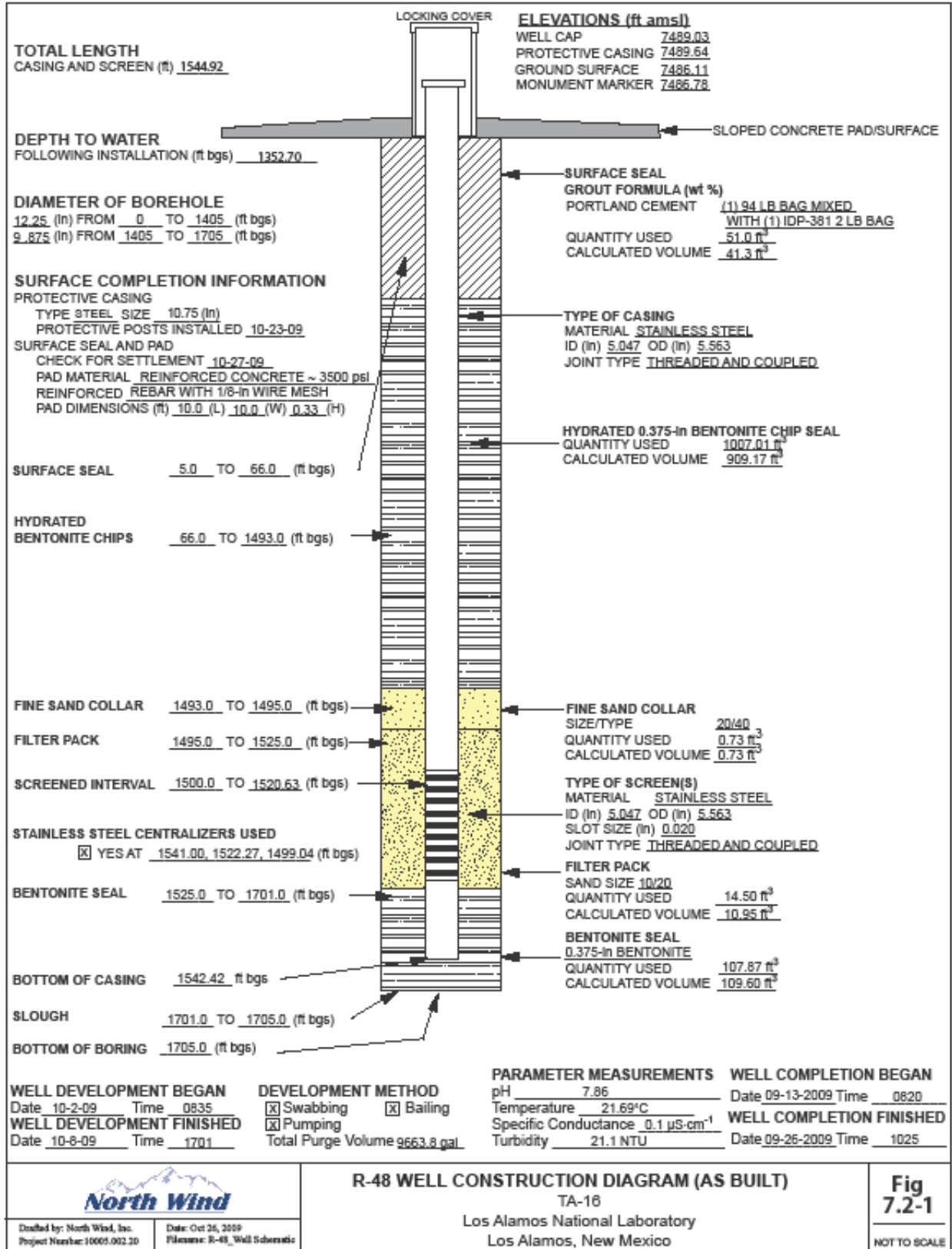


Figure 7.2-1 R-48 as-built well construction diagram



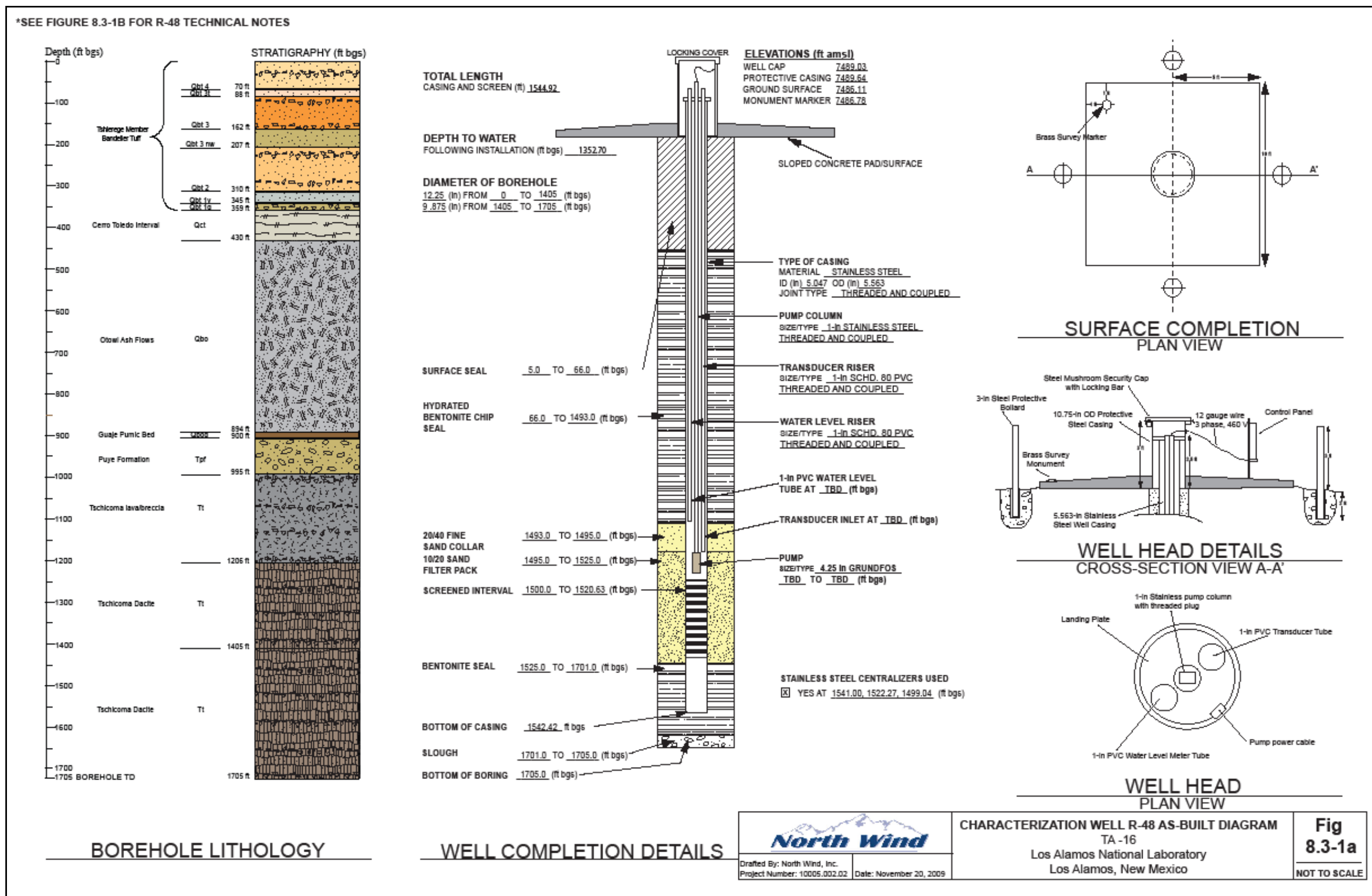


Figure 8.3-1a As-built schematic for regional well R-48

<b>R-48 TECHNICAL NOTES<sup>1</sup></b>		
<p><b>SURVEY INFORMATION<sup>2</sup></b>  <b>Brass Marker</b>                      Northing: 1762436.24 ft                      Easting: 1615977.33 ft                      Elevation: 7486.78 ft amsl</p> <p><b>Well Casing</b> (top of stainless steel)                      Northing: 1762433.08 ft                      Easting: 1615981.81 ft                      Elevation: 7489.64 ft amsl</p> <p><b>BOREHOLE GEOPHYSICAL LOGS</b>                      Jet West Geophysical:                      Schlumberger: HNGS, ECS, TLD, and APS</p> <p><b>DRILLING INFORMATION</b>  <b>Drilling Company</b>                      Layne Christensen Company</p> <p><b>Drill Rig</b>                      Atlas Copco RD-20</p> <p><b>Drilling Methods</b>                      Fluid-assisted air rotary</p> <p><b>Drilling Fluids</b>                      Air, potable water</p> <p><b>MILESTONE DATES</b>  <b>Drilling</b>                      Start: 06/11/09                      Finish: 09/08/09</p> <p><b>Well Completion</b>                      Start: 09/13/09                      Finish: 09/26/09</p> <p><b>Well Development</b>                      Start: 10/02/09                      Finish: 10/08/09</p> <p><b>WELL DEVELOPMENT</b>  <b>Development Methods</b>                      Performed swabbing, bailing, and pumping                      Volume Purged: 9663.8 gallons</p> <p><b>Parameter Measurements</b>                      pH: 7.86                      Temperature: 21.69°C                      Specific Conductance: 100 <math>\mu\text{S}\cdot\text{cm}^{-1}</math>                      Turbidity: 21.1 NTU</p> <p><small>NOTES:                      1) Additional information available in main body text of this report: "Final Well Completion Report, Characterization Well R48, Los Alamos National Laboratory, Los Alamos, New Mexico, TBD 2009".                      2) Coordinates based on New Mexico State Plane Grid Coordinates, Central Zone (NAD 83).                      Elevation expressed in feet above mean sea level using the National Geodetic Vertical Datum of 1929.</small></p>	<p><b>AQUIFER TESTING</b>                      Constant Rate Pumping Test  <b>Screened Interval</b>                      Water Produced: 3238.9 gallons                      Average Flow Rate: 2.2 gpm                      Performed on: 10/19-10/21/2009</p> <p><b>DEDICATED SAMPLING SYSTEM</b>  <b>Pump</b>                      Make: Grundfos                      Model: 896945912-P10943155                      5.0 U.S. gpm, intake at 1470.10 ft bgs                      Environmental Retrofit</p> <p><b>Motor</b>                      Make: Franklin Electric                      Model: 2343278602</p> <p><b>Pump Column</b>                      1-in OD Threaded/Coupled                      Schd. 80 Stainless Steel</p> <p><b>Transducer Tube</b>                      1-in OD Flush Threaded Schd. 80 PVC                      with 6-in long 0.010 Screen</p> <p><b>Water Level Tube</b>                      1-in OD Flush Threaded Schd. 80 PVC                      with 6-in long 0.010 Screen</p> <p><b>Transducer</b>                      Make: In-Situ                      Model: Level Troll 500, 100 psig (vented cable)                      S/N: 152950</p>	
	<p><b>R-48 TECHNICAL NOTES</b>                      TA-16                      Los Alamos National Laboratory                      Los Alamos, New Mexico</p>	<p><b>Fig</b>  <b>8.3-1b</b>                      NOT TO SCALE</p>
<p>Drafted by: North Wind, Inc.      Date: November 20, 2009                      Project Number: 10009.002.20      Filename: R-48_Tech_Spec</p>		

Figure 8.3-1b Technical notes for regional well R-48

**Table 3.1-1  
Fluid Quantities Used during  
Drilling and Well Construction**

Date	Water (gal.)	Cumulative Water (gal.)
<b>Drilling</b>		
08/29/09	2600	2600
08/30/09	420	3020
09/03/09	1200	4220
09/05/09	500	4720
09/06/09	1000	5720
09/07/09	500	6220
09/08/09	480	6700
09/14/09	1500	8200
<b>Construction</b>		
09/21/09	10,000	18,200
09/22/09	21,500	39,700
09/23/09	23,000	62,700
09/24/09	200	62,900
09/25/09	150	63,050
09/26/09	56	63,106
09/27/09	75	63,181
<b>Total Volume (gal.)</b>		
R-48	63,181	

**Table 3.1-2  
Fluids Recovered during Drilling and Well Construction**

Volume Recovered:	Dates	Amount (gal.)
from drilling (cumulative)	8/29/09–9/14/09	~7500
from development	10/3/09–10/8/09	9664
from pump test	10/16/09	394
from pump test 1	10/17/09	257
from pump test 2	10/17/09	233
from pump test 3	10/17/09	11
from 24-hour pump test	10/19/09–1-/20/09	2452
<b>Total</b>		<b>20,611</b>

**Table 4.2-1  
Summary of Groundwater Screening Samples Collected  
during Drilling, Well Development, and Aquifer Testing of Well R-48**

Location ID	Sample ID	Date Collected	Collection Depth (ft bgs)	Sample Type	Analysis
<b>Drilling</b>					
R-48	GW48-09-12356	08/20/09	1310–1354	Groundwater	Low-level tritium High explosives EPA:8260B Volatile organic analytes (VOA) EPA:8270C Semivolatile organic analytes (SVOA) Anions and target analyte list metals
R-48	GW48-09-12357	08/20/09	n/a*	Trip Blank	EPA:8260B VOA
R-48	GW48-09-13125	09/07/09	1625	Groundwater	Perchlorate Metals+boron+tin+strontium+uranium
R-48	GW48-09-13126	09/08/09	1705	Groundwater	Perchlorate Metals+boron+tin+strontium+uranium
<b>Development</b>					
R-48	WST48-10-42	10/05/09	1520	Groundwater	TOC
R-48	GW48-10-554	10/06/09	1520	Groundwater	SW-846:9060 TOC
R-48	GW48-10-555	10/07/09	1520	Groundwater	SW-846:9060 TOC
R-48	GW48-10-556	10/08/09	1520	Groundwater	SW-846:9060 TOC

\*n/a = Not applicable.

**Table 6.0-1  
R-48 Geophysical Logging Runs**

Date	Depth (ft bgs)	Description
06/03/09	0–1401	Jet West Geophysical downhole survey.
09/09/09	0–1705	Schlumberger arrives at drill site and runs geophysical logs including AIT, CMR, natural and spectral gamma, APS, caliper, and FMI logs.

**Table 7.2-1  
R-48 Annular Fill Materials**

Material	Volume (ft <sup>3</sup> )
Surface seal: cement slurry	51.0
Upper seal: 0.375-in. bentonite chips	1007.0
Fine sand collar: 20/40 silica sand	0.73
Filter Pack: 10/20 silica sand	14.50
Lower seal: 0.375-in. bentonite chips	107.9

**Table 8.5-1  
R-48 Survey Coordinates**

Identification	Northing	Easting	Elevation
R-48 brass monument embedded in NW corner of pad	1762436.24	1615977.33	7486.78
R-48 ground surface near edge of pad	1762440.05	1615971.21	7486.11
R-48 top of protective casing at center	1762433.08	1615981.81	7489.64
R-48 top of well casing at center	1762433.08	1615981.63	7489.03

Note: All coordinates are expressed as New Mexico State Plan Coordinate System Central Zone Feet (NAD 83); elevation is expressed in feet above mean sea level using the National Geodetic Vertical Datum of 1929. Surveying was completed on November 17, 2009.

**Table 8.6-1  
Summary of Waste Samples Collected during Drilling and Development of R-48**

Location ID	Sample ID	Date Collected	Description	Sample Type	Analysis
R-48	WSTR48-10-91	10/14/09	Drilling Fluids	Liquid	Cyanide (Total) EPA:8081A Pesticides EPA:8082 Polychlorinated biphenyl (PCB) EPA:8151A Herbicides EPA:8260B Volatile organic analyte (VOA) EPA:8270C Semivolatile organic analyte (SVOA) EPA:8321A High explosives Gross alpha/beta Low level tritium Target analyte list metals+boron+tin+strontium+uranium Radionuclides (isotopic americium, isotopic plutonium, isotopic uranium, strontium-90, gamma spectroscopy)
R-48	WSTR48-10-92	10/14/09	Trip Blank	n/a*	Not collected
R-48	WSTR48-10-2713	10/21/09	Frac Tank	Liquid	Radium-226 and -228 EPA8081A Pesticides EPA:8082 PCB EPA:8151A Herbicides EPA:8260B VOA EPA:8270C SVOA EPA:8321A High explosives Cyanide (Total) Gross alpha/beta Low level tritium Target analyte list metals+boron+tin+strontium+uranium Radionuclides (isotopic americium, isotopic plutonium, isotopic uranium, strontium-90, gamma spectroscopy)
R-48	WSTR48-10-2714	10/21/09	Trip Blank	n/a	EPA:8260B VOA
R-48	WST48-10-4562	10/29/09	Petroleum-contaminated soil (PCS)	Solid	EPA:8260B+total petroleum hydrocarbons (TPH) gasoline range organics Target analyte list metals TPH diesel range organics
R-48	WST48-10-4563	10/29/09	PCS	Solid	EPA:8260B VOA

\*n/a = Not applicable.

# **Appendix A**

---

*Well R-48 Lithologic Log*

**Los Alamos National Laboratory  
Regional Hydrogeologic Characterization Project  
Borehole Lithologic Log**

<b>Borehole Identification (ID):</b> R-48		<b>Technical Area (TA):</b> 16		<b>Page:</b> 1 of 6	
<b>Drilling Company:</b> Layne Christensen Co.		<b>Start Date/Time:</b> 6/11/09: 0826		<b>End Date/Time:</b> 9/8/09: 1339	
<b>Drilling Method:</b> Air Rotary		<b>MACHINE:</b> Atlas Copco RD-20		<b>Sampling Method:</b> Grab	
<b>Ground Elevation:</b> 7486.11 ft AMSL				<b>Total Depth:</b> 1705 ft bgs	
<b>Driller:</b> Ernesto Vargas		<b>Site Geologists:</b> D. Osbourne, B. Lucero, G. Kinsman, S. Thomas			
<b>Depth (ft bgs)</b>	<b>Lithology</b>			<b>Lithologic Symbol</b>	<b>Notes</b>
<b>0–1405</b>	See boring log from previous drilling.				
<b>1405–1450</b>	No cuttings returned in this interval.				
<b>1450–1465</b>	Crystalline, fine grained dacite, Light gray (N7) to medium light gray (N6) with pinkish gray (5YR8/1), angular to subrounded fragments. WR: Dacite fragments with phenocrysts composed of 50% plagioclase, 25% hornblende, 25% pyroxene. +10F: Dacite fragments with phenocrysts composed of 50-60% plagioclase, 15-25% hornblende, 10-20% pyroxene, 5-15% biotite. +35F: 80% dacite fragments with phenocrysts as stated above with minor iron staining, 5-10% plagioclase crystals, 5-10% hornblende crystals.			<b>Tt</b>	
<b>1465–1480</b>	Crystalline, fine grained dacite, Medium light gray (N6) with light brownish gray (5YR6/1), angular to subrounded fragments. WR: Dacite fragments with phenocrysts composed of 50% plagioclase, 25% hornblende, 25% pyroxene. +10F: Dacite fragments with phenocrysts composed of 50-60% plagioclase, 15-25% hornblende, 10-20% pyroxene, 5-15% biotite. +35F: 80% dacite fragments with phenocrysts as stated above with minor iron staining, 5-10% plagioclase crystals, 5-10% hornblende crystals.			<b>Tt</b>	

<b>Borehole Identification (ID):</b> R-48		<b>Technical Area (TA):</b> 16		<b>Page:</b> 2 of 6	
<b>Drilling Company:</b> Layne Christensen Co.		<b>Start Date/Time:</b> 6/11/09: 0826		<b>End Date/Time:</b> 9/8/09: 1339	
<b>Drilling Method:</b> Air Rotary		<b>MACHINE:</b> Atlas Copco RD-20		<b>Sampling Method:</b> Grab	
<b>Ground Elevation:</b> 7486.11 ft AMSL				<b>Total Depth:</b> 1705 ft bgs	
<b>Driller:</b> Ernesto Vargas		<b>Site Geologists:</b> D. Osbourne, B. Lucero, G. Kinsman, S. Thomas			
<b>1480–1500</b>		Crystalline, fine grained dacite, Light gray (N7) to medium light gray (N6) with pinkish gray (5YR8/1), angular to subrounded fragments. WR: Dacite fragments with phenocrysts composed of 50% plagioclase, 25% hornblende, 25% pyroxene. +10F: Dacite fragments with phenocrysts composed of 50-60% plagioclase, 15-25% hornblende, 10-20% pyroxene, 5-15% biotite. +35F: 80% dacite fragments with phenocrysts as stated above with minor iron staining, 5-10% plagioclase crystals, 5-10% hornblende crystals.		<b>Tt</b>	
<b>1500–1505</b>		Crystalline, fine grained dacite - medium bluish gray (5B 5/1) and light brownish gray (5Y 6/1) and with very pale orange (10YR 8/2) clay fragments (up to 10 mm in size). Dacite fragments angular to subrounded. WR: Dacite fragments (some clay coated) with phenocrysts composed of 70% plagioclase, 20% hornblende, 5% pyroxene, 5% biotite. Clay fragments. +10F: Dacite fragments with minor iron staining with phenocrysts composed of 50-60% plagioclase, 15-25% hornblende, 10-20% pyroxene, 5-15% biotite. +35F: 80% dacite fragments (some clay coating) with phenocrysts as stated above with minor iron staining, 5-10% plagioclase crystals, 5-10% hornblende crystals, trace pyroxene.		<b>Tt</b>	

<b>Borehole Identification (ID):</b> R-48		<b>Technical Area (TA):</b> 16		<b>Page:</b> 3 of 6	
<b>Drilling Company:</b> Layne Christensen Co.		<b>Start Date/Time:</b> 6/11/09: 0826		<b>End Date/Time:</b> 9/8/09: 1339	
<b>Drilling Method:</b> Air Rotary		<b>MACHINE:</b> Atlas Copco RD-20		<b>Sampling Method:</b> Grab	
<b>Ground Elevation:</b> 7486.11 ft AMSL				<b>Total Depth:</b> 1705 ft bgs	
<b>Driller:</b> Ernesto Vargas		<b>Site Geologists:</b> D. Osbourne, B. Lucero, G. Kinsman, S. Thomas			
<b>1505–1515</b>		Crystalline, fine grained dacite - medium bluish gray (5B 5/1) and light brownish gray (5Y 6/1) and with very pale orange (10YR 8/2) minor clay fragments (up to 2 mm in size). Dacite fragments angular to subrounded with minor iron staining. WR: Dacite fragments with phenocrysts composed of 70% plagioclase, 20% hornblende, 5% pyroxene, 5% biotite. Also some weathered looking fragments. +10F: Dacite fragments with minor iron staining with phenocrysts composed of 50-60% plagioclase, 15-25% hornblende, 10-20% pyroxene, 5-15% biotite. +35F: 80% dacite fragments (some clay fragments) with phenocrysts as stated above with minor iron staining, 5-10% plagioclase crystals, 5-10% hornblende crystals, trace pyroxene crystals.		<b>Tt</b>	
<b>1515–1535</b>		Crystalline, fine grained dacite - medium bluish gray (5B 5/1), light brownish gray (5Y 6/1) - and with very pale orange (10YR 8/2) minor clay fragments (up to 2 mm in size). Dacite fragments angular to subrounded with minor iron staining. WR: Dacite fragments with phenocrysts composed of 70% plagioclase, 20% hornblende, 5% pyroxene, 5% biotite. Some dacite fragments with clay coating. +10F: Dacite fragments with minor iron staining with phenocrysts composed of 50-60% plagioclase, 15-25% hornblende, 10-20% pyroxene, 5-15% biotite. +35F: 80% dacite fragments (some clay coating) with phenocrysts as stated above with minor iron staining, 5-10% plagioclase crystals, 5-10% hornblende crystals, trace pyroxene crystals.		<b>Tt</b>	

<b>Borehole Identification (ID):</b> R-48		<b>Technical Area (TA):</b> 16		<b>Page:</b> 4 of 6		
<b>Drilling Company:</b> Layne Christensen Co.		<b>Start Date/Time:</b> 6/11/09: 0826		<b>End Date/Time:</b> 9/8/09: 1339		
<b>Drilling Method:</b> Air Rotary		<b>MACHINE:</b> Atlas Copco RD-20		<b>Sampling Method:</b> Grab		
<b>Ground Elevation:</b> 7486.11 ft AMSL				<b>Total Depth:</b> 1705 ft bgs		
<b>Driller:</b> Ernesto Vargas		<b>Site Geologists:</b> D. Osbourne, B. Lucero, G. Kinsman, S. Thomas				
<b>1535–1555</b>		Crystalline, fine grained dacite - medium bluish gray (5B 5/1), light brownish gray (5Y 6/1), and brownish gray (5YR 4/1) - and with very pale orange (10YR 8/2) minor clay fragments (up to 2 mm in size). Dacite fragments angular to subrounded with minor iron staining. WR: Dacite fragments with phenocrysts composed of 60% plagioclase, 20% hornblende, 15% pyroxene, 5% biotite. +10F: Dacite fragments with minor iron staining and some clay coating with phenocrysts composed of 50-60% plagioclase, 15-25% hornblende, 15-20% pyroxene, 5-10% biotite, and minor clay fragments. +35F: 80% dacite fragments with phenocrysts as stated above with minor iron staining, 10% plagioclase crystals, 5-10% hornblende crystals, 5% pyroxene crystals, and trace clay fragments.		<b>Tt</b>		
<b>1555–1585</b>		Crystalline, fine grained dacite - medium bluish gray (5B 5/1), and pale red (5R 6/2). Dacite fragments angular to subrounded with minor iron staining. WR: Dacite fragments with phenocrysts composed of 55% plagioclase, 20% hornblende, 20% pyroxene, 5% biotite, minor clay fragments. +10F: Dacite fragments with minor iron staining with phenocrysts composed of 50-60% plagioclase, 15-25% hornblende, 15-20% pyroxene, 5-10% biotite, and minor clay fragments. +35F: 96% dacite fragments with phenocrysts as stated above with minor iron staining, 2% plagioclase crystals, 2% hornblende crystals.		<b>Tt</b>		

<b>Borehole Identification (ID):</b> R-48		<b>Technical Area (TA):</b> 16		<b>Page:</b> 5 of 6	
<b>Drilling Company:</b> Layne Christensen Co.		<b>Start Date/Time:</b> 6/11/09: 0826		<b>End Date/Time:</b> 9/8/09: 1339	
<b>Drilling Method:</b> Air Rotary		<b>MACHINE:</b> Atlas Copco RD-20		<b>Sampling Method:</b> Grab	
<b>Ground Elevation:</b> 7486.11 ft AMSL				<b>Total Depth:</b> 1705 ft bgs	
<b>Driller:</b> Ernesto Vargas		<b>Site Geologists:</b> D. Osbourne, B. Lucero, G. Kinsman, S. Thomas			
<b>1585–1620</b>		Crystalline, fine grained dacite–Brownish gray (5YR 4/1). Dacite fragments angular to subrounded with minor iron staining. WR: Dacite fragments with phenocrysts composed of 60% plagioclase, 15% hornblende, 10% pyroxene, 5% biotite. +10F: Dacite fragments with phenocrysts as stated above with minor iron staining with phenocrysts composed of 50-60% plagioclase, 15-25% hornblende, 15-20% pyroxene, and 5-10% biotite. +35F: 96% dacite fragments with minor iron staining, 2% plagioclase crystals, 2% hornblende crystals.		<b>Tt</b>	
<b>1620–1625</b>		No cuttings returned in this interval.		<b>Tt</b>	
<b>1625–1650</b>		Crystalline, fine grained dacite–Brownish gray (5YR 4/1). Dacite fragments angular to subrounded with minor iron staining. WR: Dacite fragments with phenocrysts composed of 60% plagioclase, 15% hornblende, 10% pyroxene, 5% biotite. +10F: Dacite fragments with minor iron staining with phenocrysts composed of 50-60% plagioclase, 15-25% hornblende, 15-20% pyroxene, and 5-10% biotite. +35F: 96% dacite fragments with phenocrysts as stated above with minor iron staining, 2% plagioclase crystals, 2% hornblende crystals.		<b>Tt</b>	

<b>Borehole Identification (ID):</b> R-48		<b>Technical Area (TA):</b> 16		<b>Page:</b> 6 of 6	
<b>Drilling Company:</b> Layne Christensen Co.		<b>Start Date/Time:</b> 6/11/09: 0826		<b>End Date/Time:</b> 9/8/09: 1339	
<b>Drilling Method:</b> Air Rotary		<b>MACHINE:</b> Atlas Copco RD-20		<b>Sampling Method:</b> Grab	
<b>Ground Elevation:</b> 7486.11 ft AMSL				<b>Total Depth:</b> 1705 ft bgs	
<b>Driller:</b> Ernesto Vargas		<b>Site Geologists:</b> D. Osbourne, B. Lucero, G. Kinsman, S. Thomas			
<b>1650–1655</b>		Crystalline, fine grained dacite–Grayish red purple (5RP 4/2) and medium light gray (N6). Dacite fragments angular to subrounded with minor iron staining. WR: Dacite fragments with phenocrysts composed of 60% plagioclase, 15% hornblende, 10% pyroxene, 5% biotite. +10F: Dacite fragments with minor iron staining with phenocrysts composed of 50-60% plagioclase, 15-25% hornblende, 15-20% pyroxene, and 5-10% biotite. +35F: 96% dacite fragments with phenocrysts as stated above with minor iron staining, 2% plagioclase crystals, 2% hornblende crystals.		<b>Tt</b>	
<b>1655–1660</b>		Crystalline, fine grained dacite–Grayish red purple (5RP 4/2) and medium light gray (N6). Dacite fragments angular to subrounded with minor iron staining. WR: Dacite fragments with phenocrysts composed of 60% plagioclase, 15% hornblende, 10% pyroxene, 5% biotite, and minor clay fragments. +10F: Dacite fragments with minor iron staining with phenocrysts composed of 50-60% plagioclase, 15-25% hornblende, 15-20% pyroxene, and 5-10% biotite. +35F: 96% dacite fragments with phenocrysts as stated above with minor iron staining, 2% plagioclase crystals, 2% hornblende crystals.		<b>Tt</b>	
<b>1660–1705</b>		Crystalline, fine grained dacite–Grayish red purple (5RP 4/2) and medium light gray (N6). Dacite fragments angular to subrounded with minor iron staining. WR: Dacite fragments with phenocrysts composed of 60% plagioclase, 15% hornblende, 10% pyroxene, 5% biotite. +10F: Dacite fragments with minor iron staining with phenocrysts composed of 50-60% plagioclase, 15-25% hornblende, 15-20% pyroxene, and 5-10% biotite. +35F: 96% dacite fragments with phenocrysts as stated above with minor iron staining, 2% plagioclase crystals, 2% hornblende crystals.		<b>Tt</b>	

# **Appendix B**

---

*Groundwater Analytical Results*

## **B-1.0 SAMPLING AND ANALYSIS OF GROUNDWATER AT R-48**

A total of five groundwater samples were collected during drilling (one sample) and development (four samples) at regional aquifer well R-48. The borehole-screening sample was collected at a depth interval ranging from 1310 to 1354 ft below ground surface (bgs). Groundwater screening samples were collected from a depth interval ranging from 1500.0 to 1520.6 ft bgs within the Tschicoma dacite during well development at R-48. The single borehole-screening sample was analyzed for dissolved cations, anions, perchlorate, and metals. The four groundwater-screening samples collected during well development were analyzed only for total organic carbon (TOC). A total of 9664 gal. of groundwater was pumped from well R-48 during development. During the pumping test, a total of 3239 gal. of groundwater was pumped; however, no groundwater samples were collected for chemical analyses.

### **B-1.1 Field Preparation and Analytical Techniques**

Chemical analyses of the five groundwater-screening samples collected from well R-48 were performed by Los Alamos National Laboratory's (the Laboratory's) Earth Systems Observations Group (EES-14) in the Earth and Environmental Sciences (EES) Division's Geology and Geochemical Research Laboratory. Groundwater samples were filtered (0.45 micrometer membranes) before preservation and chemical (inorganic) analyses. Samples were acidified at the EES-14 wet chemistry laboratory with analytical-grade nitric acid to a pH of 2.0 or less for metal and major cation analyses.

Groundwater samples were analyzed using techniques specified by the U.S. Environmental Protection Agency (EPA) methods for water analyses. Ion chromatography (IC) (EPA Method 300, Rev. 2.1) was the analytical method for bromide, chloride, fluoride, nitrate, nitrite, oxalate, perchlorate, phosphate, and sulfate. The analytical result for perchlorate is pending because this analyte is run in batches of at least 30 samples every 3 or 4 mo at EES-14. The instrument detection limits for perchlorate typically are 0.002 and 0.005 ppm (EPA Method 314.0, Rev. 1). Inductively coupled (argon) plasma optical emission spectroscopy (ICPOES) (EPA Method 200.7, Rev. 4.4) was used for analyses of dissolved aluminum, barium, boron, calcium, total chromium, iron, lithium, magnesium, manganese, potassium, silica, sodium, strontium, titanium, and zinc. Dissolved aluminum, antimony, arsenic, barium, beryllium, boron, cadmium, cesium, chromium, cobalt, copper, iron, lead, lithium, manganese, mercury, molybdenum, nickel, rubidium, selenium, silver, thallium, thorium, tin, vanadium, uranium, and zinc were analyzed by inductively coupled (argon) plasma mass spectrometry (ICPMS) (EPA Method 200.8, Rev. 5.4). The precision limits (analytical error) for major ions and trace elements were generally less than  $\pm 7\%$  using ICPOES and ICPMS. Total carbonate alkalinity (EPA Method 310.1) was measured using standard titration techniques. No groundwater samples were collected for TOC analyses at R-48 before well development. Analyses of TOC were performed on four groundwater samples collected during well development following EPA Method 415.1. The charge-balance error for the borehole water sample including total cations and anions was  $-5\%$  for complete analyses of the above inorganic chemicals. The negative cation-anion charge balance value for this screening sample indicates excess anions for the filtered screening sample.

### **B-1.2 Field Parameters**

#### **B-1.2.1 Well Development**

Water samples were drawn from the pump flow line into sealed containers, and field parameters were measured using a YSI multimeter. Results of field parameters, consisting of pH, temperature, percent saturation of dissolved oxygen (DO), oxidation-reduction potential (ORP), specific conductance, and

turbidity, measured during well development conducted at R-48 are provided in Table B-1.2-1. Forty-four measurements of pH and temperature varied from 6.48 to 8.86 and from 11.43 to 23.63°C, respectively, in groundwater pumped from well R-48 during development. Reliable concentrations of DO varied from 2.67 to 7.93 mg/L at well R-48 during development, suggesting that groundwater is oxic. Noncorrected ORP values varied from 62.0 to 156.9 millivolts (mV) during development of well R-48 (Table B-1.2-1). Temperature-dependent correction factors for calculating Eh values from field ORP measurements were based on an Ag/AgCl, KCl-saturated filling solution contained in the ORP electrode. The correction factors are 208.9, 203.9, and 198.5 mV at 15, 20, and 25°C, respectively. Corrected Eh values ranged from 265.9 to 360.8 mV during development of well R-48. These corrected Eh values associated with well R-48 are considered to be reliable and representative of the known relatively oxidizing conditions characteristic of the regional aquifer beneath the Pajarito Plateau, based on analytical results for redox-sensitive solutes, including detectable nitrate and sulfate and low concentrations of manganese measured at other R-wells. These DO measurements taken during well development are generally consistent with the corrected Eh values. Specific conductance generally decreased from 939 to 124 microSiemens per centimeter ( $\mu\text{S}/\text{cm}$ ) and turbidity values varied from 19.9 to 94.7 nephelometric turbidity units (NTU) during well development of R-48 (Table B-1.2-1).

### **B-1.3 Analytical Results for R-48 Groundwater Screening Samples**

#### **B-1.3.1 Borehole and Well Development Samples**

Analytical results for the groundwater-screening sample collected at well R-48 during drilling are provided in Table B-1.3-1. Anions including chloride, fluoride, nitrate, and sulfate are discussed because they can occur as contaminant tracers released from the Laboratory. Only the trace metals molybdenum, chromium, and uranium are discussed for the borehole-screening water samples. Water pumped from R-48 borehole during drilling contains regional aquifer groundwater, municipal supply water used during drilling, and dissolved and suspended minerals released from the disaggregation of aquifer material containing clay minerals, ferric (oxy)hydroxide, manganese oxide, and silicates.

Calcium and sodium are the dominant cations measured in the R-48 borehole-screening sample collected from the regional aquifer (Table B-1.3-1). Dissolved concentrations of calcium and sodium were 18.2 and 13.5 parts per million (ppm) or mg/L, respectively, in a water sample collected from the borehole on August 20, 2009. Concentrations of chloride, fluoride, nitrate (N), and sulfate in this filtered sample were 3.57, 0.01 (less than detection), 0.021, and 11.3 ppm, respectively. The dissolved concentration of bromide was 1.78 ppm in the borehole-screening sample and probably results from using potassium bromide as a tracer during drilling of CdV-16-3(i). The dissolved concentration of molybdenum was 0.017 ppm (0.017 mg/L, 17 parts per billion, or 17  $\mu\text{g}/\text{L}$ ) in the borehole sample. Dissolved concentrations of chromium and uranium were 0.003 and 0.0004 ppm, respectively (Table B-1.3-1). Lubricants used during drilling of R-48 are the most likely source of molybdenum detected in borehole water sample.

Detectable concentrations of TOC were 0.45, 0.58, 0.49, and 0.55 mgC/L in four groundwater-screening samples collected sequentially during development conducted at well R-48, as presented in Table B-1.3-2. The median, mean, and maximum background concentrations of TOC are 0.34, 0.41, and 1.37 mgC/L for regional aquifer groundwater (LANL 2007, 095817).

In summary, groundwater at well R-48 is relatively oxidizing, based on corrected Eh values and measurable concentrations of DO during development. Concentrations of TOC ranged between 0.45 mgC/L and 0.58 mgC/L, indicating residual drilling fluids have been removed from well R-48 during development. Groundwater samples collected from well R-48 during characterization sampling will provide additional data on groundwater chemistry and the presence or absence of high explosive

compounds and chlorinated aliphatic hydrocarbons within the regional aquifer. Well R-48 potentially bounds the downgradient movement of contaminants detected at well R-25, screens 5 and 6.

## **B-2.0 REFERENCES**

*The following list includes all documents cited in this appendix. Parenthetical information following each reference provides the author(s), publication date, and ER ID. This information is also included in text citations. ER IDs are assigned by the Environmental Programs Directorate's Records Processing Facility (RPF) and are used to locate the document at the RPF and, where applicable, in the master reference set.*

*Copies of the master reference set are maintained at the NMED Hazardous Waste Bureau and the Directorate. The set was developed to ensure that the administrative authority has all material needed to review this document, and it is updated with every document submitted to the administrative authority. Documents previously submitted to the administrative authority are not included.*

LANL (Los Alamos National Laboratory), May 2007. "Groundwater Background Investigation Report, Revision 3," Los Alamos National Laboratory document LA-UR-07-2853, Los Alamos, New Mexico. (LANL 2007, 095817)



**Table B-1.2-1**  
**Field Water-Quality Parameters for Well R-48 during Development**

Date	pH	Temp (°C)	DO (mg/L)	ORP, Eh* (mV)	Specific Conductivity (µS/cm)	Turbidity (NTU)
10/03/09	8.78	18.75	2.67	141.6, 345.5	939	Not measured
	8.52	18.29	6.22	94.7, 298.6	701	Not measured
	8.86	19.31	6.37	62.0, 265.9	760	Not measured
	8.81	19.07	7.58	80.2, 284.1	460	Not measured
	8.85	19.13	7.53	94.1, 298.0	433	Not measured
	8.72	19.65	8.16	84.5, 288.4	358	Not measured
	8.75	19.39	10.31	87.3, 291.2	375	Not measured
	8.47	19.45	7.92	121.4, 325.3	327	Not measured
	8.45	19.87	7.47	133.1, 337.0	329	Not measured
10/05/09	8.45	16.80	Not measured	147.6, 356.5	288	Not measured
	8.03	21.02	Not measured	123.9, 327.8	288	Not measured
	7.94	23.34	Not measured	78.3, 278.8	178	68.0
	7.20	23.44	Not measured	94.7, 293.2	166	76.7
	7.50	23.63	Not measured	93.0, 291.5	157	59.5
	7.58	23.41	Not measured	96.5, 295.0	152	49.0
	7.59	23.52	Not measured	102.1, 300.6	146	43.6
	7.52	23.45	Not measured	106.1, 304.6	142	32.1
	7.36	20.99	Not measured	117.5, 321.4	142	32.4
10/06/09	7.22	15.81	7.16	141.9, 350.8	165	73.3
	7.88	19.84	7.93	129.0, 332.9	147	34.6
	7.93	22.19	8.09	91.3, 295.2	140	27.5
	7.74	21.96	7.02	111.5, 315.4	135	24.2
	8.01	22.33	8.13	97.9, 296.4	134	22.3
	7.23	14.25	8.05	137.0, 345.9	130	41.4
	7.96	22.74	6.87	119.6, 318.1	134	20.9
	7.99	22.93	7.22	121.2, 319.7	134	20.1
	7.62	22.18	8.21	156.9, 360.8	131	19.9
10/07/09	6.48	11.43	3.04	113.2, 327.0	124	90.5
	6.99	20.01	7.50	119.1, 323.0	134	36.1
	7.86	21.32	6.39	119.5, 323.4	132	31.4
	7.73	21.74	6.71	121.9, 325.8	130	25.1

Table B-1.2-1 (continued)

Date	pH	Temp (°C)	DO (mg/L)	ORP, Eh* (mV)	Specific Conductivity (µS/cm)	Turbidity (NTU)
10/07/09	7.50	22.29	7.19	126.7, 330.6	129	26.7
	7.65	22.75	7.48	128.0, 326.5	129	24.4
	7.45	23.05	6.49	128.6, 327.1	128	23.4
	7.89	23.37	6.21	126.9, 325.4	133	22.3
	7.95	23.39	8.23	130.6, 329.1	128	21.5
	7.55	23.0	6.30	141.0, 339.5	129	22.5
	7.45	22.80	6.70	136.1, 334.6	128	23.1
10/08/09	6.98	14.05	4.13	130.7, 339.6	142	94.7
	7.70	20.79	7.30	118.7, 322.6	132	27.3
	7.67	22.57	6.27	117.5, 316.0	130	26.9
	7.76	22.2	7.86	122.6, 326.5	130	23.1
	7.86	22.27	6.31	120.3, 324.2	129	21.4
	7.86	21.69	6.76	127.6, 331.5	131	21.1

\* Eh (mV) is calculated from an Ag/AgCl saturated KCl electrode filling solution at 15.0, 20.0, and 25.0°C by adding temperature-sensitive correction factors of 208.9, 203.9, and 198.5 mV, respectively.

**Table B-1.3-1**  
**Analytical Results for Groundwater Screening**  
**Samples Collected from Well R-48, Pajarito Canyon**

<b>Sample ID</b>	GW48-09-12356
<b>Date Received</b>	8/21/2009
<b>ER/RRES-WQH</b>	09-2979
<b>Depth (ft)</b>	1310–1354
Ag result (ppm)	0.001
Standard deviation (Ag)	U*
Al result (ppm)	0.003
Standard deviation (Al)	0.000
As result (ppm)	0.003
Standard deviation (As)	0.000
B result (ppm)	0.021
Standard deviation (B)	0.000
Ba result (ppm)	0.029
Standard deviation (Ba)	0.001
Be result (ppm)	0.001
Standard deviation (Be)	U
Br(-) ppm	1.78
TOC result (ppm)	Not analyzed
Ca result (ppm)	18.19
Standard deviation (Ca)	0.1
Cd result (ppm)	0.001
Standard deviation (Cd)	U
Cl(-) ppm	3.57
ClO <sub>4</sub> (-) ppm	pending
ClO <sub>4</sub> (-) (U)	pending
Co result (ppm)	0.002
Standard deviation (Co)	0.000
Alk-CO <sub>3</sub> result (ppm)	0.000
ALK-CO <sub>3</sub> (U)	U
Cr result (ppm)	0.003
Standard deviation (Cr )	0.000
Cs result (ppm)	0.001
Standard deviation (Cs)	U
Cu result (ppm)	0.001
Standard deviation (Cu)	U
F(-) ppm	0.01
F(-) (U)	U

Table B-1.3-1 (continued)

<b>Sample ID</b>	GW48-09-12356
<b>Date Received</b>	8/21/2009
<b>ER/RRES-WQH</b>	09-2979
<b>Depth (ft)</b>	1310–1354
Fe result (ppm)	0.010
Standard deviation (Fe)	U
Alk-CO <sub>3</sub> +HCO <sub>3</sub> result (ppm)	114
Hg result (ppm)	0.00035
Standard deviation (Hg)	0.00001
K result (ppm)	1.52
Standard deviation (K)	0.01
Li result (ppm)	0.025
Standard deviation (Li)	0.000
Mg result (ppm)	5.34
Standard deviation (Mg)	0.01
Mn result (ppm)	0.677
Standard deviation (Mn)	0.005
Mo result (ppm)	0.017
Standard deviation (Mo)	0.000
Na result (ppm)	13.5
Standard deviation (Na)	0.1
Ni result (ppm)	0.004
Standard deviation (Ni)	0.000
NO <sub>2</sub> (ppm)	0.01
NO <sub>2</sub> -N result	0.003
NO <sub>2</sub> -N (U)	U
NO <sub>3</sub> (ppm)	0.090
NO <sub>3</sub> -N result	0.021
C <sub>2</sub> O <sub>4</sub> result (ppm)	0.01
C <sub>2</sub> O <sub>4</sub> (U)	U
Pb result (ppm)	0.0002
Standard deviation (Pb)	U
pH	7.69
PO <sub>4</sub> (-3) result (ppm)	0.95
Rb result (ppm)	0.004
Standard deviation (Rb)	0.000
Sb result (ppm)	0.001
Standard deviation (Sb)	U
Se result (ppm)	0.001
Standard deviation (Se)	U

Table B-1.3-1 (continued)

<b>Sample ID</b>	GW48-09-12356
<b>Date Received</b>	8/21/2009
<b>ER/RRES-WQH</b>	09-2979
<b>Depth (ft)</b>	1310–1354
Si result (ppm)	20
Standard deviation (Si)	0.1
SiO <sub>2</sub> result (ppm)	42.8
Standard deviation (SiO <sub>2</sub> )	0.3
Sn result (ppm)	0.001
Standard deviation (Sn)	U
SO <sub>4</sub> (-2) result (ppm)	11.3
Sr result (ppm)	0.096
Standard deviation (Sr)	0.000
Th result (ppm)	0.001
Standard deviation (Th)	U
Ti result (ppm)	0.002
Standard deviation (Ti)	U
Tl result (ppm)	0.001
Standard deviation (Tl)	U
U result (ppm)	0.0004
Standard deviation (U)	0.0000
V result (ppm)	0.001
Standard deviation (V)	0.000
Zn result (ppm)	0.011
Standard deviation (Zn)	0.000
TDS (ppm)	213
Cations	2.00
Anions	2.23
Balance	-0.05

\*U = The analyte was analyzed for but not detected.

**Table B-1.3-2**  
**Summary of Groundwater Screening Samples Collected during Development of Well R-48**

<b>Location ID</b>	<b>Sample ID</b>	<b>Date Collected</b>	<b>Collection Depth (ft bgs)</b>	<b>Sample Type</b>	<b>Analysis</b>
R-48	WST48-10-42	10/05/09	1520	Groundwater	TOC
R-48	GW48-10-554	10/06/09	1520	Groundwater	SW-846:9060 Total organic carbon
R-48	GW48-10-555	10/07/09	1520	Groundwater	SW-846:9060 Total organic Carbon
R-48	GW48-10-556	10/08/09	1520	Groundwater	SW-846:9060 Total organic carbon

# **Appendix C**

---

*Aquifer Testing Report*

## C-1.0 INTRODUCTION

This appendix describes the hydraulic analysis of pumping tests conducted at well R-48 located at Technical Area 16 (TA-16) at Los Alamos National Laboratory (the Laboratory). The tests on R-48 were conducted to evaluate the hydraulic properties of the aquifer in which the well was completed.

Testing consisted of brief trial pumping of R-48, background water-level data collection, and a 24-h constant-rate pumping test. As with most of the R-well pumping tests conducted on the Pajarito Plateau, an inflatable packer system was used in R-48 to minimize the effects of casing storage on the test data.

As described below, the test data showed unusual response, possibly associated with transducer drift or other malfunction. This response somewhat limited the applicability of the data for determining aquifer parameters. Thus, an additional test is planned for R-48 when the permanent pump and transducer are installed. At the time this report was prepared, the follow-up test had not yet been conducted.

The apparently malfunctioning transducer was returned to the vendor (In-Situ, Inc.) for examination following the test pumping. The vendor reported that it passed all the calibration tests and judged it to be operating satisfactorily. Acquisition of additional pumping test data with the new, permanent transducer should help evaluate the aquifer as well as the veracity of the vendor's conclusions about the transducer used in the R-48 tests.

In addition to transducer anomalies, the discharge rate fluctuated inexplicably in all of the pumping tests. The pump was operated using a variable frequency drive (VFD) control unit. While these devices are generally reliable, it was possible the unit used for the pumping tests may have failed to control the discharge rate as expected.

### Conceptual Hydrogeology

Well R-48 penetrates several hundred feet of Tschicoma dacite. It was completed with 20.6 ft of 5-in. stainless-steel well screen from 1500 to 1520.6 ft below ground surface (bgs) in a slightly fractured zone. The static water level measured on October 16, 2009, was well above the top of the well screen, at 1352.52 ft bgs.

It was assumed that all water production came from tiny fractures within the dacite. It was anticipated that both porosity and permeability of this formation would be low.

### R-48 Testing

Well R-48 was tested from October 16 to 21, 2009. After filling the drop pipe on October 16, testing consisted of brief trial pumping on October 17, background data collection, and a 24-h constant-rate pumping test that began on October 19.

Three trial tests were conducted on October 17. Trial 1 was conducted at multiple discharge rates ranging from 4.5 to 1.7 gallons per minute (gpm) for 80 min from 0800 h to 0920 h and was followed by 40 min of recovery until 1000 h.

Trial 2 was conducted for 60 min from 1000 h to 1100 h. The initial discharge rate was 4.9 gpm but declined inexplicably to 3.5 gpm. It was subsequently adjusted manually to 3.3 gpm. Following shutdown, recovery data were recorded for 30 min until 1130 h.

Trial 3 was conducted for 31 min from 1130 h to 1201 h. The initial discharge rate was 3.8 gpm, declining inexplicably to 3.3 gpm. Following shut down, recovery/background data were recorded for 2699 min until 0900 h on October 19.

At 0900 h on October 19, the 24-h pumping test was begun at a rate of 3.3 gpm. The rate inexplicably declined to 2.3 gpm within the first hour of pumping. It was then adjusted to 1.75 gpm from where the rate declined inexplicably to 1.56 gpm by the end of the test. Pumping continued until 0900 h on October 20. Following shutdown, recovery measurements were recorded for 1440 min until 0900 h on October 21 when the pump was tripped out of the well.

## **C-2.0 BACKGROUND DATA**

The background water-level data collected in conjunction with running the pumping tests allow the analyst to see what water-level fluctuations occur naturally in the aquifer and help distinguish between water-level changes caused by conducting the pumping test and changes associated with other causes.

Background water-level fluctuations have several causes, among them barometric pressure changes, operation of other wells in the aquifer, Earth tides, and long-term trends related to weather patterns. The background data hydrographs from the monitored wells were compared to barometric pressure data from the area to determine if a correlation existed.

Previous pumping tests on the Pajarito Plateau have demonstrated a barometric efficiency for most wells of between 90% and 100%. Barometric efficiency is defined as the ratio of water-level change divided by barometric pressure change, expressed as a percentage. In the initial pumping tests conducted on the early R-wells, downhole pressure was monitored using a vented pressure transducer. This equipment measures the difference between the total pressure applied to the transducer and the barometric pressure, this difference being the true height of water above the transducer.

Subsequent pumping tests, including at R-48, have utilized nonvented transducers. These devices record the total pressure on the transducer, that is, the sum of the water height plus the barometric pressure. This results in an attenuated "apparent" hydrograph in a barometrically efficient well. For example, at a 90% barometrically efficient well monitored using a vented transducer, an increase in barometric pressure of 1 unit causes a decrease in recorded downhole pressure of 0.9 unit because the water level is forced downward 0.9 unit by the barometric pressure change. However, when a nonvented transducer is used, the total measured pressure increases by 0.1 unit (the combination of the barometric pressure increase and the water-level decrease). Thus, the resulting apparent hydrograph changes by a factor of 100 minus the barometric efficiency, and in the same direction as the barometric pressure change, rather than in the opposite direction.

Barometric pressure data were obtained from TA-54 tower site from the Waste and Environmental Services Division-Environmental Data and Analysis (WES-EDA). The TA-54 measurement location is at an elevation of 6548 ft above mean sea level (amsl), whereas the wellhead elevation is reportedly 7486.8 ft amsl. The static water level in R-48 was 1352.5 ft below land surface, making the calculated water-table elevation 6134.3 ft amsl. Therefore, the measured barometric pressure data from TA-54 had to be adjusted to reflect the pressure at the elevation of the water table within R-48.

The following formula was used to adjust the measured barometric pressure data:

$$P_{WT} = P_{TA54} \exp \left[ - \frac{g}{3.281R} \left( \frac{E_{R-48} - E_{TA54}}{T_{TA54}} + \frac{E_{WT} - E_{R-48}}{T_{WELL}} \right) \right] \quad \text{Equation C-1}$$

Where  $P_{WT}$  = barometric pressure at the water table inside R-48

$P_{TA54}$  = barometric pressure measured at TA-54

$g$  = acceleration of gravity, in m/sec<sup>2</sup> (9.80665 m/sec<sup>2</sup>)

$R$  = gas constant, in J/Kg/degree Kelvin (287.04 J/Kg/degree Kelvin)

$E_{R-48}$  = land surface elevation at R-48 site, in ft (7486.8 ft)

$E_{TA54}$  = elevation of barometric pressure measuring point at TA-54, in ft (6548 ft)

$E_{WT}$  = elevation of the water level in R-48, in ft (6134.3 ft)

$T_{TA54}$  = air temperature near TA-54, in degrees Kelvin (assigned a value of 52.9 degrees Fahrenheit, or 284.8 degrees Kelvin)

$T_{WELL}$  = air temperature inside R-48, in degrees Kelvin (assigned a value of 58.2 degrees Fahrenheit, or 287.7 degrees Kelvin)

This formula is adapted from an equation WES-EDA provided. It can be derived from the ideal gas law and standard physics principles. An inherent assumption in the derivation of the equation is that the air temperature between TA-54 and the well is temporally and spatially constant, and that the temperature of the air column in the well is similarly constant.

The corrected barometric pressure data reflecting pressure conditions at the water table were compared to the water-level hydrograph to discern the correlation between the two and determine whether water level corrections would be needed prior to data analysis.

### C-3.0 IMPORTANCE OF EARLY DATA

When pumping or recovery first begins, the vertical extent of the cone of depression is limited to approximately the well screen length, the filter pack length, or the aquifer thickness in relatively thin permeable strata. For many pumping tests on the Pajarito Plateau, the early pumping period is the only time the effective height of the cone of depression is known with certainty because soon after startup the cone of depression expands vertically through permeable materials above and/or below the screened interval. Thus, the early data often offer the best opportunity to obtain hydraulic conductivity information because conductivity would equal the earliest-time transmissivity divided by the well-screen length.

Unfortunately, in many pumping tests, casing-storage effects dominate the early-time data, potentially hindering the effort to determine the transmissivity of the screened interval. The duration of casing-storage effects can be estimated using the following equation (Schafer 1978, 098240).

$$t_c = \frac{0.6(D^2 - d^2)}{\underline{Q}} \quad \text{Equation C-2}$$

Where  $t_c$  = duration of casing storage effect, in min

$D$  = inside diameter of well casing, in in.

$d$  = outside diameter of column pipe, in in.

$Q$  = discharge rate, in gpm

$s$  = drawdown observed in pumped well at time  $t_c$ , in ft

The calculated casing storage time is quite conservative. Often, the data show that significant effects of casing storage have dissipated after about half the computed time.

For wells screened across the water table (not applicable here), there can be an additional storage contribution from the filter pack around the screen. The following equation provides an estimate of the storage duration accounting for both casing and filter pack storage.

$$t_c = \frac{0.6[(D^2 - d^2) + S_y(D_B^2 - D_C^2)]}{\frac{Q}{s}} \quad \text{Equation C-3}$$

Where  $S_y$  = short-term specific yield of filter media (typically 0.2)

$D_B$  = diameter of borehole, in in.

$D_C$  = outside diameter of well casing, in in.

This equation was derived from Equation C-2 on a proportional basis by increasing the computed time in direct proportion to the additional volume of water expected to drain from the filter pack. (To prove this, note that the left hand term within the brackets is directly proportional to the annular area [and volume] between the casing and drop pipe while the right hand term is proportional to the area [and volume] between the borehole and the casing, corrected for the drainable porosity of the filter pack. Thus, the summed term within the brackets accounts for all of the volume [casing water and drained filter pack water] appropriately.)

In some instances, it is possible to eliminate casing storage effects by setting an inflatable packer above the tested screen interval before conducting the test. Therefore, this option has been implemented for the R-well testing program, including R-48.

#### C-4.0 TIME-DRAWDOWN METHODS

$$s = \frac{114.6Q}{T} W(u) \quad \text{Equation C-4}$$

Where

$$W(u) = \int_u^{\infty} \frac{e^{-x}}{x} dx \quad \text{Equation C-5}$$

and

$$u = \frac{1.87r^2S}{Tt} \quad \text{Equation C-6}$$

and where  $s$  = drawdown, in ft

$Q$  = discharge rate, in gpm

$T$  = transmissivity, in gallons per day (gpd)/ft

$S$  = storage coefficient (dimensionless)

$t$  = pumping time, in d

$r$  = distance from center of pumpage, in ft

To use the Theis method of analysis, the time-drawdown data are plotted on log-log graph paper. Then, Theis curve matching is performed using the Theis type curve—a plot of the Theis well function  $W(u)$  versus  $1/u$ . Curve matching is accomplished by overlaying the type curve on the data plot and, while keeping the coordinate axes of the two plots parallel, shifting the data plot to align with the type curve, effecting a match position. An arbitrary point, referred to as the match point, is selected from the overlapping parts of the plots. Match-point coordinates are recorded from the two graphs, yielding four values:  $W(u)$ ,  $1/u$ ,  $s$ , and  $t$ . Using these match-point values, transmissivity and storage coefficient are computed as follows:

$$T = \frac{114.6Q}{s} W(u) \quad \text{Equation C-7}$$

$$S = \frac{Tut}{2693r^2} \quad \text{Equation C-8}$$

Where  $T$  = transmissivity, in gpd/ft

$S$  = storage coefficient

$Q$  = discharge rate, in gpm

$W(u)$  = match-point value

$s$  = match-point value, in ft

$u$  = match-point value

$t$  = match-point value, in min

An alternative solution method applicable to time-drawdown data is the Cooper–Jacob method (1946, 098236), a simplification of the Theis equation that is mathematically equivalent to the Theis equation for most pumped well data. The Cooper–Jacob equation describes drawdown around a pumping well as follows:

$$s = \frac{264 Q}{T} \log \frac{0.3Tt}{r^2 S} \quad \text{Equation C-9}$$

The Cooper–Jacob equation is a simplified approximation of the Theis equation and is valid whenever the  $u$  value is less than about 0.05. For small radius values (e.g., corresponding to borehole radii),  $u$  is less than 0.05 at very early pumping times and therefore is less than 0.05 for most or all measured drawdown values. Thus, for the pumped well, the Cooper–Jacob equation usually can be considered a valid approximation of the Theis equation.

According to the Cooper–Jacob method, the time-drawdown data are plotted on a semilog graph, with time plotted on the logarithmic scale. Then a straight line of best fit is constructed through the data points and transmissivity is calculated using:

$$T = \frac{264Q}{\Delta s} \quad \text{Equation C-10}$$

Where  $T$  = transmissivity, in gpd/ft

$Q$  = discharge rate, in gpm

$\Delta s$  = change in head over one log cycle of the graph, in ft

Because many of the test wells completed on the Plateau are severely partially penetrating, an alternate solution considered for assessing aquifer conditions is the Hantush equation for partially penetrating wells (Hantush 1961, 098237; Hantush 1961, 106003). The Hantush equation is as follows:

**Equation C-11**

$$s = \frac{Q}{4\pi T} \left[ W(u) + \frac{2b^2}{\pi^2(l-d)(l'-d')} \sum_{n=1}^{\infty} \frac{1}{n^2} \left( \sin \frac{n\pi l}{b} - \sin \frac{n\pi d}{b} \right) \left( \sin \frac{n\pi l'}{b} - \sin \frac{n\pi d'}{b} \right) W \left( u, \sqrt{\frac{K_z}{K_r} \frac{n\pi r}{b}} \right) \right]$$

Where, in consistent units,  $s$ ,  $Q$ ,  $T$ ,  $t$ ,  $r$ ,  $S$ , and  $u$  are as previously defined and

$b$  = aquifer thickness

$d$  = distance from top of aquifer to top of well screen in pumped well

$l$  = distance from top of aquifer to bottom of well screen in pumped well

$d'$  = distance from top of aquifer to top of well screen in observation well

$l'$  = distance from top of aquifer to bottom of well screen in observation well

$K_z$  = vertical hydraulic conductivity

$K_r$  = horizontal hydraulic conductivity

In this equation,  $W(u)$  is the Theis well function and  $W(u, \beta)$  is the Hantush well function for leaky aquifers where:

$$\beta = \sqrt{\frac{K_z}{K_r} \frac{n\pi r}{b}} \quad \text{Equation C-12}$$

Note that for single-well tests,  $d = d'$  and  $l = l'$ .

### C-5.0 RECOVERY METHODS

Recovery data were analyzed using the Theis recovery method. This is a semilog analysis method similar to the Cooper–Jacob procedure.

In this method, residual drawdown is plotted on a semilog graph versus the ratio  $t/t'$ , where  $t$  is the time since pumping began and  $t'$  is the time since pumping stopped. A straight line of best fit is constructed through the data points and  $T$  is calculated from the slope of the line as follows:

$$T = \frac{264Q}{\Delta s} \quad \text{Equation C-13}$$

The recovery data are particularly useful compared with time-drawdown data. Because the pump is not running, spurious data responses associated with dynamic discharge rate fluctuations are eliminated. The result is that the data set is generally “smoother” and easier to analyze.

## C-6.0 FRACTURED ROCK METHODS

In fractured rock settings, there are two primary approaches to analyzing water-level data from constant-rate pumping tests. In one approach, porous media assumptions are applied and the fractured aquifer is analyzed as though it were a homogeneous, equivalent porous medium. This approach is often called the *radial* conceptual model because groundwater is assumed to move radially toward the pumped well. If there are a large number of interconnected fractures, this conceptual model may be reasonable, and the response to pumping may be similar to what would be observed in typical unconsolidated sediments. At sufficiently large scales (time or distance), many fractured rock environments show response consistent with the radial flow model.

In another approach, the pumped well is assumed to intersect a fully penetrating fracture having infinite conductivity and embedded in an otherwise homogeneous aquifer. This approach is called the *linear* conceptual model because, for a very long fracture, groundwater flows along straight lines that are approximately perpendicular to the orientation of the fracture. If there is one dominant fracture in the vicinity of the pumped well (actually penetrated by the well), this conceptual model may describe the flow regime more accurately than the radial model. At late time, as the cone of depression expands to a sufficiently large size compared to the fracture length, the transient flow response gradually transitions to radial flow. Thus, linear flow systems often exhibit radial flow response at large pumping times.

It is important to note that sometimes in fractured rock aquifers, neither conceptual model adequately describes the response to pumping because there are often several dominant fractures, rather than just one, and numerous other fractures of various sizes. The resulting heterogeneous flow system may be too complex to be described accurately by either the radial model or the linear model. In these cases careful review of the data is required and the limitations of the available analytical methods must be considered in the analysis.

Another common conceptual description of fractured systems is the *fracture and block* model in which the aquifer is assumed to be composed of a large number of uniform, permeable fractures with blocks of tighter materials between the fractures. However, this is nothing more than a radial flow model with special features. During pumping, the fractures draw down rapidly and then are gradually recharged by water contained in the low-permeability blocks. This dual porosity representation of the aquifer produces a bimodal drawdown curve analogous to the delayed yield response seen in typical unconfined aquifers. Except for the bimodal character of the drawdown curve, the analysis is similar to that applicable to standard radial flow systems.

Most radial flow systems are described adequately by the Theis and Cooper-Jacob equations described above. Linear flow to a single primary fracture, on the other hand, is generally described by the

Gringarten-Witherspoon solution. For a well drilled into a fracture of length  $2x_f$  oriented along the x-axis and centered at the origin of an x-y coordinate system, the following equation applies:

$$s = \frac{Q}{8\sqrt{\pi T}} \int_0^{t_D} \left[ \operatorname{erf} \frac{1-x_D}{2\sqrt{\tau}} + \operatorname{erf} \frac{1+x_D}{2\sqrt{\tau}} \right] \exp\left(\frac{-y_D^2}{4\tau}\right) \frac{d\tau}{\sqrt{\tau}} \quad \text{Equation C-14}$$

Where, in consistent units

$$t_D = \frac{Tt}{Sx_f^2} \quad \text{Equation C-15}$$

$$x_D = \frac{x}{x_f} \quad \text{Equation C-16}$$

$$y_D = \frac{y}{x_f} \quad \text{Equation C-17}$$

The term  $\operatorname{erf}$  is the error function, defined as follows:

$$\operatorname{erf}(z) = \frac{2}{\sqrt{\pi}} \int_0^z \exp(-\tau^2) d\tau \quad \text{Equation C-18}$$

One of the drawbacks of interpreting pumping tests using the linear model is that the parameter  $x_f$ , the half-length of the fracture, is not known. Introduction of this additional unknown parameter often makes it impossible to determine a unique solution for the hydraulic aquifer parameters. Nevertheless, application of the linear analysis provides insight into the system response and can provide an explanation for multiple slopes that may be observed in conventional plots of the drawdown data. This information, in turn, can aid subsequent interpretation of the data using the Theis method by clarifying those instances when the Theis analysis must be restricted to the late-time data.

Another drawback of the linear model is that curve-matching methods based on log-log plots often fail because well losses or head loss within the fracture (assumed in the theory to be infinitely permeable) alter both the position and shape of the data plot, resulting in poor curve matches and calculation of erroneous aquifer coefficients.

For drawdown data in the pumped well (and any observation wells located within the same fracture as the pumped well) the Gringarten-Witherspoon equation can be simplified for early pumping times as follows:

$$s = \frac{Q}{2x_f \sqrt{\pi TS}} \sqrt{t} \quad \text{Equation C-19}$$

This equation shows that the initial drawdown response is related to the square root of the pumping time. Thus, a linear plot of  $s$  versus the square root of  $t$  yields a straight line. Further, because of this relationship, a log-log plot of  $s$  versus  $t$  yields a straight line having a slope of one half. Again, these simplified responses only occur in the pumped well and observation wells installed in the same fracture as the pumped well and only at early time. At late time, as the flow transitions from linear to radial, the response is more similar to the Theis type curve.

Part of the analyst's job in reviewing and interpreting pumping test data is choosing which model—radial or linear—does the better job of describing the flow system. This decision cannot be deduced from the geologic setting alone but must consider the drawdown response as well. As stated above, radial flow data generally exhibit a Theis-type curve shape on log-log plots and a straight-line trend on semilog plots. In contrast, early-time linear flow data from wells completed within the same fracture as the pumped well typically show a straight-line trend on both log-log plots (with a slope of one half) and linear plots of  $s$  versus the square root of  $t$ . These combinations of plotting trends are the strongest indicators of which flow regime is prevalent in a given pumping test.

### C-7.0 SPECIFIC CAPACITY METHOD

The specific capacity of the pumped well can be used to obtain a lower-bound value of hydraulic conductivity. The hydraulic conductivity is computed using formulas based on the assumption that the pumped well is 100% efficient. The resulting hydraulic conductivity is the value required to sustain the observed specific capacity. If the actual well is less than 100% efficient, it follows that the actual hydraulic conductivity would have to be greater than calculated to compensate for well inefficiency. Thus, because the efficiency is not known, the computed hydraulic conductivity value represents a lower bound. The actual conductivity is known to be greater than or equal to the computed value.

For fully penetrating wells, the Cooper–Jacob equation can be iterated to solve for the lower-bound hydraulic conductivity. However, the Cooper–Jacob equation (assuming full penetration) ignores the contribution to well yield from permeable sediments above and below the screened interval. To account for this contribution, it is necessary to use a computation algorithm that includes the effects of partial penetration. One such approach was introduced by Brons and Marting (1961, 098235) and augmented by Bradbury and Rothchild (1985, 098234).

Brons and Marting introduced a dimensionless drawdown correction factor,  $s_p$ , approximated by Bradbury and Rothschild as follows:

$$s_p = \frac{1 - \frac{L}{b}}{\frac{L}{b}} \left[ \ln \frac{b}{r_w} - 2.948 + 7.363 \frac{L}{b} - 11.447 \left( \frac{L}{b} \right)^2 + 4.675 \left( \frac{L}{b} \right)^3 \right] \quad \text{Equation C-20}$$

In this equation,  $L$  is the well screen length, in ft. Incorporating the dimensionless drawdown parameter, the conductivity is obtained by iterating the following formula:

$$K = \frac{264Q}{sb} \left( \log \frac{0.3Tt}{r_w^2 S} + \frac{2s_p}{\ln 10} \right) \quad \text{Equation C-21}$$

The Brons and Marting procedure can be applied to both partially penetrating and fully penetrating wells.

To apply this procedure, a storage coefficient value must be assigned. Confined conditions were assumed for R-48 because of the water level rise above the well screen. Storage coefficient values for confined conditions can be expected to range from about  $10^{-3}$  to  $10^{-5}$  (Driscoll 1986, 104226). A value of  $10^{-4}$  was used for the R-48 calculations. The calculation result is not particularly sensitive to the choice of storage coefficient value, so a rough estimate of the storage coefficient is generally adequate to support the calculations.

The analysis also requires assigning a value for the saturated aquifer thickness,  $b$ . For the purposes of this exercise, the fracture zone was assumed to be fully penetrated by the well screen. Limited fracturing was encountered during drilling, so it was unclear whether or not a substantial thickness of fractures existed at R-48. Discharge rate fluctuations and possible transducer drift, described earlier, made it impossible to see the effects of late-time flattening of the drawdown and recovery curves associated with possible vertical growth of the cone of depression. These factors limited somewhat the usefulness of the lower-bound transmissivity calculation.

It is important to note that in a fractured setting, the actual specific capacity is greater than what would be observed in an equivalent fractured medium—often several times greater. The presence of a fracture essentially increases the effective radius of the well resulting in increased yield. Therefore, the Brons and Marting calculations were performed knowing that the resulting value could easily have been greater than the true lower bound transmissivity.

### **C-8.0 BACKGROUND DATA ANALYSIS**

Background aquifer pressure data collected during the R-48 tests were plotted along with barometric pressure to determine the barometric effect on water levels.

Figure C-8.0-1 shows aquifer pressure data from R-48 along with barometric pressure data from TA-54 that have been corrected to equivalent barometric pressure in feet of water at the water table. The R-48 data are referred to in the figure as the “apparent hydrograph” because the measurements reflect the sum of water pressure and barometric pressure, having been recorded using a nonvented pressure transducer. The times of the pumping periods for the R-48 pumping tests are included on the figure for reference.

In examining the data in Figure C-8.0-1, the recovery data following the brief pumping event on October 16 appeared normal, but subsequent recovery episodes showed unusual response. For example, recovery following the trial pumping on October 17 showed a water level rebound about 4 ft above the original static water level, followed by a gradual linear decline over the next 2 d of monitoring. Likewise, following the 24-h test, the water level rebounded to an even higher elevation and subsequently declined throughout the balance of the monitoring period. As stated above, the manufacturer examined the transducer, claiming that it was working properly and that the data response appeared normal. It seems more likely that the transducer actually malfunctioned, displaying some sort of gradual drift or similar effect.

The data from the initial, normal-appearing recovery response were replotted in Figure C-8.0-2 at the same scale as the barometric pressure data. At late time, the recovery curve appeared to flatten despite an ongoing increase in barometric pressure, suggesting a highly barometrically efficient aquifer zone, typical of most deep wells on the plateau.

Figure C-8.0-3 shows an expanded-scale plot of the recovery data following the October 17 trial testing that illustrates the nearly linear change in reported head over time as indicated by the close correspondence between the straight line on the graph and the data plot. It was suspected that this was an indication of some sort of transducer drift or other malfunction, although the manufacturer claimed that it was not.

## C-9.0 WELL R-48 DATA ANALYSIS

This section presents the data obtained from the R-48 pumping tests and the results of the analytical interpretations. Data are presented for drawdown and recovery for trials 1, 2 and 3, as well as the 24-h constant-rate pumping test.

### C-9.1 Well R-48 Trial 1

Figure C-9.1-1 shows a semilog plot of the drawdown data collected from trial 1. As indicated on the graph, the discharge rate was varied through several steps—4.5, 3.7, 2.7, and 1.7 gpm. Table C-9.1-1 summarizes the drawdown observed at each pumping rate along with the computed specific capacities. The specific capacity declined slightly for the later steps because of increased cumulative pumping time. There was no discernable decline in specific capacity at the greater discharge rates, suggesting largely laminar flow conditions at all pumping rates.

Figure C-9.1-2 shows the recovery data collected following shutdown of the trial 1 pumping test. Using the late recovery data in conjunction with the average discharge rate from the test of 3.2 gpm, the transmissivity was estimated at about 120 gpd/ft. Based on an assumed aquifer thickness (fractured zone) equal to the well screen length (20.6 ft), this corresponded to an average hydraulic conductivity value of 5.8 gpd/ft<sup>2</sup>, or 0.78 ft/d. Naturally, a thicker or thinner contributing zone would imply lower or greater hydraulic conductivity values, respectively.

During the early recovery, there was a slight flattening of the curve at a  $t/t'$  value of about 200. This effect may be attributed to various causes including vertical expansion of the cone of depression, lateral variations in formation permeability, or a subdued “block and fracture” effect sometimes seen in bedrock aquifers. Of these possibilities, vertical expansion of the cone of depression may be the least likely cause because the steep slope was resumed subsequently, belying ongoing vertical growth of the cone.

### C-9.2 Well R-48 Trial 2

Figure C-9.2-1 shows a semilog plot of the drawdown data collected from trial 2. The pump performance appeared to be erratic in that the discharge rate started at 4.9 gpm and declined to 3.5 gpm after about a half-hour. The decline in rate could not be attributed to increased drawdown and pumping lift because there was little decline in yield during the first several minutes of the test when most of the drawdown was incurred. The data suggested the possibility that the VFD was not providing constant electrical current frequency and concomitant constant pump speed and discharge rate.

The discharge rate was adjusted to 3.3 gpm for the second half of the test, resulting in an average pumping rate of 3.9 gpm.

Figure C-9.2-2 shows the recovery data collected following shutdown of the trial 2 pumping test. The gradual increase in slope over time is consistent with the linear conceptual flow regime with a gradual transition to radial. The late data suggested a formation transmissivity of 117 gpd/ft with a corresponding average hydraulic conductivity for the screened interval of 5.7 gpd/ft<sup>2</sup>, or 0.76 ft/d. The same transient flattening of the recovery curve seen in trial 1 was apparent in Figure C-9.2-2, again possibly from a subdued “block and fracture” effect.

### C-9.3 Well R-48 Trial 3

Figure C-9.3-1 shows a semilog plot of the drawdown data collected from trial 3. About half way through the pumping period, the discharge rate inexplicably declined gradually from 3.8 to 3.3 gpm, resulting in an average rate of 3.6 gpm for the test.

Figure C-9.3-2 shows the recovery data collected following shutdown of the trial 3 pumping test. As in trial 2 recovery, the early flat slope was consistent with the linear flow model, likely transitioning to radial flow at later time. The middle data on the graph suggested a formation transmissivity of 139 gpd/ft with a corresponding average hydraulic conductivity for the screened interval of 6.7 gpd/ft<sup>2</sup>, or 0.90 ft/d. The data showed the same ripple effect seen in the previous trials, consistent with a subdued “block and fracture” response.

The late data in Figure C-9.3-2 showed the strange overshoot of the original static water level by several feet, followed by a gradual decline. These data presumably reflected transducer error rather than actual water levels.

The recovery data were plotted in Figure C-9.3-3 on a log-log scale as feet of recovery versus time since pumping stopped. The early data were compared to the theoretically expected straight line having a slope of 0.5. As shown on the graph, the data fit deviated from expectations in that the initial slope was greater while the later slope was less than expected. The data fit shown revealed an estimated value for  $TSx_f^2$  of 655 ft<sup>4</sup>/d. This parameter was used to evaluate transmissivity for a range of assumed storage coefficient values and fracture lengths.

Figure C-9.3-4 shows the results of the calculations. Because both storage coefficient and fracture length can vary over more than an order of magnitude, the resulting range of transmissivity values covers several orders of magnitude. This confirms that the log-log analysis cannot be used to accurately quantify the transmissivity. Based on the relatively low transmissivity values obtained from the semilog analyses (between 100 and 200 gpd/ft), the graphical results in Figure C-9.3-4 implied relatively large storage coefficient and fracture length (the only area of the graph where low to moderate transmissivity values were predicted).

### C-9.4 Well R-48 24-H Constant-Rate Pumping Test

Figure C-9.4-1 shows a semilog plot of the drawdown data collected during the 24-h pumping test. Note that the drawdown reference point shown on the graph started at –2 ft. This was an artifact of referencing all water levels to the original static level measured at the onset of testing combined with the final trial 3 water level being well above the initial static level. The performance of both the pump and the transducer appeared to be erratic during this test.

The data looked fairly normal for the first 19 min of pumping, transitioning from a flat slope (linear model) to a steep, steady slope (radial model). However, between 19 and 35 min of pumping, there was a distinct reduction in the drawdown reported by the transducer. Field records showed, however, that the measured discharge rate remained fairly constant during this period. For example, the rate remained between about 2.75 and 2.80 gpm from 8 to 35 min. Thus, it appeared that the transducer was recording erroneous information. Typically, a response such as that seen between 19 and 35 min could indicate a gradual increase in well efficiency during pumping. In this case, however, drawing this conclusion was uncertain because of other transducer data anomalies observed during testing.

After 35 minutes of pumping, the discharge rate inexplicably declined from 2.75 to 2.30 gpm. The transducer output seemed to be consistent with this change in discharge rate. After about an hour of

pumping, the rate was adjusted manually to 1.75 gpm, after which it inexplicably declined gradually to 1.56 gpm. Again, the transducer data seemed to reflect the associated water level changes properly during this period.

Figure C-9.4-2 shows the recovery data collected following shutdown of the 24-h pumping test. As in trials 2 and 3, the early flat slope was consistent with the linear flow model, likely transitioning to radial flow at later time. The middle data on the graph suggested a formation transmissivity of 143 gpd/ft with a corresponding average hydraulic conductivity for the screened interval of 6.9 gpd/ft<sup>2</sup> or 0.93 ft/d. The data showed the same subtle ripple effect consistent with a subdued “block and fracture” response.

The late data shown in Figure C-9.4-2 repeated the strange overshoot of the original static water level by several feet followed by a gradual decline, similar to what was seen in the extended recovery data set after trial 3. As before, these data were presumed to reflect transducer error rather than actual water levels.

The recovery data were plotted in Figure C-9.4-3 on a log-log scale as feet of recovery versus time since pumping stopped. The early data were compared to the theoretically expected straight line having a slope of 0.5. As shown on the graph, the data fit revealed an estimated value for  $TSx_f^2$  of 1190 ft<sup>4</sup>/d. This parameter was used to evaluate transmissivity for a range of assumed storage coefficient values and fracture lengths.

Figure C-9.4-4 shows the results of the calculations. Again, the resulting range of transmissivity values covered several orders of magnitude, confirming the difficulty in using the log-log analysis to quantify the transmissivity. Based on the relatively low transmissivity values obtained from the semilog analyses (between 100 and 200 gpd/ft), the graphical results in Figure C-9.4-4 implied relatively large storage coefficient and fracture length (the only area of the graph where low to moderate transmissivity values were predicted).

### C-9.5 Well R-48 Specific Capacity Data

Specific capacity data were used along with well geometry to estimate a lower-bound transmissivity value for the permeable zone penetrated by R-48. This was done to provide a frame of reference for evaluating the above analyses.

In addition to specific capacity, other input values used in the calculations included a storage coefficient value of  $10^{-4}$ , a borehole radius of 0.51 ft and a pumping time of 1440 min.

The final pumping rate from R-48 at the end of the 24-h test was 1.56 gpm. The drawdown from the starting water level was 6.1 ft while the net recovery from the final pumping level was 8.19 ft, the discrepancy presumably because of transducer errors. The drawdown value implied a specific capacity of 0.26 gpm/ft while the recovery value yielded a specific capacity of 0.19 gpm/ft. Applying the Brons and Marting method to these inputs for fully penetrating conditions yielded a lower-bound transmissivity of 453 gpd/ft for the drawdown value and 331 gpd/ft for the recovery value. Averaging these two values yielded a lower-bound transmissivity estimate of 392 gpd/ft.

The lower-bound transmissivity estimates were on the same order of magnitude as the transmissivity values determined from previous analysis (117 to 143 gpd/ft), although a few times greater. This is the expected result when using the radial flow model to estimate pumping performance. In other words, it is expected that the specific capacity of a well in a fractured system will be several times greater than that of a well completed in porous sediments having similar transmissivity. The large computed lower-bound

transmissivity estimates provided good corroboration of fracture flow response and the existence of a significant linear flow component.

### **C-10.0 SUMMARY**

Constant-rate pumping tests were conducted on R-48. The tests were performed to gain an understanding of the hydraulic characteristics of the fractured Tshicoma dacite in the vicinity of the R-48 well screen. Numerous observations and conclusions were drawn for the tests as summarized below.

Both the submersible pump and pressure transducer appeared to operate erratically during all of the pumping tests. The transducer seemed to exhibit drift problems while the submersible pump (driven by a VFD) showed unusual discharge rate fluctuations.

A comparison of barometric pressure and R-48 water level data suggested a high barometric efficiency.

The pumping test data suggested that the linear flow model was applicable to the early test data with the flow transitioning to radial at later time.

The transmissivity values computed from the test ranged from 117 to 143 gpd/ft, averaging 130 gpd/ft. Assuming this value represented the screened interval (20.6 ft), the average hydraulic conductivity computed to 6.3 gpd/ft<sup>2</sup>, or 0.84 ft/d.

The flow regime was essentially laminar at all test rates.

R-48 produced 1.56 gpm after 1440 min of pumping with observed water level changes of 6.1 ft (drawdown) and 8.19 ft (recovery), resulting in estimated specific capacities of 0.26 and 0.19 gpm/ft, respectively. The lower-bound transmissivity values computed from these data using the radial flow conceptual model were 453 and 331 gpd/ft, respectively—several times greater than the pumping test values. This discrepancy suggested linear flow near the well, associated with discrete fractures in the dacite.

If possible, a follow-up pumping test will be conducted using the permanent pump and transducer after they are installed.

### **C-11.0 REFERENCES**

*The following list includes all documents cited in this appendix. Parenthetical information following each reference provides the author(s), publication date, and ER ID. This information is also included in text citations. ER IDs are assigned by the Environmental Programs Directorate's Records Processing Facility (RPF) and are used to locate the document at the RPF and, where applicable, in the master reference set.*

*Copies of the master reference set are maintained at the New Mexico Environment Department Hazardous Waste Bureau and the Directorate. The set was developed to ensure that the administrative authority has all material needed to review this document, and it is updated with every document submitted to the administrative authority. Documents previously submitted to the administrative authority are not included.*

Bradbury, K.R., and E.R. Rothschild, March-April 1985. "A Computerized Technique for Estimating the Hydraulic Conductivity of Aquifers from Specific Capacity Data," *Ground Water*, Vol. 23, No. 2, pp. 240-246. (Bradbury and Rothschild 1985, 098234)

- Brons, F., and V.E. Marting, 1961. "The Effect of Restricted Fluid Entry on Well Productivity," *Journal of Petroleum Technology*, Vol. 13, No. 2, pp. 172-174. (Brons and Marting 1961, 098235)
- Cooper, H.H., Jr., and C.E. Jacob, August 1946. "A Generalized Graphical Method for Evaluating Formation Constants and Summarizing Well-Field History," *American Geophysical Union Transactions*, Vol. 27, No. 4, pp. 526-534. (Cooper and Jacob 1946, 098236)
- Driscoll, F.G., 1986. Excerpted pages from *Groundwater and Wells*, 2nd Ed., Johnson Filtration Systems Inc., St. Paul, Minnesota. (Driscoll 1986, 104226)
- Hantush, M.S., July 1961. "Drawdown around a Partially Penetrating Well," *Journal of the Hydraulics Division, Proceedings of the American Society of Civil Engineers*, Vol. 87, No. HY 4, pp. 83-98. (Hantush 1961, 098237)
- Hantush, M.S., September 1961. "Aquifer Tests on Partially Penetrating Wells," *Journal of the Hydraulics Division, Proceedings of the American Society of Civil Engineers*, pp. 171-195. (Hantush 1961, 106003)
- Schafer, D.C., January-February 1978. "Casing Storage Can Affect Pumping Test Data," *The Johnson Drillers Journal*, pp. 1-6, Johnson Division, UOP, Inc., St. Paul, Minnesota. (Schafer 1978, 098240)



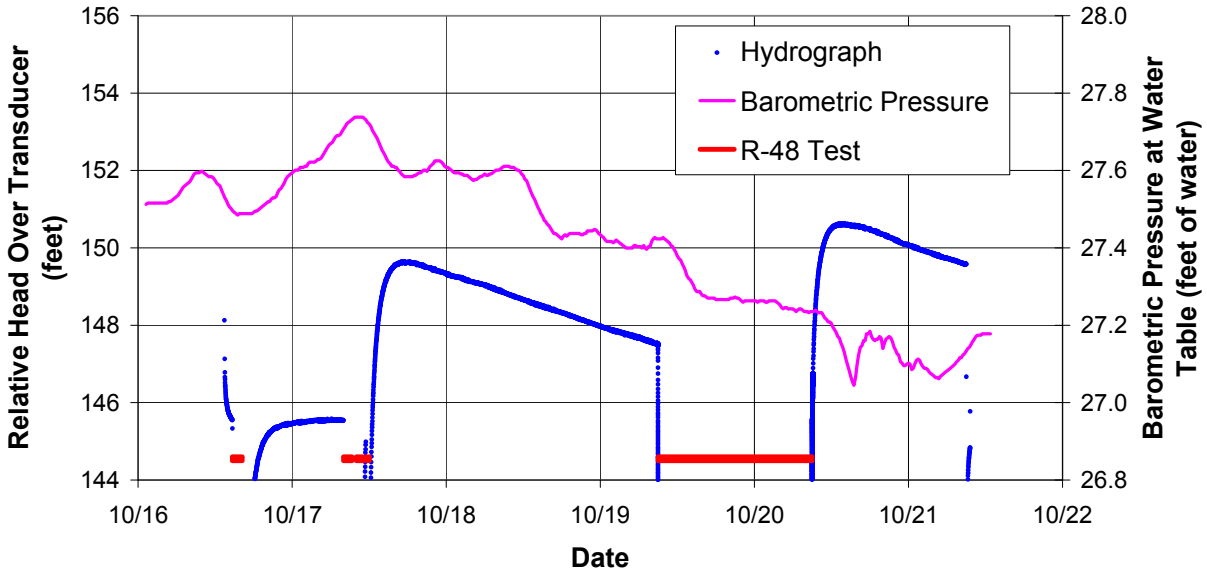


Figure C-8.0-1 Well R-48 apparent hydrograph

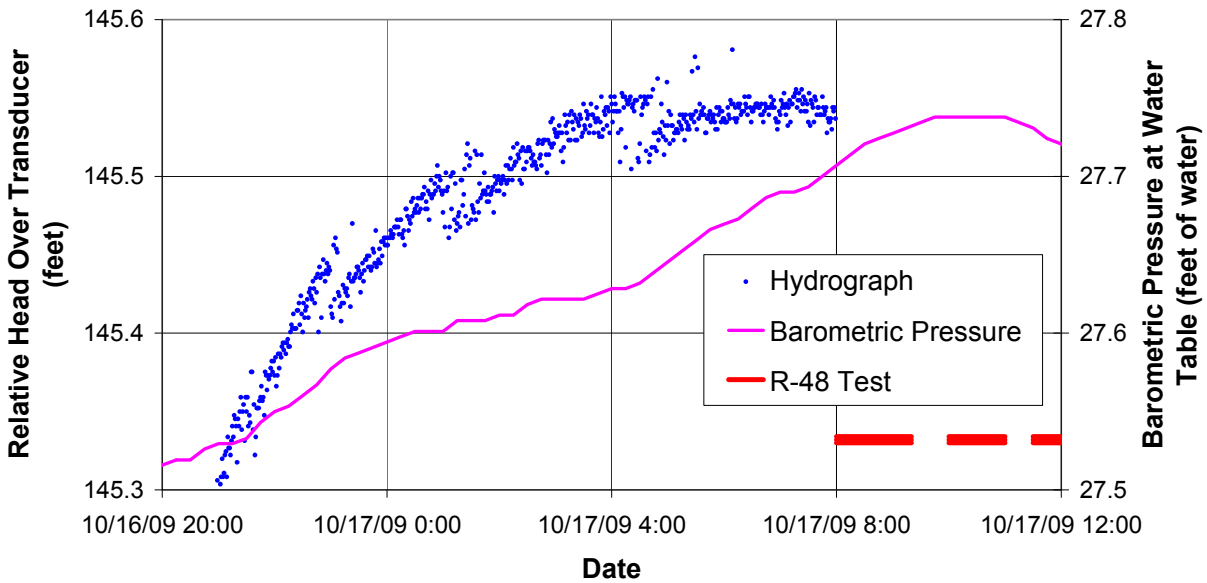


Figure C-8.0-2 Well R-48 apparent hydrograph – early data

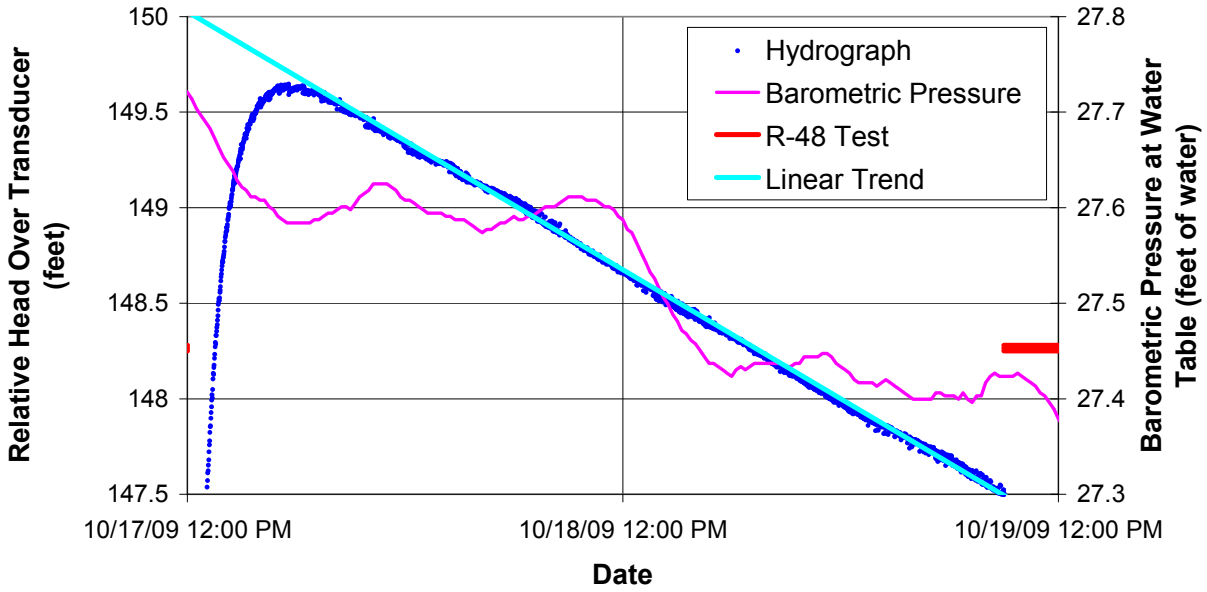


Figure C-8.0-3 Well R-48 apparent hydrograph and linear trend

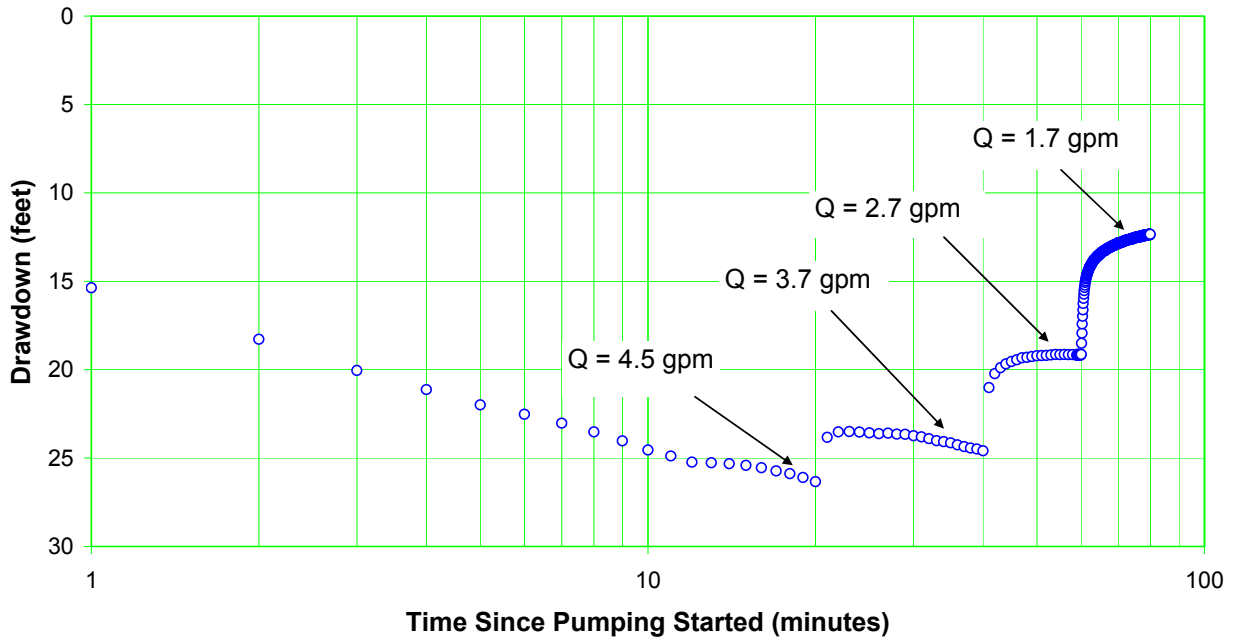


Figure C-9.1-1 Well R-48 trial 1 drawdown

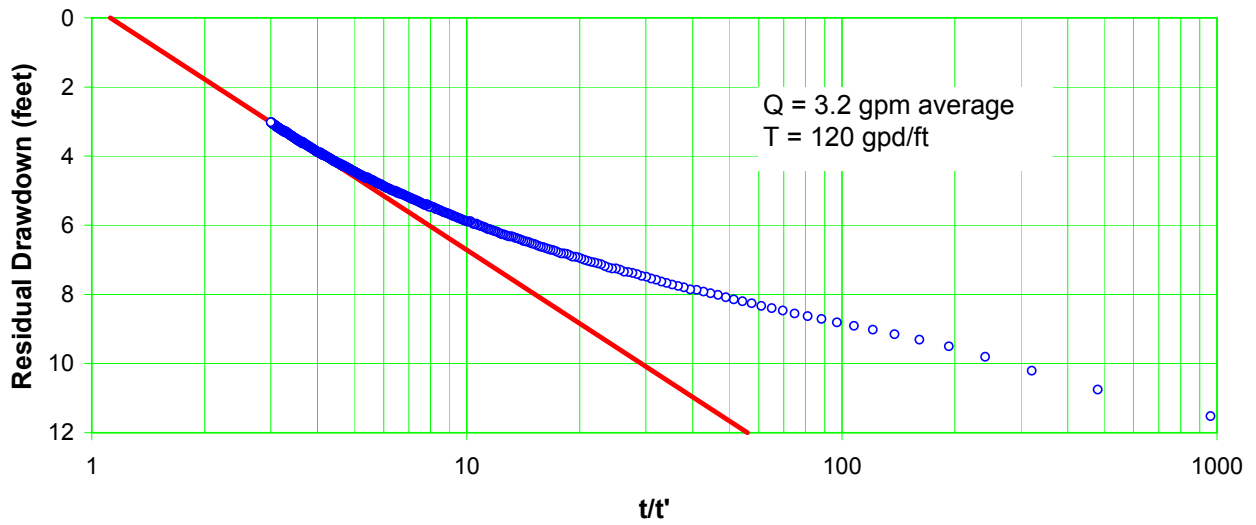


Figure C-9.1-2 Well R-48 trial 1 recovery

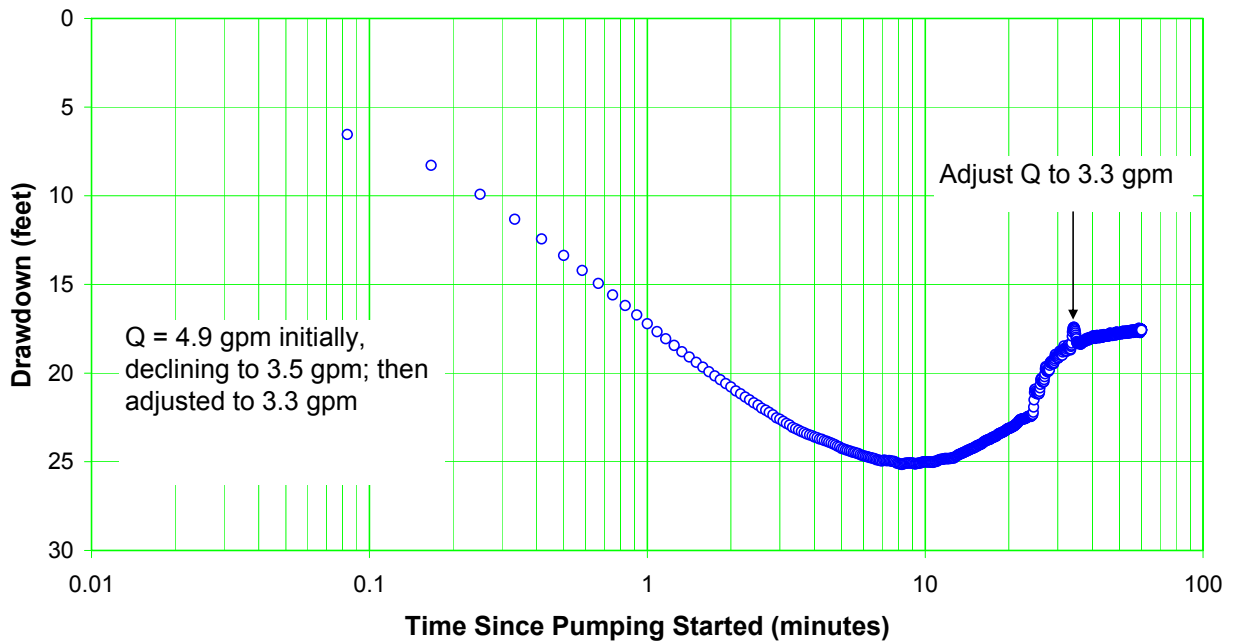


Figure C-9.2-1 Well R-48 trial 2 drawdown

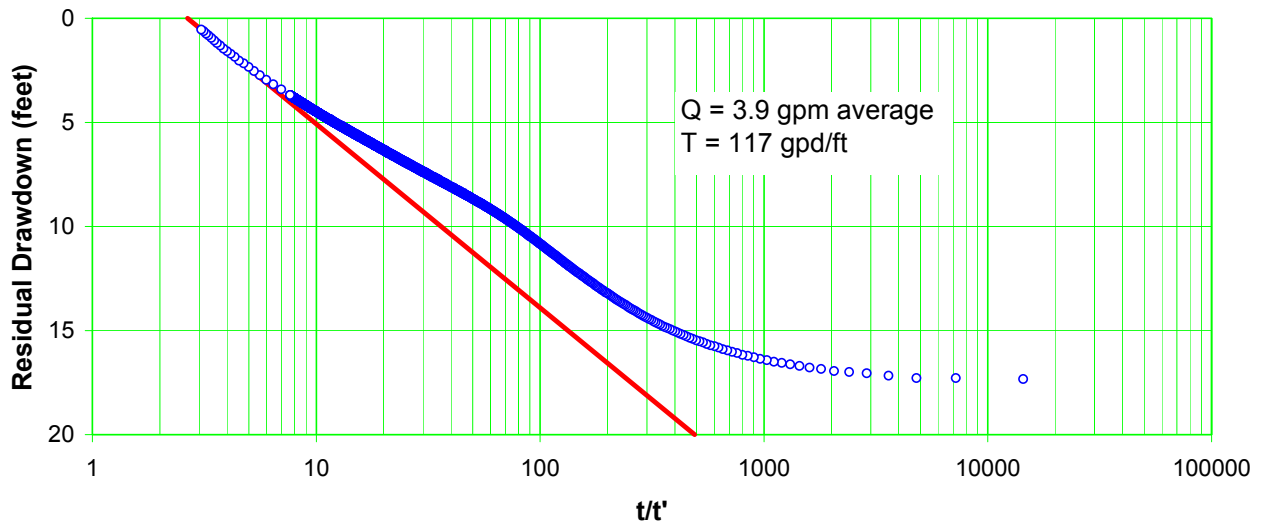


Figure C-9.2-2 Well R-48 trial 2 recovery

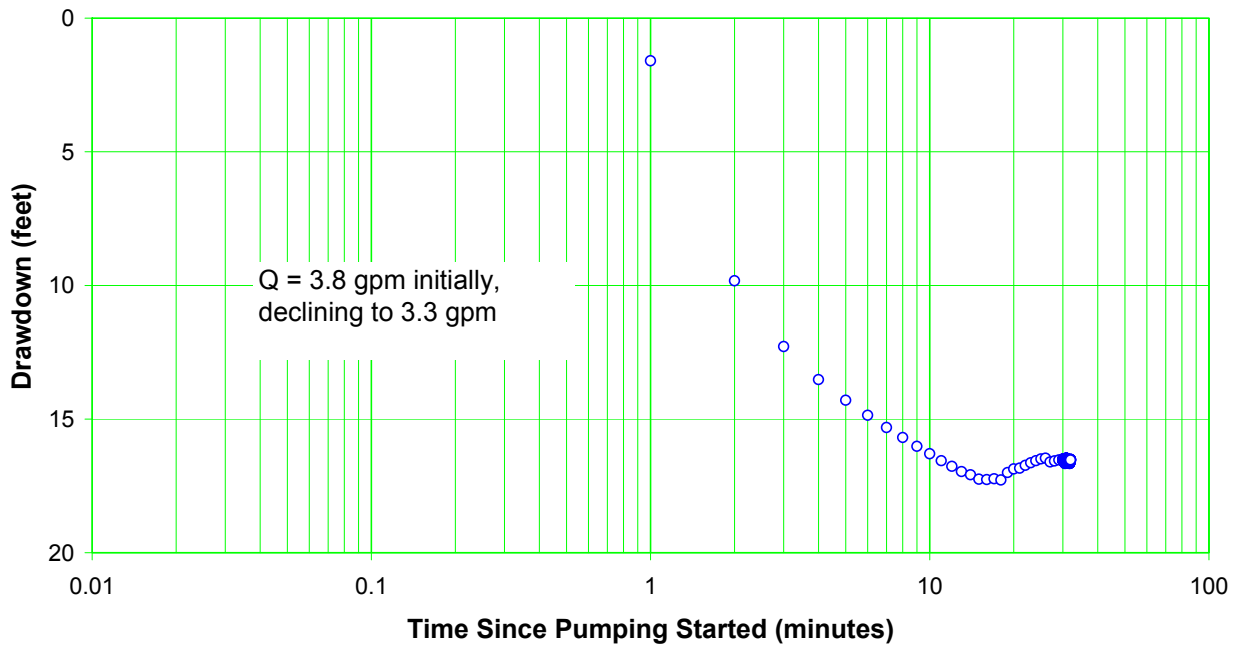


Figure C-9.3-1 Well R-48 trial 3 drawdown

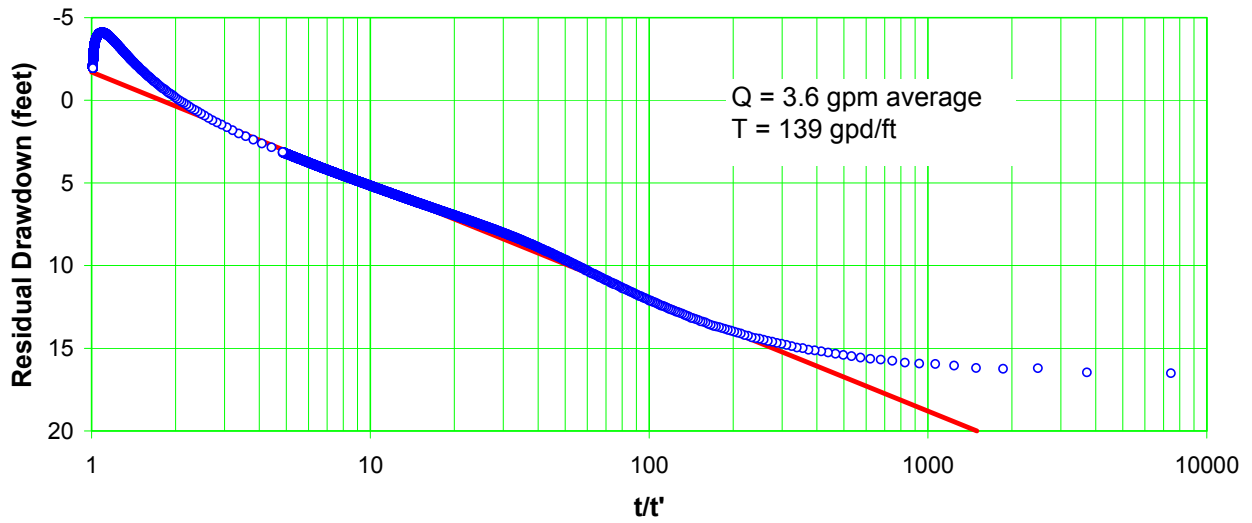


Figure C-9.3-2 Well R-48 trial 3 recovery

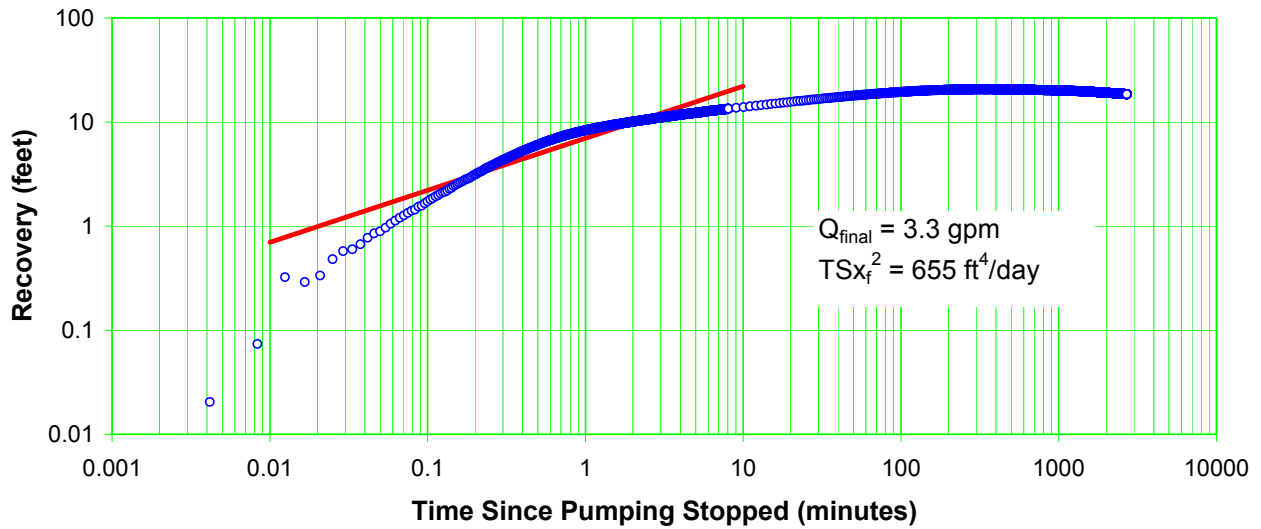


Figure C-9.3-3 Well R-48 trial 3 recovery versus time

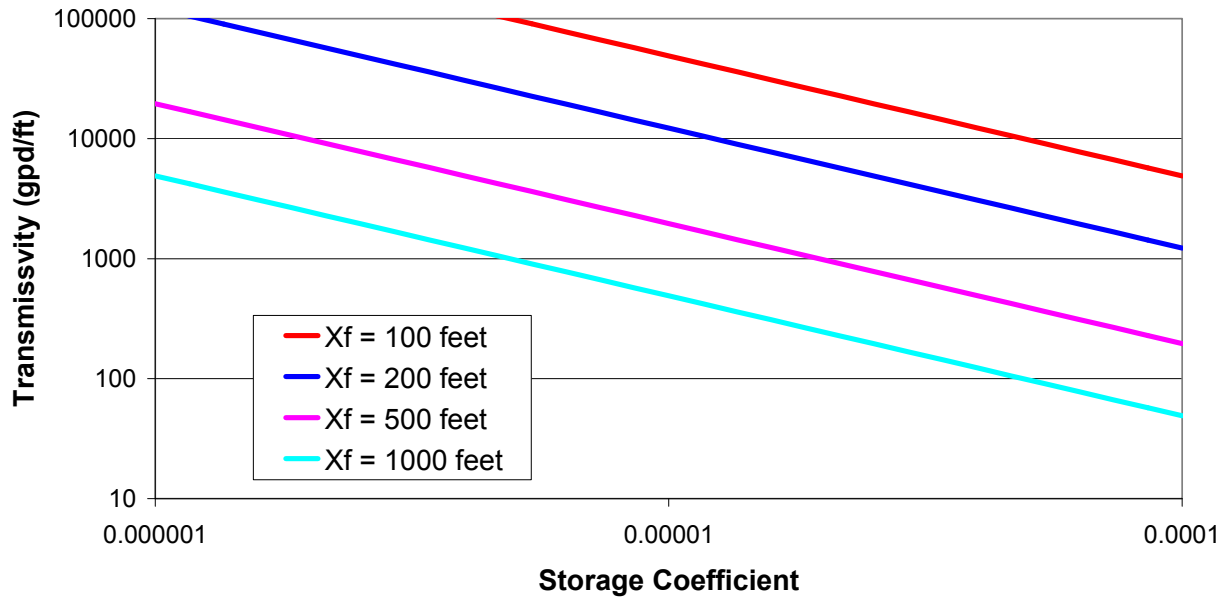


Figure C-9.3-4 Range of T values based on trial 3 recovery

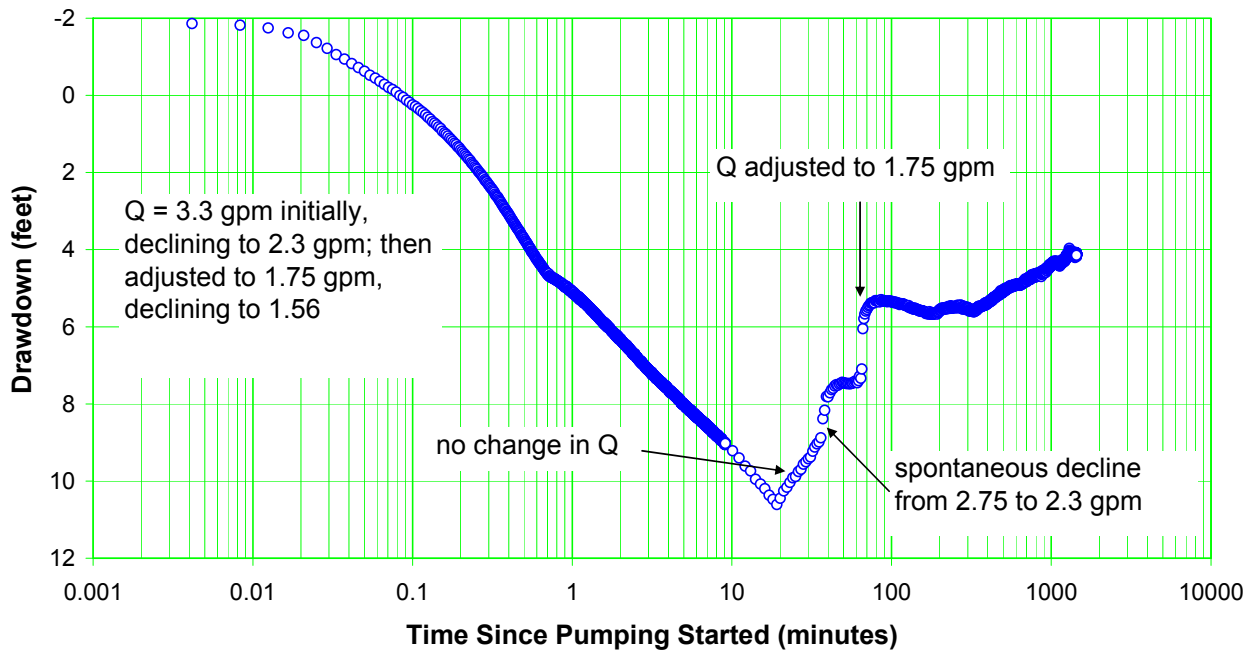


Figure C-9.4-1 Well R-48 drawdown

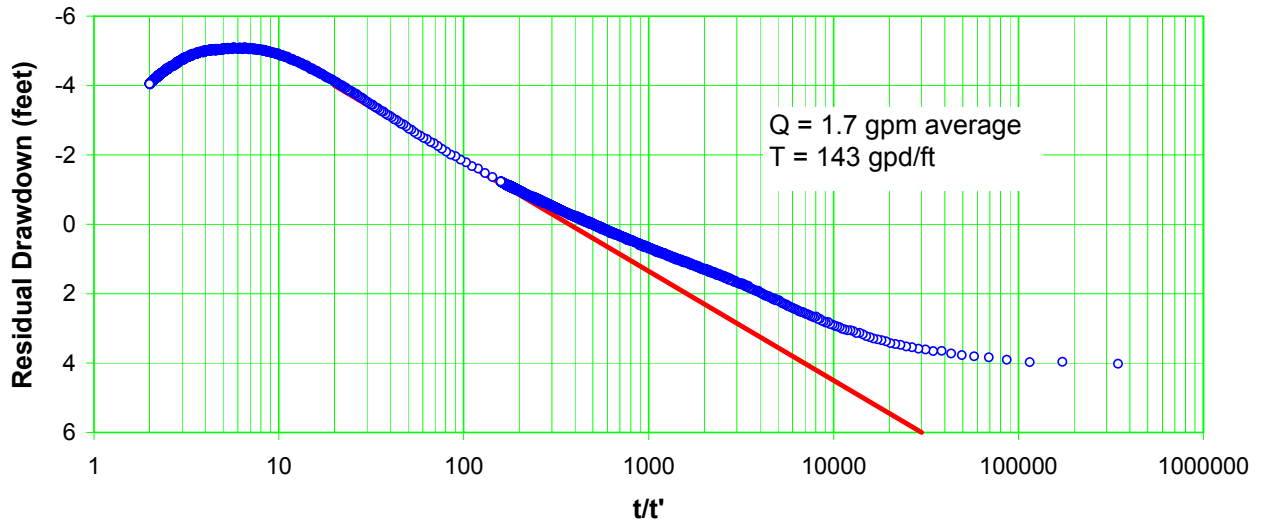


Figure C-9.4-2 Well R-48 recovery

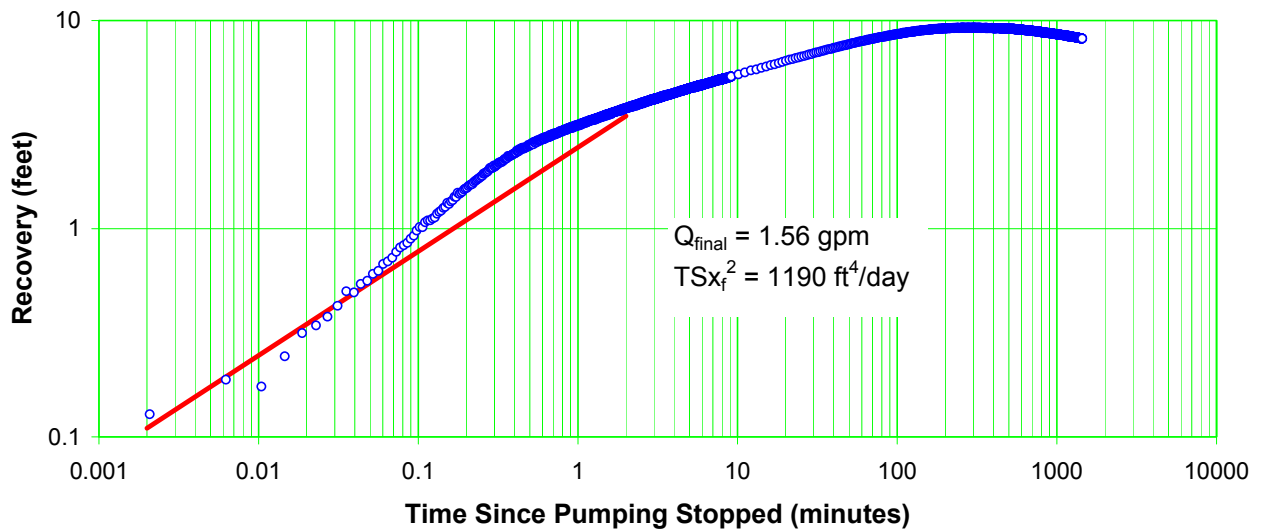


Figure C-9.4-3 Well R-48 recovery versus time

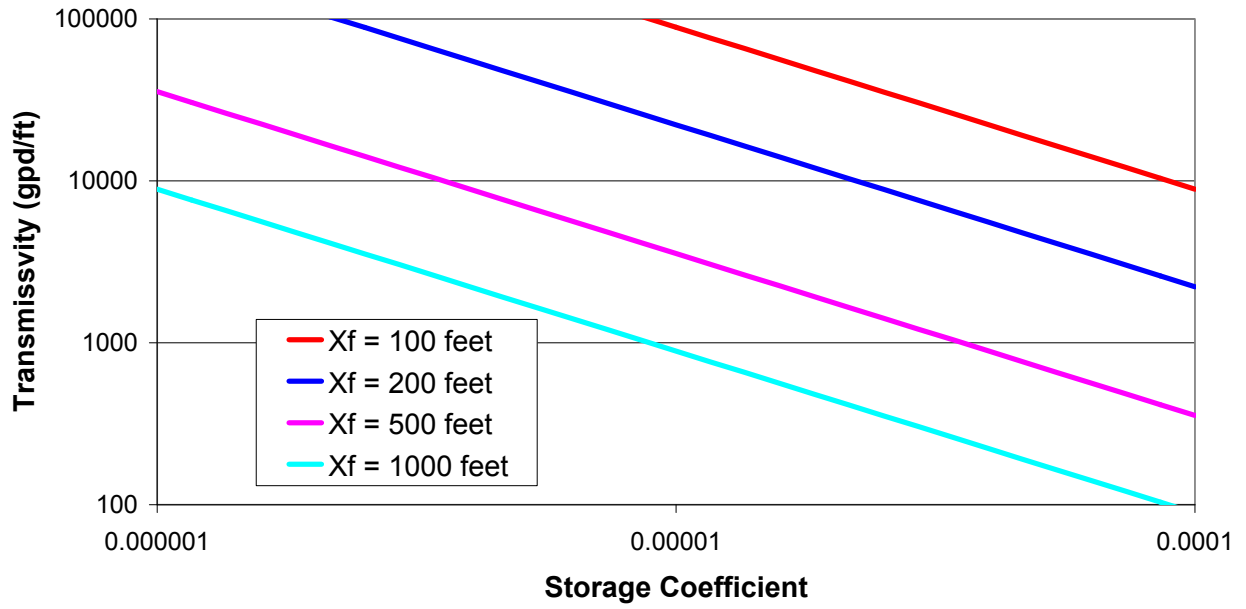


Figure C-9.4-4 Range of T values based on 24-hour recovery

**Table C-9.1-1**  
**Specific Capacity Values**

<b>Time (min)</b>	<b>Q (gpm)</b>	<b>s (ft)</b>	<b>Q/s (gpm/ft)</b>
20	4.5	26.33	0.17
40	3.7	24.59	0.15
60	2.7	19.14	0.14
80	1.7	12.35	0.14



## **Appendix D**

---

*Geophysical Logs and  
Schlumberger Geophysical Logging Report  
(on CD included with this document)*

## **Appendix D**

---

*Geophysical Logs and  
Schlumberger Geophysical Logging Report  
(on CD included with this document)*

*Report on:*  
**Advanced Borehole Geophysical Logging of  
LANL Regional Monitoring and  
Characterization Well R-48**

**Los Alamos National Laboratory,  
New Mexico**

Prepared for  
North Wind Inc.

By



*January 2010*

**EXECUTIVE SUMMARY**

Geophysical logging was performed by Schlumberger to characterize well R-48 in September 2009 before well completion. The logging measurements were acquired from 19 to 903 ft below ground surface (bgs), when the borehole was open (uncased) from 1,200 to 1,702 ft (bottom of hole, as measured by the logs), drilled with an approximately 9.75-in. diameter bit size below 1,440 ft and 12.25 in. above.

The primary purpose of the geophysical logging was to characterize the geologic/hydrogeologic section intersected by the well, with emphasis on determining regional aquifer groundwater level, relative water saturation, moisture content, depths of permeable aquifer zones, and the stratigraphy and lithology of geologic units. A secondary purpose of the geophysical logging was to evaluate the borehole conditions such as borehole diameter versus depth, deviation versus depth, and degree of drilling fluid invasion. These objectives were accomplished by measuring, nearly continuously, along the length of the well (1) total and effective water-filled porosity and pore-size distribution from which an estimate of hydraulic conductivity is made; (2) bulk electrical resistivity at multiple radial depths of investigation; (3) neutron capture cross-section, sensitive to lithology and water; (4) spectral natural gamma ray, including potassium, thorium, and uranium concentrations; (5) bedding and fracture orientation, fracture aperture, and geologic texture; (6) borehole inclination and azimuth; and (8) borehole diameter.

The following Schlumberger geophysical logging tools were used in the project (Table ES-1):

**Table ES-1: Geophysical Logging Tool, Technology, Corresponding Measured Properties**

<b>Tool</b>	<b>Technology</b>	<b>Parameters</b>
Combinable Magnetic Resonance (CMR)	Magnetic resonance proton precession	Effective (moveable) versus bound water-filled porosity, estimated hydraulic conductivity and relative flow capacity versus depth
Accelerator Porosity Sonde (APS*)	Epithermal neutron porosity at several radial depths of investigation, neutron capture cross section	Water/moisture content, lithologic variations
Array Induction Tool (AIT*)	Bulk electrical resistivity at multiple radial depths of investigation; spontaneous potential and borehole fluid resistivity	Stratigraphic delineation, relative permeability and water saturation from borehole fluid invasion profile, clay content
Micro-Cylindrically Focused Log (MCFL*)	High-resolution, focused micro-resistivity	Thin bed delineation, formation pore water salinity
Fullbore Formation Micro-Imager (FMI*)	Fully-oriented electrical resistivity imaging	Bedding, geologic texture and structure, discrete fracture characterization; borehole diameter

\* Mark of Schlumberger

A more detailed description of these geophysical logging tools can be found on the Schlumberger website (<http://www.slb.com/content/services/evaluation/index.asp?>).

To prepare for geophysical well logging, the Schlumberger district in Farmington, NM, mobilized a wireline logging truck, the appropriate wireline logging tools and associated equipment, and crew to the job site. Table 2 summarizes the geophysical logging runs performed in R-48.

**Table ES-2: Geophysical logging services, their combined tool runs and intervals logged, as performed by Schlumberger in well R-48**

Date of Logging	Run #	Tool 1 (bottom)	Tool 2 (top)	Tool 3	Depth Interval (ft bgs)
9-Sep-2009	1	AIT	MCFL	GR	1160–1694
	2	APS	GR	n/a*	1203–1696
	3	CMR	GR	n/a	1335–1699
	4	FMI	HNGS	GR	1182–1700

\*n/a = Not applicable.

Preliminary results of these measurements were generated in the logging truck at the time the geophysical services were performed and are documented in field logs provided on site. The measurements presented in the field results are not fully corrected for borehole conditions. Some require additional correction for “full results” (such as the FMI oriented electrical image) and are provided as separate logs. The field results were reprocessed by Schlumberger to: (1) correct/improve the measurements, as best as possible, for borehole/formation environmental conditions; (2) generate additional outputs through more refined workstation processing; (3) perform an integrated analysis of the log measurements so that they are all coherent and provide consistent hydrogeologic and geologic results; and (4) combine the logs in a single presentation, enabling integrated interpretation. The reprocessed log results provide better quantitative property estimates that are consistent for all applicable measurements, as well as estimates of properties that otherwise could not be reliably estimated from the single measurements alone (e.g., lithology).

The geophysical log measurements from Well R-48 provide, overall, good quality results that are consistent with each other through most of the borehole. The quality of some measurements was degraded across a few intervals where the borehole contained washouts and/or rugose hole. The measurements most affected by the adverse borehole conditions were ones that have a shallow depth of investigation and that require close contact to the borehole wall—primarily the porosity measurements from the magnetic resonance tool. The greatest impact on the log processing was erroneously high water-filled porosity in the adverse borehole conditions – as estimated from the CMR magnetic resonance logs (the other logs were not significantly impacted). The depth intervals where the CMR measurements were most affected are 1504–1510, 1514–1519, 1540–1545, 1558–1570, 1611–1621, 1626–1634, 1648–1654, 1670–1674, and 1688–1696 ft bgs. Through the integrated analysis and interpretation of all the logs, the individual shortcomings of the specific measurements are reduced. Thus, the results derived from integrated log analysis (e.g., the optimized water-filled porosity log) are the most robust single representation of the geophysical log measurements—providing a wealth of valuable high-resolution information on the geologic and hydrogeologic environment of the R-48 locale.

Important results from the processed geophysical logs in R-48 include the following:

1. The well standing water level in R-48 was 1352 ft bgs at the time of logging, and did not vary much between the different logging runs.
2. The processed logs indicate that the intersected geologic section is fully saturated with water from the bottom of the log borehole (1702 ft bgs measured from the geophysical logs) to at least 1490 ft bgs, which is the top of a porous zone overlain by much lower porosity, competent lava. The logs results indicate that there is a significant lithologic/textural boundary at 1495 ft, with porous breccia or possibly alluvium lying below (as seen on the FMI electrical image) and much more competent bedrock material (likely lava) above. Below 1490 ft, the log-estimated water content ranges from 15% to over 40% of total rock/sediment volume (see Figure 1, 3<sup>rd</sup> track from right, bright blue curve). Directly above 1490 ft, the water content drops to 7% then to less than 5% above 1475 ft. Also, above 1475 ft the shallow resistivity measurement becomes significantly less than the deep resistivity, suggesting a large difference between the rock near the water-filled borehole (saturated with water from the borehole) and the rock distant from the borehole (dry conditions). It is possible the lava is saturated above 1475 ft up to 1349 ft (the depth of the borehole water level at the time of the logging), but the rock is so tight it is very difficult to assess water saturation from the geophysical logs, although the logs indicate the non-porous rock would not produce much water anyways. The non-radioactive source open-hole logging suite does not provide a measurement of air-filled or total porosity, so a quantitative assessment of water saturation is not possible. These results suggest that the depth of the regional aquifer water level (depth at which there is full water saturation) may be as high as 1349 ft, but the top of the aquifer effectively resides at 1475 to 1490 ft, the top of porous rock, in the immediate vicinity of R-48.
3. Above 1475 ft bgs, which the processed logs indicate to be the likely top of the Regional Aquifer, the measured water content remains below 5% of total rock volume through most of the log interval, except it increases to 15% at the very top (1200–1210 ft) where there is also a borehole washout that possibly contained some water.
4. The relative hydraulic conductivity estimate and flow capacity profile generated from the processed magnetic resonance logs suggest that there are many productive zones in the porous breccia/undifferentiated alluvium below 1500 ft to the bottom of the log interval at 1700 ft (see Figure 1, 2<sup>nd</sup> track from right, blue hashed zones are the most productive). From these estimates, the most productive zones are: 1500–1520 ft, 1538–1546 ft, 1568–1580 ft, 1610–1620 ft, 1626–1634 ft, 1647–1660 ft, 1670–1675 ft, and 1688–1696 ft (although most of the interval below 1500 ft appears to be water producing).
5. The processed geophysical log results clearly delineate that the saturated/water-filled section of the borehole, below 1495 ft bgs, consists of lava breccia and possibly some zones of undifferentiated alluvium. Above 1495 ft bgs the processed logs indicate competent, low porosity lava, fractured below 1490 ft where it transitions into breccia, that extends to the top of the log interval at 1200 ft. There is a distinct, albeit small, increase in the measured potassium concentration above 1495 ft (see Figure 1, green curve in right most track) that correlates with the textural change on the electrical resistivity image.

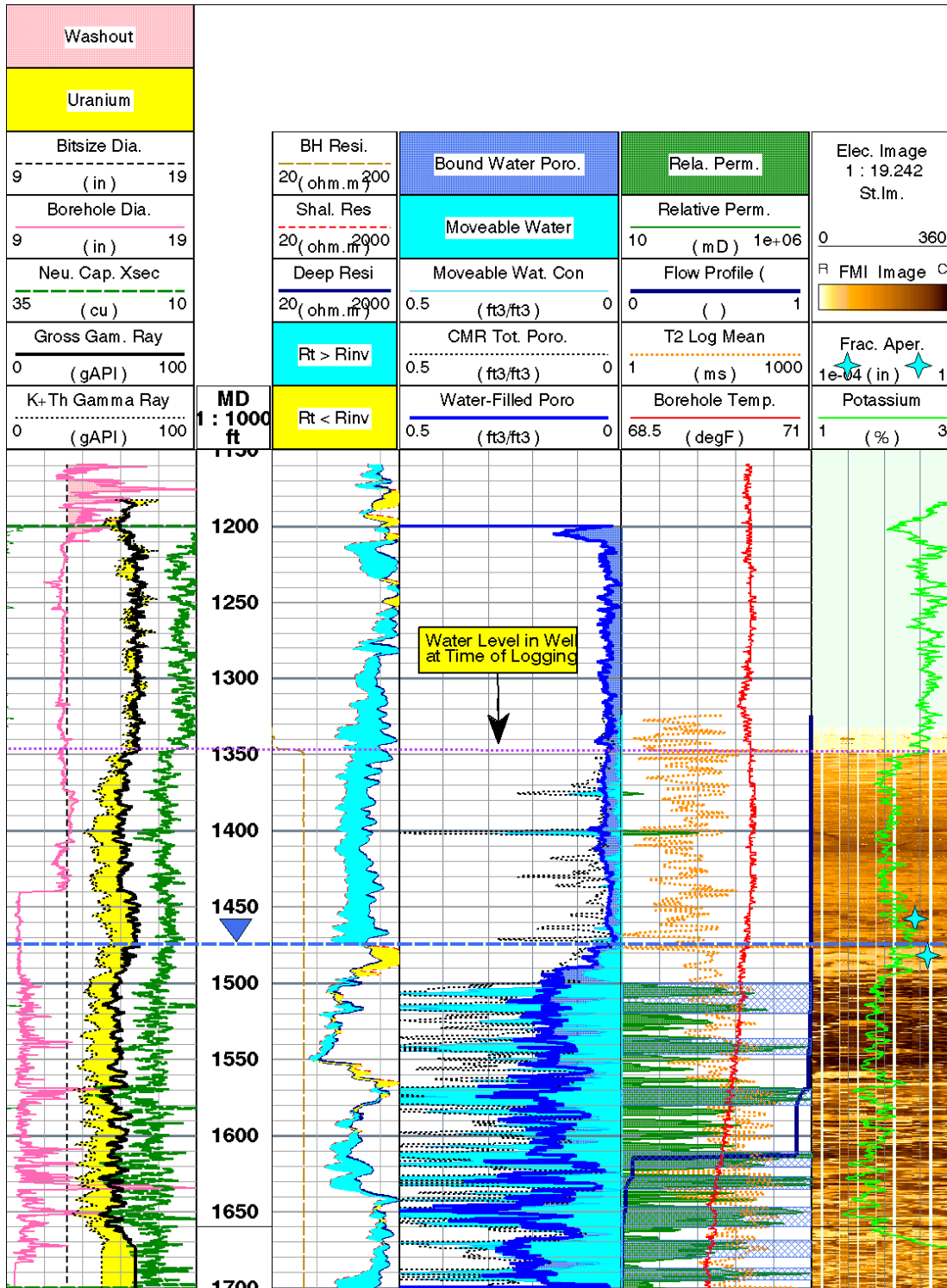


**Figure ES-1:** Initial post-processed geophysical log summary composite displaying in the 1<sup>st</sup> track (from the left) borehole diameter, gamma ray, and neutron capture cross section; in the 2<sup>nd</sup> track depth below ground surface; in the 3<sup>rd</sup> track resistivity logs; in the 4<sup>th</sup> track water-filled porosity logs; in the 5<sup>th</sup> track estimated relative permeability, flow profile, and T2 log mean (sensitive to mean pore size) from the magnetic resonance tool, as well as borehole temperature; in the 6<sup>th</sup> track is the electrical image with calculated apertures of delineated fractures and potassium concentration overlain.

## TABLE OF CONTENTS

1.0	SUMMARY .....	1
2.0	INTRODUCTION.....	4
3.0	METHODOLOGY.....	5
3.1	ACQUISITION PROCEDURE.....	5
3.2	LOG QUALITY CONTROL AND ASSESSMENT .....	6
3.3	PROCESSING PROCEDURE .....	7
3.3.1	Environmental Corrections and Raw Measurement Reprocessing.....	7
3.3.2	Depth-Matching and Splicing .....	8
3.3.3	Integrated Log Analysis .....	8
4.0	RESULTS.....	10
4.1	Well Fluid Level.....	10
4.2	Regional Aquifer .....	10
4.3	Vadose Zone Perched Water.....	11
4.4	Geology.....	11
4.5	SUMMARY LOGS.....	12
4.6	INTEGRATED LOG MONTAGE .....	17
4.6.1	Track 1–Depth.....	17
4.6.2	Track 2–Basic Logs .....	17
4.6.3	Track 3–Resistivity.....	17
4.6.4	Track 4–Porosity .....	18
4.6.5	Track 5–Density .....	18
4.6.6	Track 6–HNGS Spectral Gamma.....	18
4.6.7	Track 7–CMR Porosity.....	19
4.6.8	Track 8–Pore Size Distribution .....	19
4.6.9	Track 9–CMR T2 Distribution (Waveforms).....	20
4.6.10	Track 10–CMR T2 Distribution (Heated Amplitude) .....	20
4.6.11	Track 11–CMR Hydraulic Conductivity .....	20
4.6.12	Track 12– FMI Image (Dynamic Normalization) .....	21
4.6.13	Track 13– FMI Bedding and Fractures .....	21
4.6.14	Track 14– FMI Image (Static Normalization) .....	21
4.6.15	Track 15– Fracture Properties and High Resolution Porosity .....	21
4.6.16	Track 16 – ELAN Mineralogy Model Results (Dry Weight Fraction).....	22
4.6.17	Track 17 –ELAN Mineralogy and Pore Space Model Results (Wet Volume Fraction).....	22
4.6.18	Track 18–Water Saturation.....	23

---

4.6.19	Track 19–Predicted Flow (Production Potential) Profile .....	23
4.6.20	Track 20–Summary Logs.....	23
4.6.21	Track 21–Depth.....	23
5.0	REFERENCES.....	24

## 1.0 SUMMARY

Geophysical logging was performed by Schlumberger in characterization well R-48 in September 2009 before well completion. Well R-48 is a deepening of previously drilled well CDV-16-3i that was geophysically logged by Schlumberger in January 2004 from near surface to 1,408 ft.

The primary purpose of the geophysical logging was to characterize the geologic/hydrogeologic section intersected by the well, with emphasis on determining regional aquifer groundwater level, relative water saturation, moisture content, depths of permeable aquifer zones, and the stratigraphy and lithology of geologic units. A secondary purpose of the geophysical logging was to evaluate the borehole conditions such as borehole diameter versus depth, deviation versus depth, and degree of drilling fluid invasion. These objectives were accomplished by measuring, nearly continuously, along the length of the well (1) total and effective water-filled porosity and pore-size distribution from which an estimate of hydraulic conductivity is made; (2) bulk electrical resistivity at multiple radial depths of investigation; (3) neutron capture cross-section, sensitive to lithology and water; (4) spectral natural gamma ray, including potassium, thorium, and uranium concentrations; (5) bedding and fracture orientation, fracture aperture, and geologic texture; (6) borehole inclination and azimuth; and (8) borehole diameter.

The following Schlumberger geophysical logging tools were used in the project (Table 1.1):

**Table 1.1: Geophysical Logging Tool, Technology, Corresponding Measured Properties**

Tool	Technology	Properties Measured
Combinable Magnetic Resonance tool (CMR*)	Magnetic resonance proton precession	Effective (moveable) versus bound water-filled porosity, estimated hydraulic conductivity and relative flow capacity versus depth
Accelerator Porosity Sonde (APS*)	Epithermal neutron porosity at several radial depths of investigation, neutron capture cross section	Water/moisture content, lithologic variations
Array Induction Tool (AIT)	Bulk electrical resistivity at multiple radial depths of investigation; spontaneous potential and borehole fluid resistivity	Stratigraphic delineation, relative permeability and water saturation from the borehole fluid invasion profile, clay content
Micro-Cylindrically Focused Log (MCFL*)	High-resolution, focused micro-resistivity	Thin bed delineation, formation pore water salinity
Fullbore Formation Micro-Imager (FMI)	Fully-oriented electrical resistivity imaging	Bedding, geologic texture and structure, discrete fracture characterization; borehole diameter
Hostile Natural Gamma Spectroscopy (HNGS*) and gamma ray (GR)	Gross and spectral natural gamma ray, including potassium, thorium, and uranium concentrations	Formation matrix geochemistry, lithology and mineralogy

\* Mark of Schlumberger

Once the North Wind, Inc. (NWI) well drilling project team provided Schlumberger final notification that R-48 was ready for geophysical well logging, the Schlumberger district in Farmington, NM, mobilized a wireline logging truck, the appropriate wireline logging tools and associated equipment, and crew to the job site. Table 1.2 summarizes the geophysical logging runs performed in R-48.

**Table 1.2: Geophysical logging services, their combined tool runs and intervals logged, as performed by Schlumberger in well R-48**

Date of Logging	Run #	Tool 1 (bottom)	Tool 2 (top)	Tool 3	Depth Interval (ft bgs)
9-Sep-2009	1	AIT	MCFL	GR	1160–1694
	2	APS	GR	n/a*	1203–1696
	3	CMR	GR	n/a	1335–1699
	4	FMI	HNGS	GR	1182–1700

\*n/a = Not applicable.

Preliminary results of these measurements were generated in the logging truck at the time the geophysical services were performed and are documented in field logs provided on site. However, the measurements presented in the field results are not fully corrected for borehole conditions, some require additional correction for full results (such as the FMI oriented electrical image) and are provided as separate, individual logs. The field results were reprocessed by Schlumberger to (1) correct/improve the measurements, as best as possible, for borehole/formation environmental conditions; (2) generate additional outputs through more refined workstation processing; (3) perform an integrated analysis of the log measurements so that they are all coherent and provide consistent hydrogeologic and geologic results; and (4) combine the logs in a single presentation, enabling integrated interpretation. The reprocessed log results provide better quantitative property estimates that are consistent for all applicable measurements, as well as estimates of properties that otherwise could not be reliably estimated from the single measurements alone (e.g., lithology).

The geophysical log measurements from Well R-48 provide, overall, good quality results that are consistent with each other through most of the borehole. The quality of some measurements was degraded across a few intervals where the borehole contained washouts and/or rugose hole. The measurements most affected by the adverse borehole conditions were ones that have a shallow depth of investigation and that require close contact to the borehole wall—primarily the porosity measurements from the magnetic resonance tool. The greatest impact on the log processing was erroneously high water-filled porosity in the adverse borehole conditions – as estimated from the CMR magnetic resonance logs (the other logs were not significantly impacted). The depth intervals where the CMR measurements were most affected are 1504–1510, 1514–1519, 1540–1545, 1558–1570, 1611–1621, 1626–1634, 1648–1654, 1670–1674, and 1688–1696 ft bgs. Through the integrated analysis and interpretation of all the logs, the individual shortcomings of the specific measurements are reduced. Thus, the results derived from integrated log analysis (e.g., the optimized water-filled porosity log) are the most robust single representation of the geophysical log measurements—providing a wealth of valuable high-resolution information on the geologic and hydrogeologic environment of the R-48 locale.

Important results from the processed geophysical logs in R-48 include the following:

1. The well standing water level in R-48 was 1352 ft bgs at the time of logging, and did not vary much between the different logging runs.
2. The processed logs indicate that the intersected geologic section is fully saturated with water from the bottom of the log borehole (1702 ft bgs measured from the geophysical logs) to at least 1490 ft bgs, which is the top of a porous zone overlain by much lower porosity, competent lava. The logs results indicate that there is a significant lithologic/textural boundary at 1495 ft, with porous breccia or possibly alluvium lying below (as seen on the FMI electrical image) and much more competent bedrock material (likely lava) above. Below 1490 ft, the log-estimated water content ranges from 15% to over 40% of total rock/sediment volume (see Figure 1, 3rd track from right, bright blue curve). Directly above 1490 ft, the water content drops to 7% then to less than 5% above 1475 ft. Also, above 1475 ft the shallow resistivity measurement becomes significantly less than the deep resistivity, suggesting a large difference between the rock near the water-filled borehole (saturated with water from the borehole) and the rock distant from the borehole (dry conditions). It is possible the lava is saturated above 1475 ft up to 1349 ft (the depth of the borehole water level at the time of the logging), but the rock is so tight it is very difficult to assess water saturation from the geophysical logs, although the logs indicate the non-porous rock would not produce much water anyways. The non-radioactive source open-hole logging suite does not provide a measurement of air-filled or total porosity, so a quantitative assessment of water saturation is not possible. These results suggest that the depth of the regional aquifer water level (depth at which there is full water saturation) may be as high as 1349 ft, but the top of the aquifer effectively resides at 1475 to 1490 ft, the top of porous rock, in the immediate vicinity of R-48.
3. Above 1475 ft bgs, which the processed logs indicate to be the likely top of the Regional Aquifer, the measured water content remains below 5% of total rock volume through most of the log interval, except it increases to 15% at the very top (1200–1210 ft) where there is also a borehole washout that possibly contained some water.
4. The relative hydraulic conductivity estimate and flow capacity profile generated from the processed magnetic resonance logs suggest that there are many productive zones in the porous breccia/undifferentiated alluvium below 1500 ft to the bottom of the log interval at 1700 ft (see Figure 1, 2nd track from right, blue hashed zones are the most productive). From these estimates, the most productive zones are: 1500–1520 ft, 1538–1546 ft, 1568–1580 ft, 1610–1620 ft, 1626–1634 ft, 1647–1660 ft, 1670–1675 ft, and 1688–1696 ft (although most of the interval below 1500 ft appears to be water producing).
5. The processed geophysical log results clearly delineate that the saturated/water-filled section of the borehole, below 1495 ft bgs, consists of lava breccia and possibly some zones of undifferentiated alluvium. Above 1495 ft bgs the processed logs indicate competent, low porosity lava, fractured below 1490 ft where it transitions into breccia, that extends to the top of the log interval at 1200 ft. There is a distinct, albeit small, increase in the measured potassium concentration above 1495 ft (see Figure 1, green curve in right most track) that correlates with the textural change on the electrical resistivity image.
6. The interpreted planar bedding features across the electrically imaged interval 1325–1700 ft bgs have fairly widely varying dip azimuths (direction beds are dipping towards) and dip angles (angle from horizontal), although there is consistency within different lithotypes. Within the competent lava beds above 1470 ft the foliation is very consistent to the northeast. In the heterogeneous breccia section below 1195 ft the bedding features that can be delineated have quite variable dip

azimuths, but appear to cluster in the northeast and northwest. The bed boundary at 896 ft between this breccia and the well-sorted channel sands below dips towards the south at an angle of 12 degrees and the cross-bedding in the channel sands is dipping primarily towards the east. Bedding feature dip angles (angle from horizontal) range mostly from 5 to 25 degrees in the lava beds and 8 to 75 degrees in the breccia. A number of fractures are discernable in the lava bed (all in the depth interval 1157–1194 ft, except one at 1107 ft), with widely varying dip azimuth directions, but predominantly orthogonal directions to the northeast, southeast, southwest and northwest, with dip angles ranging from 10 to 85 degrees. Computed fracture apertures show higher apertures and, thus, bulk fracture porosity at the bottom of the lava (1175–1194 ft) near the transition to breccia below.

## 2.0 INTRODUCTION

Geophysical logging services were performed in characterization well R-48 by Schlumberger in September 2009 before initial well completion. Well R-48 is a deepening of previously drilled well CDV-16-3i that was geophysically logged by Schlumberger in January 2004 from near surface to 1,408 ft. The purpose of these services was to acquire in-situ measurements to help characterize the borehole, near-borehole, and abutting geologic formation environment. The primary objective of the geophysical logging was to provide in-situ evaluation of formation properties (hydrogeology and geology) intersected by the well. This information was (and is) used by scientists, engineers, and project managers in the Los Alamos Characterization and Monitoring Well Project to design the well completion, to better understand subsurface site conditions, and assist in overall decision-making.

The primary geophysical logging tools used by Schlumberger in well R-48 included the following:

Combinable Magnetic Resonance (CMR\*) tool, which measures the nuclear magnetic resonance response of the formation to evaluate total and effective water-filled porosity of the shallow formation and to estimate pore size distribution and in-situ hydraulic conductivity;

Accelerator Porosity Sonde (APS\*) which measures volumetric water content of the formation to evaluate moist/porous zones;

Array Induction Tool (AIT\*), which measures formation electrical resistivity at five depths of investigation and borehole fluid resistivity to evaluate drilling fluid invasion into the formation (a qualitative indicator of permeability and water saturation), presence of moist zones far from the borehole wall, and presence of clay-rich zones;

Micro-Cylindrically Focused Log (MCFL\*), which is a focused, high vertical resolution electrical resistivity measurement in fluid filled borehole, and is used optimize resistivity measurement environmental corrections;

Formation Micro-Imager (FMI\*) tool, which measures electrical conductivity images of the borehole wall in fluid-filled open-hole and borehole diameter with a two-axis caliper to evaluate geologic bedding and fracturing, including strike and dip of these features and fracture apertures, and rock/sediment texture;

General Purpose Inclinerometry Tool (GPIT\*), run as part of the FMI, which measures borehole deviation and azimuth in open-hole to evaluate borehole position versus depth and to orient FMI images; and

Hostile Natural Gamma Spectroscopy (HNGS\*) tool, which measures gross natural gamma and spectral natural gamma ray activity, including potassium, thorium, and uranium concentrations, to evaluate geology/lithology, particularly the amount of clay and potassium-bearing minerals.

\* Mark of Schlumberger

In addition, calibrated gross gamma ray (GR) was recorded with every service for the purpose of correlating depths between the different logging runs. Table 2.1 summarizes the geophysical logging runs performed in R-48.

**Table 2.1: Geophysical logging services, their combined tool runs and intervals logged, as performed by Schlumberger in borehole R-48**

Date of Logging	Borehole Status	Run #	Tool 1	Tool 2	Tool 3	Depth Interval (ft bgs)
9-Sep-2009	Open hole across logged interval. Bit size of 12 in. above 1440 ft and 10 in. below	1	AIT	MCFL	GR	1160–1694
		2	APS	GR	n/a*	1203–1696
		3	CMR	GR	n/a	1335–1699
		4	FMI	HNGS	GR	1182–1700

\*n/a = Not applicable.

A more detailed description of these geophysical logging tools can be found on the Schlumberger website (<http://www.slb.com/content/services/evaluation/index.asp?>).

### 3.0 METHODOLOGY

This section describes the methods Schlumberger employed for geophysical logging of Well R-48, including the following stages/tasks:

- Measurement acquisition at the well site
- Quality assessment of logs
- Reprocessing of field data

#### 3.1 Acquisition Procedure

Once the well drilling project team notified Schlumberger that R-48 was ready for geophysical well logging, the Schlumberger district in Farmington, NM, mobilized a wireline logging truck, the appropriate wireline logging tools and associated equipment, and crew to the job site. Upon arriving at the LANL site, the crew completed site-entry paperwork and received a site-specific safety briefing.

After arriving at the well site, the crew proceeded to rig up the wireline logging system, including:

- Parking and stabilizing the logging truck in a position relative to the borehole that is best for performing the surveys
- Setting up a lower and an upper sheave wheel (the latter attached to, and hanging above, the borehole from the drilling rig/mast truck)

- Threading the wireline cable through the sheaves
- Attaching to the end of the cable the appropriate sonde(s) for the first run

Next, pre-logging checks and any required calibrations were performed on the logging sondes, and the tool string was lowered into the borehole. The tool string was lowered to the bottom of the borehole and brought up at the appropriate logging speed as measurements were made. At least two logging runs (one main and one repeat) were made with each tool string.

Upon reaching the surface, post-logging measurement checks were performed as part of log quality control and assurance. The tool string was cleaned as it was pulled out of the hole, separated, and disconnected.

The second tool string was attached to the cable for another logging run, followed by subsequent tool strings and logging runs. After the final logging run was completed, the cable and sheave wheels were rigged down.

Before departure, the logging engineer printed field logs and created a compact disc containing the field log data for on-site distribution and sent the data via satellite to the Schlumberger data storage center. The Schlumberger data processing center was alerted that the data were ready for post-acquisition processing.

### **3.2 Log Quality Control and Assessment**

Schlumberger has a thorough set of procedures and protocols for ensuring that the geophysical logging measurements are of very high quality. This includes full calibration of tools when they are first built, regular recalibrations and tool measurement/maintenance checks, and real-time monitoring of log quality as measurements are made. One of the primary responsibilities of the logging engineer is to ensure, before and during acquisition, that the log measurements meet prescribed quality criteria.

A tool-specific base calibration that directly relates the tool response to the physical measurement using the designed measurement principle is performed on all Schlumberger logging tools when first assembled in the engineering production centers. This is accomplished through a combination of computer modeling and controlled measurements in calibration models with known chemical and physical properties.

The base calibration for most Schlumberger tools is augmented through regular “master calibrations” typically performed every one to six months in local Schlumberger shops (such as Farmington, NM), depending on tool design. Master calibrations consist of controlled measurements using specially designed calibration tanks/jigs and internal calibration devices that are built into the tools, both with known physical properties. The measurements are used to fine-tune the tool’s calibration parameters and to verify that the measurements are valid.

In addition, on every logging job, before and after on-site “calibrations” are executed for most Schlumberger tools directly before/after lowering/removing the tool string from the borehole. For most tools, these represent a measurement verification instead of an actual calibration used to confirm the validity of the measurements directly before acquisition and to ensure that they have not drifted or been corrupted during the logging job.

All Schlumberger logging measurements have a number of associated depth-dependent quality control (QC) logs and flags to assist with identifying and determining the magnitude of log quality problems.

These QC logs are monitored in real-time by the logging engineer during acquisition and are used in the post-acquisition processing of the logs to determine the best processing approach for optimizing the overall validity of the property estimates derived from the logs.

Additional information on specific tool calibration procedures can be found on the Schlumberger web page (<http://www.slb.com/content/services/evaluation/index.asp?>).

### **3.3 Processing Procedure**

After the geophysical logging job was completed in the field and the data was archived, the data was downloaded to the Schlumberger processing center. There, the data were processed in the following sequence: (1) the measurements were corrected for near-wellbore environmental conditions and the measurement field processing for certain tools (in this case the CMR) was redone or refined using better processing algorithms and parameters, (2) the log curves from different logging runs were depth matched and spliced, and (3) the near-wellbore substrate lithology/mineralogy and pore fluids were modeled through integrated log analysis. Separately, the FMI electrical image was processed to produce scaled and normalized high-resolution images that were interpreted to identify geologic features and compute fracture apertures. Afterwards, an integrated log montage was built to combine and compile all the processed log results.

#### **3.3.1 Environmental Corrections and Raw Measurement Reprocessing**

If required, the field log measurements were processed to correct for conditions in the well, including fluid type (water or air), presence of steel casing (not applicable for this well since the top of all logs is below casing), and (to a much lesser extent) pressure, temperature, and fluid salinity. Basically, these environmental corrections entail subtracting from the measurement response the known influences of the set of prescribed borehole conditions. In R-48, the log measurements requiring these corrections are the APS porosity and HNGS spectral gamma ray logs, although the AIT field resistivity logs were also re-processed to improve the environmental corrections.

Two neutron porosity measurements are available – one that measures thermal (“slow”) neutrons, and one that measures epithermal (“fast”) neutrons. Measurement of epithermal neutrons is required to make neutron porosity measurements in air-filled holes. In water/mud-filled holes, both the epithermal and thermal neutron measurements are valid. The APS makes epithermal porosity measurements. In R-48 the borehole was partly water-filled (below 1349 ft during the logging) and partly air-filled (above 1349 ft). The APS epithermal neutron porosity was processed at the field site for borehole fluid type (air versus water) and other environmental conditions and didn’t require any further processing. However, the APS field porosity measurements were re-processed to confirm the validity of the environmental corrections.

The HNGS spectral gamma ray is affected by the material (fluid, air, and casing) in the borehole because different types and amounts of these materials have different gamma ray shielding properties; the HNGS measures incoming gamma rays emitted by radioactive elements in the formation surrounding the borehole. The processing algorithms try to correct for the damping influence of the borehole material. The HNGS logs from R-48 were reprocessed to fully account for the environmental effects of the borehole fluid (water below 1349 ft and air above) and hole size.

The measurements cannot be fully corrected for borehole washouts or rugosity since the specific characteristics (e.g., geometry) of these features are unknown and their effects on the measurements are often too significant to account for. Thus, the compromising effects of these conditions on the measurements should be accounted for in the interpretation of the log results.

### 3.3.2 Depth-Matching and Splicing

Once the logs were environmentally corrected for the conditions in the borehole and the raw measurement reprocessing was completed, the logs from different tool runs were depth-matched to each other using the FMI tool run as the base reference. Gross gamma ray and measurements sensitive to water content were used as the common correlation log measurements for depth-matching the different runs. The depth reference for all the processed logs in this report is ground surface, as was the depth reference for logs presented in the field (field logs).

### 3.3.3 Integrated Log Analysis

An integrated log analysis, using as many of the processed logs as possible, was performed to model the near-wellbore substrate lithology/mineralogy and pore fluids. This analysis was performed using the Elemental Log Analysis (ELAN<sup>\*</sup>) program (Mayer and Sibbit, 1980; Quieren et al, 1986) – a petrophysical interpretation program designed for depth-by-depth quantitative formation evaluation from borehole geophysical logs. ELAN estimates the volumetric fractions of user-defined rock matrix and pore constituents at each depth based on the known log measurement responses to each individual constituent by itself<sup>1</sup>. ELAN requires an a priori specification of the volume components present within the formation, i.e., fluids, minerals, and rocks. For each component, the relevant response parameters for each measurement are also required. For example, if one assumes that quartz is a volume component within the formation and the bulk density tool is used, then the bulk density parameter for this mineral is well known to be 2.65 grams per cubic centimeter (g/cc).

The logging tool measurements, volume components, and measurement response parameters used in the ELAN analysis for R-48 are provided in Table 3.1. The final results of the analysis – an optimized mineral-fluid volume model – are shown on the integrated log montage (see Attachment D-1), 3<sup>rd</sup> track from the right (inclusive of the depth track). In addition, the ELAN program provides a direct comparison of the modeled versus the actual measured geophysical logs, as well as a composite log of all of the key ELAN-derived results. To make best use of all the measurement data and to perform the analysis across as much of the logged interval as possible (1204 to 1700 ft bgs), as many as possible of the processed logs were included in the analysis, with less weighting applied to less robust logs. Not all of the tool measurements shown in Table 3.1 and the ELAN modeled versus measured log display are used for the entire interval analyzed, as not all the measurements are available, or of good quality, across certain sections of the borehole. To accommodate fewer tool measurements, certain model constituents are removed from the analysis in some intervals. Most notably, above 1325 ft bgs moveable/free water had to be removed from the analysis because no CMR measurement is available (CMR has the only

---

\*Mark of Schlumberger

<sup>1</sup>Mathematically this corresponds to an inverse problem – solving for constituent volume fractions from an (over)determined system of equations relating the measured log results to combinations of the tool measurement response to individual constituents.

measurement that is independently sensitive to moveable and bound water independently) and above 1475 ft total porosity had to be set since no bulk density measurement is available.

The ELAN analysis was performed with as few constraints or prior assumptions as possible. A considerable effort was made to choose a set of minerals or mineral types for the model that is representative of Los Alamos area geology and its volcanic origins. For the ELAN analysis, the entire log interval was assumed to be andesite/dacite lava or breccia/sediments derived from it, and a mineral suite considered representative of this volcanic material, based on LANL cuttings mineral analysis, was used (primary “minerals” plagioclase and potassium feldspar; possible secondary minerals montmorillonite clay, hornblende, augite, hematite, and magnetite).

Initially, no prior assumption was made about water saturation—where the boundary between saturated and unsaturated zones lies (e.g., the depth to the top of the regional aquifer or perched zones)—in order to not bias where the analysis indicated full saturation was, even though there were no measurements in the open-hole logging suite specifically sensitive to air-filled or total porosity. Because of this, once the distinct change in water content at 1475 ft was verified, an arbitrary total porosity was chosen for the interval above (zoned to differentiate between competent, non-porous lava and brecciated, more porous lava). There is no way to objectively correct for the adverse effect on the log measurements from borehole washouts; therefore the decision was made to perform the ELAN analysis so as to honor the log measurements. Accordingly, interpretations should be made from the ELAN results with the understanding that the mineral-fluid model represents a mathematically optimized solution that is not necessarily a physically accurate representation of the native geologic formation. Within this context, the ELAN model is a robust estimate of the bulk mineral-fluid composition that accounts for the combined response from all the geophysical measurements.

**Table 3.1: Tool measurements, volumes, and respective parameters used in the R-48 ELAN analysis**

Volume	Air	Capillary Bound Water	Water	Hornblende	Hematite	Labradorite	Magnetite	Augite	Montmorillonite	Orthoclase
Epithermal neutron poro. (ft <sup>3</sup> /ft <sup>3</sup> )	0	1.00	1.00	0.045	0.0556	-0.01	0.022	-0.01	0.55	-0.01
Total CMR porosity (ft <sup>3</sup> /ft <sup>3</sup> )	0	1.0	1.0	0	0	0	0	0	0.55	0
CMR bound fluid volume (ft <sup>3</sup> /ft <sup>3</sup> )	0	1.0	0	0	0	0	0	0	0.55	0
Resistivity (ohm-m)	Infinite	36.2	36.2	Infinite	Infinite	Infinite	Infinite	Infinite	0.92	Infinite
Wet weight potassium (lbf/lbf)	0	0	0	0.01	0	0	0	0.003	0.004	0.102
Wet weight thorium (ppm)	0	0	0	50	0	1.75	20	25	44	5
Neutron capture cross section (cu)	0	22.2	22.2	9	101.4	7.87	103	25.66	20	15.82

Volume	Air	Capillary Bound Water	Water	Hornblende	Hematite	Labradorite	Magnetite	Augite	Montmorillonite	Orthoclase
Clay bound water volume (ft <sup>3</sup> /ft <sup>3</sup> )	0	0	0	0	0	0	0	0	0.55	0

ohm-m = ohm x meters  
 ft<sup>3</sup> = cubic feet

g/cc = grams per cubic centimeter  
 ppm = parts per million

cu = neutron capture units  
 lbf = pounds force

#### 4.0 RESULTS

Preliminary results from the wireline geophysical logging measurements acquired by Schlumberger in R-48 were generated in the logging truck at the time the geophysical services were performed and were documented in the field logs provided on site. However, the measurements presented in the field results are not fully corrected for undesirable (from a measurement standpoint) borehole and geologic conditions and are provided as separate, individual logs. The field log results have been processed (1) to correct/improve the measurements, as best as possible, for borehole/formation environmental conditions, and (2) to depth-match the logs from different tool runs in the well. Additional logs were generated from integrated analysis of processed measured logs, providing valuable estimates of key geologic and hydrologic properties.

The processed log results are presented as continuous curves of the processed measurement versus depth and are displayed as (1) a one-page, compressed summary log display for selected directly related sets of measurements (see Figures 4.1, 4.2, and 4.3); (2) an integrated log montage that contains all the key processed log curves, on depth and side by side (see Attachment D-1); and (3) an expanded scale composite log of the processed and interpreted FMI electrical resistivity image log, also containing other useful log results for high resolution interpretation (see Attachment D-2). The summary log displays address specific characterization needs, such as moisture content, water saturation, and lithologic changes. The purpose of the integrated log montage is to present, side by side, all the most salient processed logs and log-derived models, depth-matched to each other, so that correlations and relationships between the logs can be identified. The electrical image composite log provides a very high resolution visual representation of the geologic section, including characterization of rock/sediment texture and fracturing.

Important results from the processed geophysical logs in R-48 are described below.

##### 4.1 Well Fluid Level

The well standing water level in R-48 was 1349 ft bgs at the time of logging, and did not vary much between the different logging runs.

##### 4.2 Regional Aquifer

The processed logs indicate that the intersected geologic section is fully saturated with water from the bottom of the log borehole (1702 ft bgs measured from the geophysical logs) to at least 1490 ft bgs, which is the top of a porous zone overlain by much lower porosity, competent lava. The logs results

indicate that there is a significant lithologic/textural boundary at 1495 ft, with porous breccia or possibly alluvium lying below (as seen on the FMI electrical image) and much more competent bedrock material (likely lava) above. Below 1490 ft, the log-estimated water content ranges from 15% to over 40% of total rock/sediment volume (see Figure 4.1, middle track). Directly above 1490 ft, the water content drops to 7% then to less than 5% above 1475 ft. Also, above 1475 ft the shallow resistivity measurement becomes significantly less than the deep resistivity (see Attachment D-1, integrated log montage, 2<sup>nd</sup> track from left), suggesting a large difference between the rock near the water-filled borehole (saturated with water from the borehole) and the rock distant from the borehole (dry conditions). It is possible the lava is saturated above 1475 ft up to 1349 ft (the depth of the borehole water level at the time of the logging), but the rock is so tight it is very difficult to assess water saturation from the geophysical logs, although the logs indicate the non-porous rock would not produce much water anyways. The non-radioactive source open-hole logging suite does not provide a measurement of air-filled or total porosity, so a quantitative assessment of water saturation is not possible. These results suggest that the depth of the regional aquifer water level (depth at which there is full water saturation) may be as high as 1349 ft, but the top of the aquifer effectively resides at 1475 to 1490 ft, the top of porous rock, in the immediate vicinity of R-48.

The hydraulic conductivity estimate and predicted relative flow capacity profile generated from the integrated log analysis results suggest that there are many productive zones in the porous breccia/undifferentiated alluvium below 1492 ft to the bottom of the log interval at 1700 ft (see Figure 4.1, right most track). From these estimates, the most productive zones are. 1540–1546 ft, 1564–1568 ft, 1574–1578 ft, 1585–1595 ft, 1625–1633 ft, 1645–1651 ft, 1656–1660 ft, 1674–1680 ft, and 1690–1693 ft (although much of the interval below 1500 ft appears to be water producing). The single most productive zone from the log analysis appears to be 1656–1660 ft, followed by 1625–1633 ft and 1585–1595 ft.

#### 4.3 Vadose Zone Perched Water

Above 1475 ft bgs, which the processed logs indicate to be the likely top of the Regional Aquifer, the measured water content remains below 5% of total rock volume through most of the log interval, except it increases to 15% at the very top (1200 to 1210 ft) where there is also a borehole washout that possibly contained some water.

#### 4.4 Geology

The processed geophysical log results clearly delineate that the saturated/water-filled section of the borehole, below 1495 ft bgs, consists of lava breccia and possibly some zones of undifferentiated alluvium. Above 1495 ft bgs the processed logs indicate competent, low porosity lava, fractured below 1490 ft where it transitions into breccia, that extends to the top of the log interval at 1200 ft. There is a distinct, albeit small, increase in the measured potassium concentration above 1495 ft (see Figure 4.1, green curve in right most track) that correlates with the textural change on the electrical resistivity image.

The generalized geologic stratigraphy observed from the logs across the measured interval is as follows (depth below ground surface):

- **1200–1350 ft bgs (top of processed log interval): Low porosity, highly competent lava flow (likely andesite or dacite in composition)** – characterized by very low water content (7-20%) that is likely associated with low total porosity (less than 5% except at very top); high

plagioclase feldspar; moderate potassium feldspar; and variably trace to minor amounts of magnetite, hornblende, and/or montmorillinite

- **1350–1455 ft bgs: Low porosity, highly competent lava flows (likely andesite or dacite in composition)** – characterized by very water content/porosity (mostly 5% or less); high plagioclase feldspar; moderate potassium feldspar; and variably trace to minor amounts of magnetite and/or montmorillinite
- **1455–1495 ft bgs: Low porosity, fractured lava flows (likely andesite or dacite in composition)** – characterized by very low content/porosity (mostly 5% or less) and fractures (increasing towards bottom); high plagioclase feldspar; moderate potassium feldspar; and variably trace to minor amounts of magnetite and/or montmorillinite
- **1495–1555 ft bgs: Moderate porosity, highly heterogeneous unconsolidated material (likely andesite/dacite lava flow breccia)** – characterized by moderate porosity (average about 20%); high plagioclase feldspar; moderate potassium feldspar; and variably trace to minor amounts of magnetite and/or montmorillinite
- **1555–1670 ft bgs: Highly variable moderate to high porosity, highly heterogeneous unconsolidated material (likely andesite/dacite lava flow breccia)** – characterized by highly variable moderate to high porosity (10-40%); high plagioclase feldspar; moderate potassium feldspar; and variably trace to minor amounts of magnetite
- **1670–1700 ft bgs (bottom of log interval): Moderately high porosity unconsolidated material (likely andesite/dacite lava flow breccia)** – characterized by moderate to high porosity (20-30%); high plagioclase feldspar; moderate potassium feldspar; and variably trace amounts of magnetite

The interpreted planar bedding features across the electrically imaged interval 1325 to 1700 ft bgs have fairly widely varying dip azimuths (direction beds are dipping towards) and dip angles (angle from horizontal), although there is consistency within different lithotypes. Within the competent lava beds above 1470 ft) the foliation is very consistent to the northeast. In the heterogeneous breccia section below 1195 ft the bedding features that can be delineated have quite variable dip azimuths, but appear to cluster in the northeast and northwest. The bed boundary at 896 ft between this breccia and the well-sorted channel sands below dips towards the south at an angle of 12 degrees and the cross-bedding in the channel sands is dipping primarily towards the east. Bedding feature dip angles (angle from horizontal) range mostly from 5 to 25 degrees in the lava beds and 8 to 75 degrees in the breccia. A number of fractures are discernable in the lava bed (all in the depth interval 1157–1194 ft, except one at 1107 ft), with widely varying dip azimuth directions, but predominantly orthogonal directions to the northeast, southeast, southwest and northwest, with dip angles ranging from 10 to 85 degrees. Computed fracture apertures show higher apertures and, thus, bulk fracture porosity at the bottom of the lava (1175–1194 ft) near the transition to breccia below.

#### 4.5 Summary Logs

Three summary log displays have been generated for R-48 to highlight the key hydrogeologic and geologic information provided by the processed geophysical log results:

- Porosity summary log showing continuous hydrogeologic property logs, including total and moveable water content and water saturation; highlights hydrologic information obtained from the integrated log results (Figure 4.1)
- Density and clay content summary showing a continuous logs of formation bulk density and estimated grain density, as well as photoelectric factor (sensitive to mineralogy) and estimated clay volume, highlights key geologic rock matrix information obtained from the log results (Figure 4.2)
- Spectral natural gamma ray and lithology summary showing a high vertical resolution, continuous volumetric analysis of formation mineral and pore fluid composition (based on an integrated analysis of the logs), and key lithologic/stratigraphic correlation logs from the spectral gamma ray measurement (concentrations of gamma-emitting elements); highlights the geologic lithology, stratigraphy, and correlation information obtained from the log results (Figure 4.3).

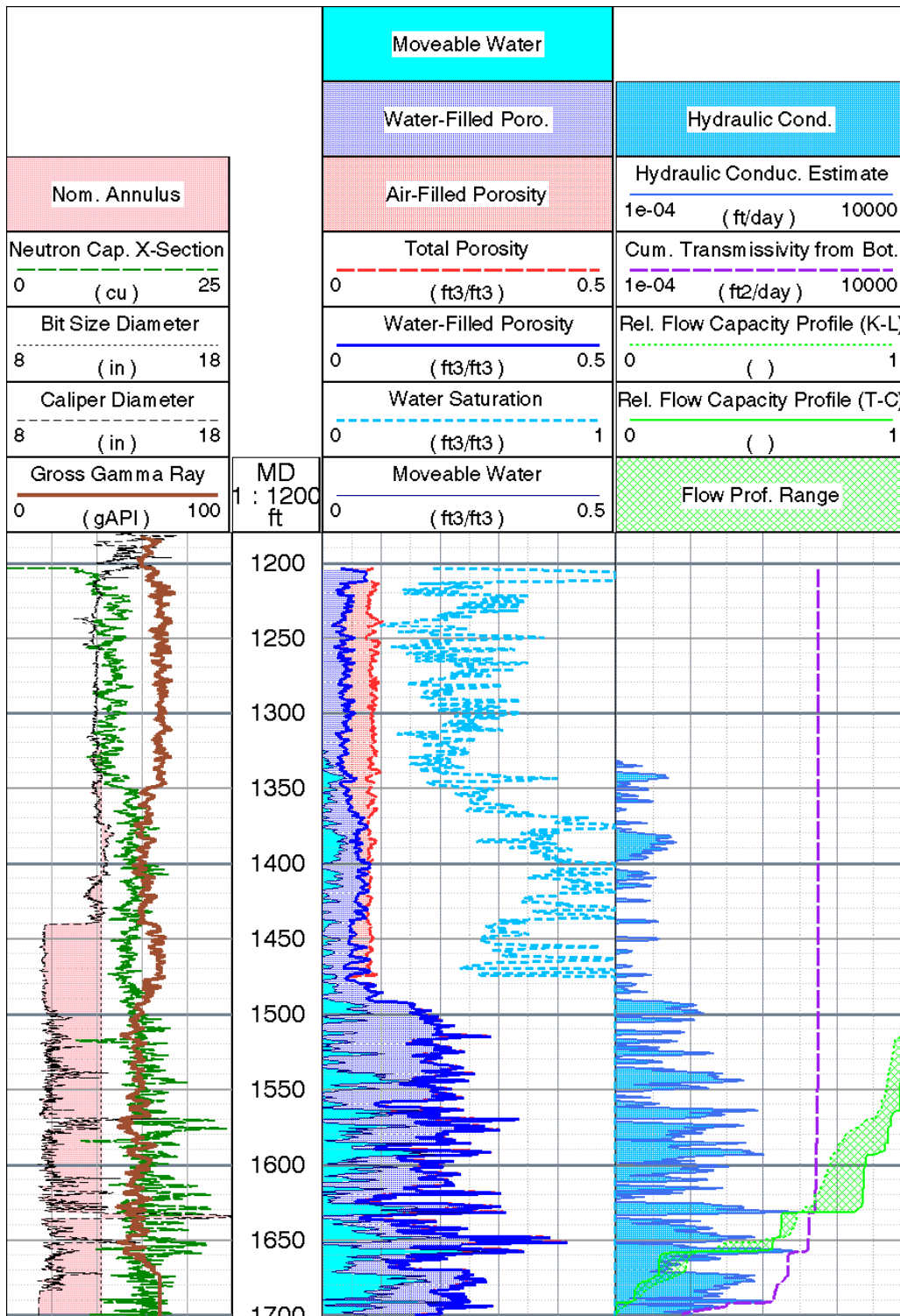


**Figure 4.1** Summary of porosity logs in R-48 borehole from processed geophysical logs, interval of 1200 to 1700 ft bgs, with caliper, gross gamma, neutron capture cross section, water saturation, estimated relative flow capacity profile, hydraulic conductivity, and transmissivity logs also displayed. Porosity, water saturation, and hydraulic conductivity logs are derived from the ELAN integrated log analysis.

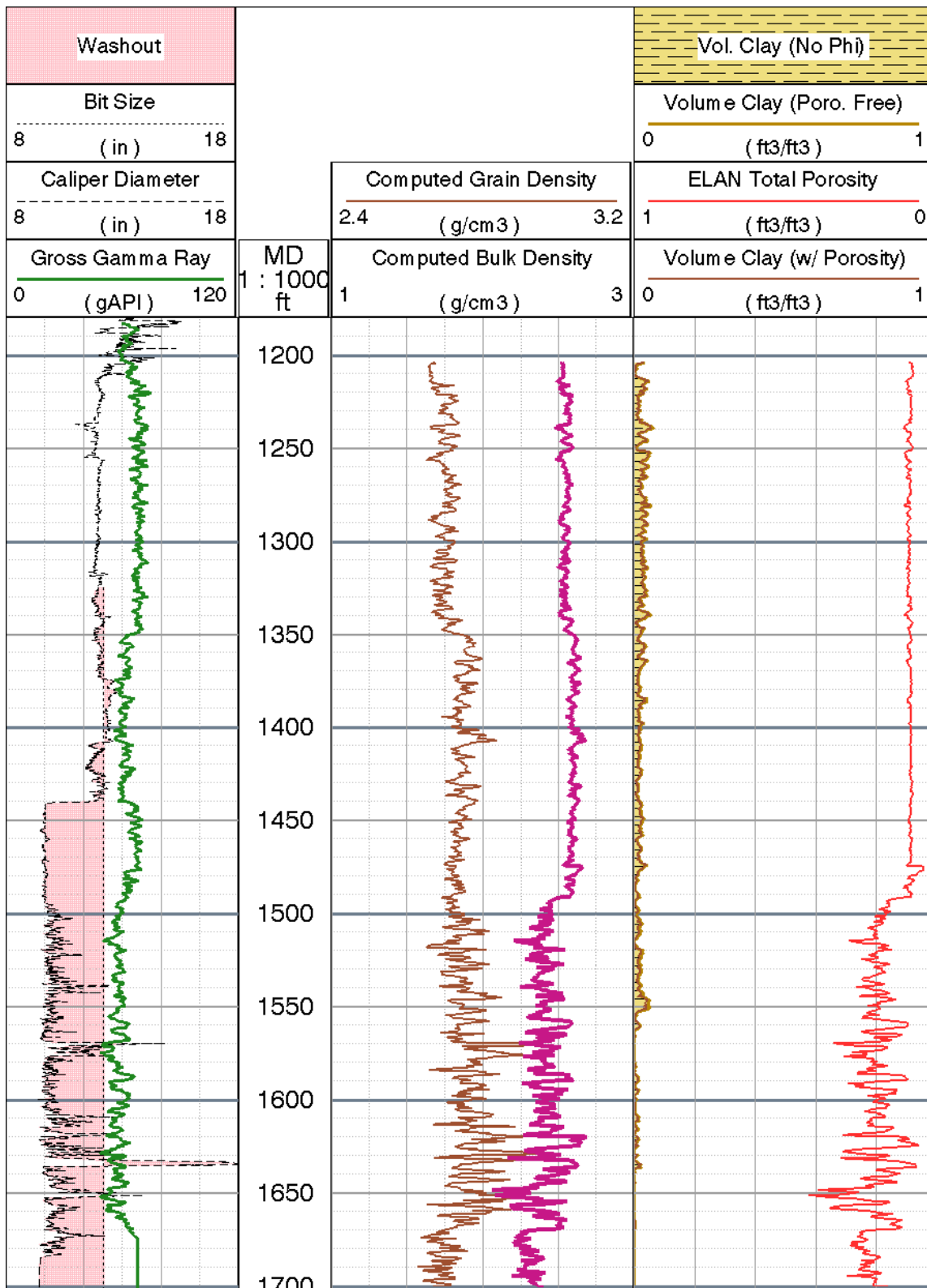


**Figure 4.2** Summary of computed bulk density and volume clay logs in R-48 borehole from processed geophysical logs, interval of 1200 to 1700 ft bgs. Also shown are caliper, gross gamma, computed grain density, and total porosity logs (the latter two derived from the ELAN analysis).



## 4.6 Integrated Log Montage

This section summarizes the integrated geophysical log montage for R-48. The montage is provided in Attachment D-1. A description of each log curve in the montage follows, organized under the heading of each track, starting from track 1 on the left-hand side of the montage. Note that the descriptions in this section focus on what the curves are and how they are displayed; the specific characteristics and interpretations of the R-48 geophysical logs are provided in the previous section

### 4.6.1 Track 1–Depth

The first track on the left contains the depth below ground surface in units of feet, as measured by the geophysical logging system during the FMI-HNGS logging run. All the geophysical logs are depth-matched to the gross gamma log acquired with this logging run.

### 4.6.2 Track 2–Basic Logs

The second track on the left (inclusive of the depth track) presents basic curves:

- gamma ray (thick black), recorded in American Petroleum Institute gamma ray standard units (gAPI) and displayed on a scale of 0 to 250 gAPI units;
- two orthogonal calipers from the FMI (thin dotted and dashed pink) and one from the TLD (thin solid pink) with bit size as a reference (dashed-dotted black) to show washout (pink shading), recorded as hole diameter in inches and displayed on a scale of 8 to 18 in.;
- borehole deviation displayed as a tadpole every ten feet (light blue dots and connected line segments) – the “head” marks the angular deviation from vertical at that particular depth, on a scale of 0 to 10 degrees, and the “tail” shows the azimuth of the deviation, true north represented by the tail facing straight towards the top of the page.
- neutron capture cross section from the APS (bold long-dashed red), recorded in standard capture units (cu) and displayed on a scale of 0 to 25 cu (left to right)

Two gamma ray curves from the NGS are:

- total gross gamma (thick solid black curve) and
- gross gamma minus the contribution of uranium (dashed black).

### 4.6.3 Track 3–Resistivity

The third track displays the resistivity measurements from the AIT, spanning most of the open hole section at the time of the logging. All the resistivity logs are recorded in units of ohmmeters (ohm-m) and are displayed on a logarithmic scale of 2 to 2000 ohm-m.

The six resistivity logs from the AIT that are displayed are

- Borehole fluid resistivity (solid orange curve)—only valid in water-filled hole
- Bulk electrical resistivity at five median depths of investigation—10 in. (black solid), 20 in. (long-dashed blue), 30 in. (short-dashed red), 60 in. (dashed-dotted green), and 90 in. (solid purple)—each having a 2-foot vertical resolution.

The area between the 20 in. and 90 in. resistivity curves, representing radial variations in bulk resistivity (potentially from invasion of drilling fluids), is shaded

- blue when the 20-in. resistivity is greater than the 90-in. resistivity (labeled “resistive invasive”) and
- yellow when the 90-in. resistivity is greater than the 20-in. resistivity (labeled “conductive invasive”).

A high vertical resolution (~8 in.), shallow-reading (~2 in.) micro-resistivity log from the MCFL is also displayed in this track (solid pink curve) – only valid in the fluid-filled, uncased section of the borehole. In addition, an optimized “true” formation resistivity log computed from all the measured resistivities is displayed (bold dotted sky blue).

#### 4.6.4 Track 4–Porosity

The fourth track displays the primary porosity log results. All the porosity logs are recorded in units of volumetric fraction and are displayed on a linear scale of 0.75 (left side) to -0.1 (right side). Specifically, these logs consist of

- APS epithermal neutron porosity derived from near-far detector pairing in water-filled hole and slowing down time measurement in air-filled hole (solid dark blue curve);
- CMR total water-filled porosity (short-dashed black);
- CMR effective water-filled porosity (long-dashed green with green area shading);
- CMR bound water porosity (cyan area shading) – representing by the area between the CMR total and effective water-filled porosities;
- Total porosity derived from bulk density and ELAN water-filled porosity using a grain density of 2.85 g/cc (dotted red curve), 2.75 g/cc (long-dashed red curve), and 2.65 g/cc (dashed red curve)–with red shading between the 2.85 g/cc and 2.65 g/cc porosity curves to show the range; and
- ELAN total water-filled porosity (bold dashed-dotted cyan)–derived from the ELAN integrated analysis of all log curves to estimate optimized matrix and pore volume constituents.

#### 4.6.5 Track 5–Density

The fifth track displays the

- computed bulk density (thick solid maroon curve), derived from the ELAN analysis, on a scale of 1 to 3 g/cc; and
- apparent grain density (dashed-dotted brown curve), derived from the ELAN analysis, on a scale of 2.4 to 3.2 g/cc.

#### 4.6.6 Track 6–HNGS Spectral Gamma

The sixth track from the left displays the spectral components of the HNGS measurement results as wet weight concentrations:

- potassium (solid green curve) in units of percent weight fraction and on a scale of -5% to 5%;

- thorium (dashed brown) in units of parts per million (ppm) and on a scale of 25 to -25 ppm; and
- uranium (dotted blue) in units of parts per million (ppm) and on a scale of 10 to 0 ppm.

#### 4.6.7 Track 7–CMR Porosity

Track 7 displays various CMR water-filled porosities along with measurement quality flags – valid only in the open-hole section. The porosity and measurement quality logs are presented on a scale of 0.5 to 0 volume fraction and discrete blocks originating from the left side, respectively. Specifically, the CMR logs shown in this track are

- High vertical resolution total water-filled porosity (solid black curve) – representing the total water volume fraction measured by the CMR;
- Three millisecond (ms) porosity (short-dashed brown) – representing the water volume fraction corresponding to the portion of the CMR measured T2 distribution that is above 3 ms, a cutoff that is considered to be representative of the break between clay-bound water (less than 3 ms) and all other types of water (greater than 3 ms);
- High vertical resolution effective water-filled, or free-fluid, porosity (solid pink) – representing the water volume fraction that is moveable (can flow), based on a 33 ms T2 distribution cutoff that is considered representative of the break between bound water (less than 33 ms) and moveable water (greater than 33 ms) in clastic rocks;
- Clay-bound water (brown area shading between total and 3 ms porosity logs) – representing the water volume fraction that is bound within clays;
- Capillary-bound water (pink area shading between 3 ms and effective porosity logs) – representing the water volume fraction that is bound within matrix pores by capillary forces;
- CMR magnetic field variation (dotted yellow) – representing the variation in the measured magnetic field versus the baseline magnetic field used for the logging (used as an indicator of the presence of magnetic minerals which requires a lower T2 cutoff)
- CMR wait-time flag (red area shading) – activates when there is significant measurement response at late T2 times, corresponding to large amounts of completely free (“bathtub”) water and often associated with washouts or very large pores;
- CMR measurement noise flag (yellow and orange area shading) – activates when there is potentially detrimental amounts of measurement noise detected by the tool, at moderate (yellow) and high (orange) levels.

#### 4.6.8 Track 8–Pore Size Distribution

Track 8 displays the water-filled pore size distribution as determined by the CMR – shown as binned water-filled porosities and valid only in the open-hole section. The binned porosity logs are presented on a scale of 0.5 to 0 volume fraction with colored area shading corresponding to the different bins:

- Clay-bound water–brown area shading
- Micro-pore and small-pore water (the sum comprising capillary-bound water)–gray and blue area shading, respectively

- Medium-pore, large-pore, and late-decay (the sum comprising effective water-filled porosity)– yellow, red, and green area shading, respectively

In addition, hydroxyl hydrogen is approximated as the difference between the CMR total porosity and environmentally corrected epithermal neutron porosity (shaded as diagonal purple stripes).

#### **4.6.9 Track 9–CMR T2 Distribution (Waveforms)**

The CMR T2 distribution is displayed in Track 9 as green waveform traces at discrete depths. The horizontal axis, corresponding to relaxation time in milliseconds, is on a logarithmic scale from 0.3 to 3000 ms. Also plotted are the:

- T2 logarithmic mean (solid blue curve) and
- T2 cutoff time used for differentiating between bound and free water (solid red line) – chosen as 33 ms

#### **4.6.10 Track 10–CMR T2 Distribution (Heated Amplitude)**

Track 10 displays the T2 distribution in another way – on a heated color scale where progressively “hotter” color (green to yellow to red) corresponds to increasing T2 amplitude. The remaining aspects of the display are the same as in Track 9, except that the high vertical resolution T2 logarithmic mean is shown as a solid white curve and the T2 cutoff is displayed as a solid black line.

#### **4.6.11 Track 11–CMR Hydraulic Conductivity**

Track 11 displays several estimates of hydraulic conductivity (K) derived from the ELAN integrated log analysis, presented on a logarithmic scale of  $10^{-5}$  to  $10^5$  feet per day (ft/day):

- K-versus-depth estimate derived from using the Timur-Coates permeability equation with total and moveable water content derived from the ELAN analysis, converted to hydraulic conductivity (solid sky blue curve with gradational coloring to represent the range of hydraulic conductivity relative to standard unconsolidated clastic sediments); and
- K-versus-depth estimate derived from using the SDR permeability equation applied to the processed CMR results, converted to hydraulic conductivity (long-dashed purple curve);
- K-versus-depth estimate derived from using the ELAN permeability equation with water-filled porosity and matrix mineral weight fraction values derived from the ELAN analysis, converted to hydraulic conductivity (dashed dark blue curve);
- Intrinsic K-versus-depth estimate (assuming full saturation) using the Timur-Coates permeability equation with total porosity and matrix mineral weight fraction values derived from the ELAN analysis, converted to hydraulic conductivity (dotted light blue).

In addition, an estimate of cumulative transmissivity from the bottom of the log interval is displayed in units of feet squared per day [ $\text{ft}^2/\text{day}$ ] (bold dashed-dotted green curve) – computed by integrating from bottom to top the ELAN Timur-Coates hydraulic conductivity estimate.

#### 4.6.12 Track 12– FMI Image (Dynamic Normalization)

Track 12 displays the FMI image, processed with dynamic normalization so that small-scale electrical resistivity features are amplified in the image. (With dynamic normalization, the range of electrical resistivity amplitudes – colors in the image – is normalized across a small moving depth window.) The image is fully oriented and corresponds to the inside of the borehole wall unwrapped, such that the left-hand side represents true north, half-way across the image is south, and the right-hand side is north again. The four color tracks in the image correspond to portions of the borehole wall contacted by the four FMI caliper pads; the blank space in between is the portion of the borehole wall not covered by the pads.

Also displayed are interpreted planar bedding features (thin green sinusoids), bed boundaries (bold dark green sinusoids), and electrically conductive fractures (bold blue).

#### 4.6.13 Track 13– FMI Bedding and Fractures

Track 13 displays the interpreted planar bedding features and bed boundaries picked from the FMI image, shown in two ways:

- Individually, as tadpoles at the depths the bedding plane or fracture plane crosses the midpoint of the borehole – where the “heads” (circles/triangles) represent the dip angle, and the “tails” (line segments) represent the true dip azimuth (direction the bed is dipping towards). Bedding features are shown as circular headed light green tadpoles, bed boundaries as circular headed dark green tadpoles, and conductive fractures as blue tadpoles.
- Summed, as dip azimuth fan plot histograms (green colored fan plots for bed boundaries) – where the number of bedding features having a dip direction within a particular sector are summed and normalized, thus highlighting the predominant dip directions.

#### 4.6.14 Track 14– FMI Image (Static Normalization)

Track 14 displays the FMI image again, but in a different way – processed with static normalization to highlight larger scale features and trends. (With static normalization, the range of electrical resistivity amplitudes – colors in the image – is normalized across the entire length of the log interval.) Also shown is the high-resolution scaled resistivity from one of the FMI pads.

#### 4.6.15 Track 15– Fracture Properties and High Resolution Porosity

Track 15 displays the estimated discrete hydraulic aperture of any interpreted electrically conductive fractures (blue circles on logarithmic scale of 0.001 to 10 inch) – computed using an FMI image scaled to the AIT shallow resistivity. Also displayed are the following fracture attributes:

- Fracture trace length (dashed purple curve) – representing the summed trace length of all interpreted fractures per unit surface area of borehole wall, in units of  $\text{ft}/\text{ft}^2$  (or  $1/\text{ft}$ ) and on a scale of 0 to  $4 \text{ ft}^{-1}$ ;
- Fracture density (solid green curve) – representing the number of fractures per unit surface area of borehole wall, in units of  $\text{ft}/\text{ft}^2$  (or  $1/\text{ft}$ ) and on a scale of 0 to  $4 \text{ 1}/\text{ft}$ ;

- Fracture porosity (bold solid blue curve) – representing the estimated fraction of the bulk rock volume occupied by open fracture apertures, in units of  $\text{ft}^3/\text{ft}^3$  and on a scale of 0.04 to 0  $\text{ft}^3/\text{ft}^3$  (left to right);
- Cumulative number of fractures from the deepest to the shallowest interpreted fractures (dotted black curve), in dimensionless units on a scale of 0 to 20 number of fractures.

#### **4.6.16 Track 16 – ELAN Mineralogy Model Results (Dry Weight Fraction)**

Track 16 displays the results from the ELAN integrated log analysis (the matrix portion)—presented as dry-weight fraction of mineral types chosen in the model:

- Montmorillonite clay (brown/tan)
- Hematite (orange with small black dots)
- Orthoclase or other potassium feldspar (lavender)
- Labradorite or similar plagioclase feldspar (pink)
- Hornblende or similar amphibole (green)
- Augite or similar pyroxene (maroon)
- Magnetite or similar heavy mafic mineral (dark green)

#### **4.6.17 Track 17 –ELAN Mineralogy and Pore Space Model Results (Wet Volume Fraction)**

Track 17 displays the results from the ELAN integrated log analysis—presented as wet mineral and pore fluid volume fractions:

- Montmorillonite clay (brown/tan)
- Hematite (orange with small black dots)
- Orthoclase or other potassium feldspar (lavender)
- Labradorite or similar plagioclase feldspar (pink)
- Hornblende or similar amphibole (green)
- Augite or similar pyroxene (maroon)
- Magnetite or similar heavy mafic mineral (dark green)
  
- Air (red)
- Moveable water (white)
- Capillary-bound (irreducible) water (light blue)
- Moved air (orange)
- Moved water (blue)

#### 4.6.18 Track 18–Water Saturation

Track 18 displays the continuous-in-depth water saturation logs estimated from the processed logs, recorded in units of volumetric fraction of pore space filled with water (ratio of cubic feet per cubic feet [ $\text{ft}^3/\text{ft}^3$ ]) and presented on a scale of 0 to 1  $\text{ft}^3/\text{ft}^3$  (left to right).

- Optimized estimate of water saturation (volumetric fraction of pore space filled with water) from the ELAN analysis (bold dashed-dotted purple curve with blue shading to the right and red shading to the left, corresponding to water-filled and air-filled pore space, respectively);
- Water saturation as calculated directly from the bulk density and ELAN-estimated porosity using a grain density of 2.65 g/cc (dashed cyan curve), 2.75 g/cc (solid cyan curve), and 2.85 g/cc (dotted cyan curve) – with stippled cyan shading between the 2.65 g/cc and 2.85 g/cc water saturation curves to show the range.

#### 4.6.19 Track 19–Predicted Flow (Production Potential) Profile

Track 19 displays the integrated predicted relative flow (production potential) profile from the permeability (hydraulic conductivity) logs that mimics a flow meter (spinner) acquired under flowing conditions:

- Predicted relative water flow profile derived from the ELAN Timur-Coates water permeability log (bold solid blue curve), displayed on a unitless linear scale of 0 to 1 relative volumetric flow rate (ratio of flow rate to flow rate);
- Predicted relative water flow profile derived from the CMR SDR water permeability log (thin solid blue curve), displayed on a unitless linear scale of 0 to 1 relative volumetric flow rate;
- Predicted hypothetical well water flow versus depth profile for the entire log interval (dotted green), assuming a well radius of 4 in., entirely open to flow, and pumping is occurring under steady state conditions with a drawdown of 25 ft (incremental flow computed using the Thiem steady state flow equation) – derived from the ELAN Timur-Coates water permeability log (bold solid blue), displayed on a linear scale of 0 to 10,000 gallons per day (gal/day).

#### 4.6.20 Track 20–Summary Logs

Track 20, the second track from the right, displays several summary logs that describe the fluid and air-filled volume measured by the geophysical tools:

- Optimized estimate of total volume fraction water from the ELAN analysis (solid blue curve and blue plus cyan area shading);
- Optimized estimate of volume fraction moveable water (effective water-filled porosity) from the ELAN analysis (dashed cyan curve and green area shading); and
- Optimized estimate of total volume fraction of air-filled porosity from the ELAN analysis (long dashed red curve and dotted red area shading).

The porosity and volumetric water content scales are from 0 to 0.5 total volume fraction, left to right.

#### 4.6.21 Track 21–Depth

The final track on the right, the same as the first track on the left, displays the depth below ground surface in units of feet, as measured by the geophysical logging system during the APS-GR logging run.

## 5.0 REFERENCES

Mayer, C. and A. Sibbit, 1980. "GLOBAL, A New Approach to Computer-Processed Log Interpretation." Paper SPE 9341 presented at the 1980 SPE Annual Technical Conference and Exhibition.

Quirein, J., S. Kimminau, J. LaVigne, J. Singer, and F. Wendel. 1986. "A Coherent Framework for Developing and Applying Multiple Formation Evaluation Models." Paper DD in 27th Annual Logging Symposium Transactions: Society of Professional Well Log Analysts.

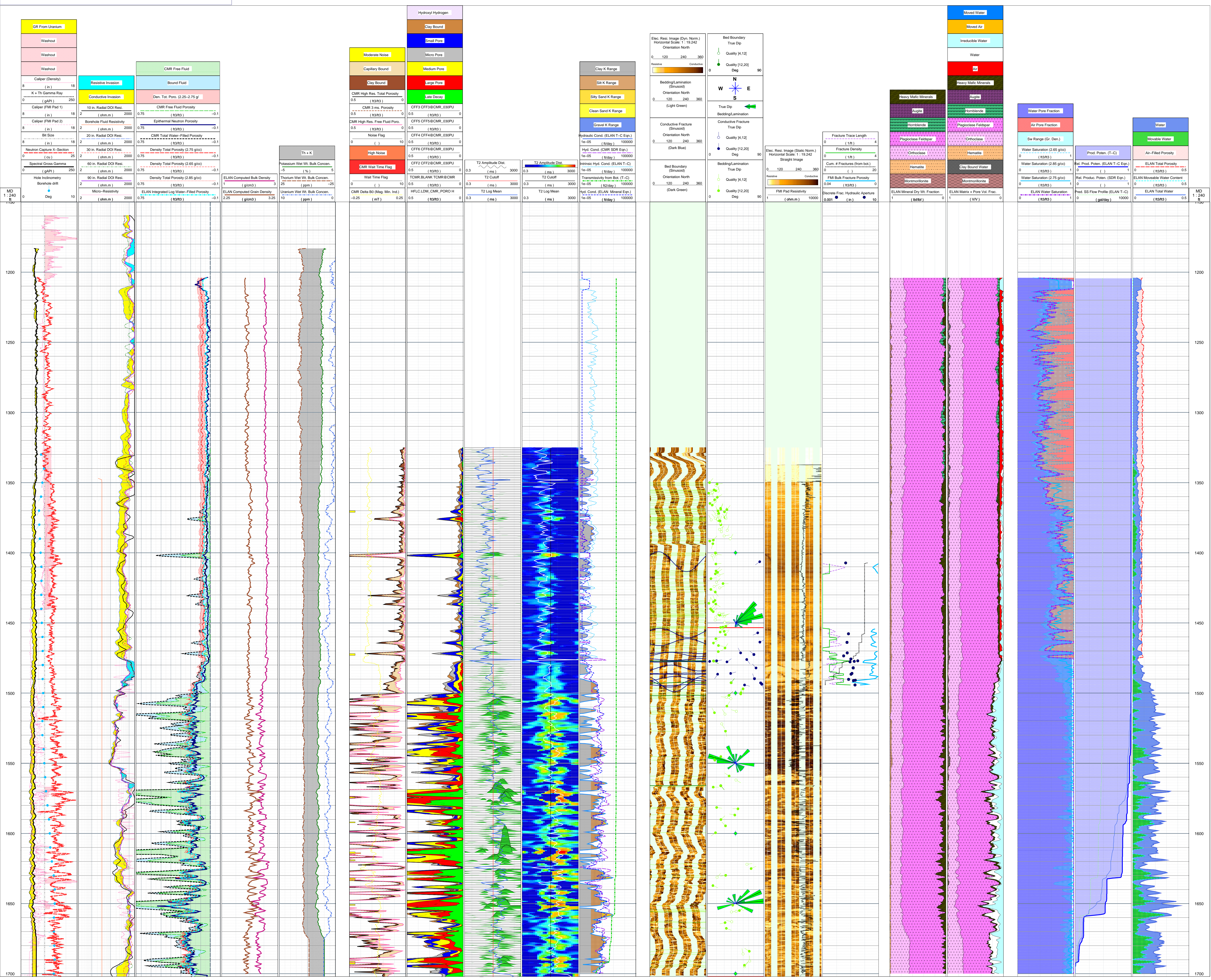
FOLD HERE The well name, location and borehole reference data were furnished by the customer.

All interpretations are opinions based on information from electrical and other measurements and are carried, and do not guarantee the accuracy or correctness of any interpretation, and we will not, except in the case of gross or willful negligence on our part, be liable or responsible for any loss, costs, damages or expenses incurred or sustained by anyone resulting from any interpretation made by any of our clients, agents or employees. These interpretations are also subject to Clause 4 of our General Terms and Conditions as set out in our Price Schedule.

**OP Vars:** 1700-154 Process Date: Nov-2009 Center: SWS Tucson Baseline: GP4.2 Log Analyst: N. Clayton

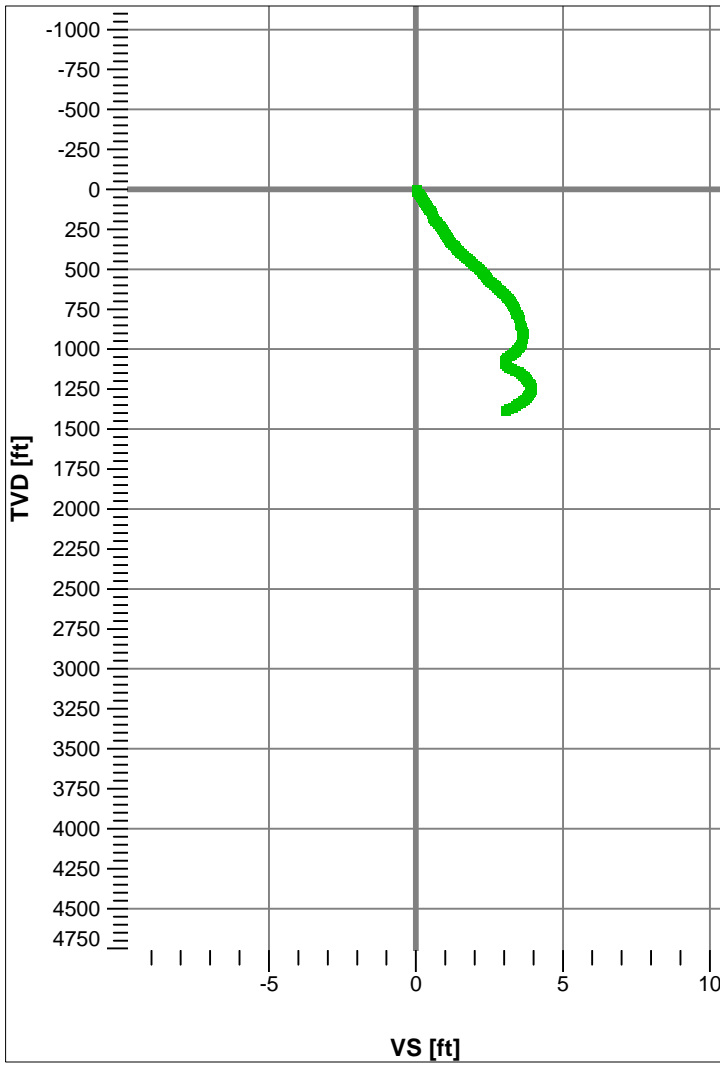
**Mud and Borehole Measurements:**  
 Rm @ Measured Temperature: 36 ohm.m @ 70 ft BHT: 70 degF Bitsize: 9.75 in  
 Rmf @ Measured Temperature: NA Type Fluid in Hole: Water FGM:  
 Rmc @ Measured Temperature: NA Mud density: 8.34 lbm/gal FGM:

**Remarks:**  
 Depth reference is ground surface. Well was uncased across log interval.  
 Well water level was 1349 ft at time of logging.  
 ELAN\* performed without total porosity measurement (unavailable in open hole).  
 Total poro. set to constant value in ELAN\* anal. above 1475 ft to account for lack of bulk den. meas.  
 Interpretation should account for borehole conditions (particularly washouts).

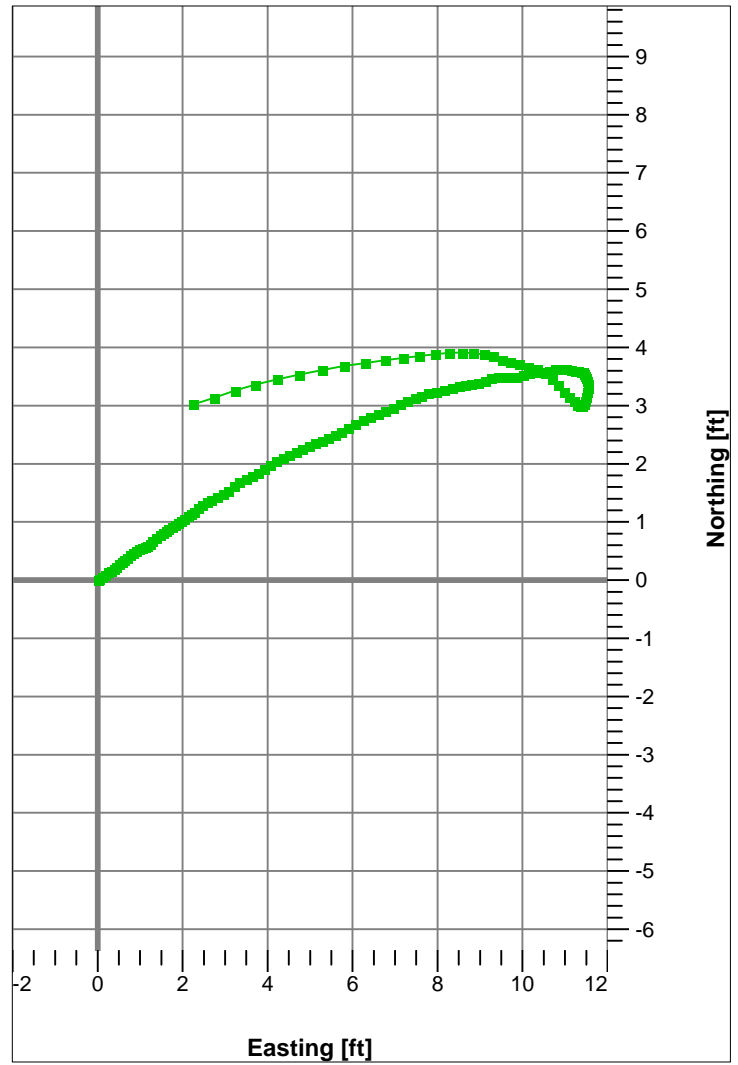


Name : Computed from R#48-2.BIN's HighSpeed: InRun  
 Generated : 2009/06/03 18:31:37 Mountain Daylight Time

VS View



Plan View





# Scientific Drilling

Gyroscopic Survey Report  
for  
Layne Christensen  
11001 Etiwanda Ave.  
Fontana CA, 92337

<b>Well Location</b>	R #48
<b>Well Name</b>	R #48
<b>Rig Name</b>	T-25
<b>Survey Date</b>	2009/06/03
<b>Latitude</b>	35.84 deg
<b>North Reference</b>	True North
<b>Grid Correction</b>	0.00 deg
<b>Depth Reference</b>	5.3 RKB
<b>Calculation Method</b>	Minimum Curvature
<b>Section (VS) Ref</b>	0.00N (ft), 0.00E (ft), 0.00Azim (deg)
<b>Definitive Survey</b>	Computed from R#48-2.BIN's HighSpeed: InRun
<b>Operator</b>	Layne Christensen

## Comments

Survey from RKB to 1380', in 4.5" Drill Pipe



Well Name: R #48  
 Survey: Computed from R#48-2.BIN's HighSpeed: InRun  
 Survey Date: 2009/06/03

MD ft	Inc deg	Azim deg	TVD ft	VS ft	Northing ft	Easting ft	DLS deg/100ft	Closure Distance ft	Closure Angle deg
0.00	0.00	0.00	0.00	0.00	0.00	0.00	Invalid	0.00	0.00
10.00	0.46	59.40	10.00	0.02	0.02	0.03	4.60	0.04	59.40
20.00	0.44	62.18	20.00	0.06	0.06	0.10	0.27	0.12	60.31
30.00	0.47	61.45	30.00	0.10	0.10	0.17	0.30	0.20	60.91
40.00	0.43	64.31	40.00	0.13	0.13	0.24	0.48	0.28	61.45
50.00	0.44	70.01	50.00	0.16	0.16	0.31	0.43	0.35	62.68
60.00	0.38	63.60	60.00	0.19	0.19	0.38	0.74	0.42	63.40
70.00	0.42	57.76	70.00	0.22	0.22	0.44	0.59	0.49	63.00
80.00	0.49	55.44	80.00	0.27	0.27	0.51	0.67	0.57	62.10
90.00	0.38	51.28	90.00	0.31	0.31	0.57	1.10	0.65	61.12
100.00	0.41	61.67	100.00	0.35	0.35	0.62	0.77	0.72	60.69
110.00	0.45	61.39	110.00	0.39	0.39	0.69	0.41	0.79	60.77
120.00	0.43	62.71	120.00	0.42	0.42	0.76	0.21	0.87	60.88
130.00	0.51	56.90	130.00	0.46	0.46	0.83	0.91	0.95	60.77
140.00	0.44	70.24	140.00	0.50	0.50	0.90	1.28	1.03	60.96
150.00	0.41	67.98	150.00	0.53	0.53	0.97	0.40	1.11	61.50
160.00	0.40	73.98	160.00	0.55	0.55	1.04	0.43	1.18	62.07
170.00	0.40	82.33	170.00	0.57	0.57	1.11	0.58	1.24	62.95
180.00	0.40	52.88	180.00	0.59	0.59	1.17	2.02	1.31	63.19
190.00	0.37	54.91	189.99	0.63	0.63	1.22	0.35	1.38	62.74
200.00	0.59	58.10	199.99	0.68	0.68	1.29	2.28	1.46	62.40
210.00	0.59	61.65	209.99	0.73	0.73	1.38	0.37	1.56	62.23
220.00	0.46	61.00	219.99	0.77	0.77	1.46	1.35	1.65	62.19
230.00	0.45	59.57	229.99	0.81	0.81	1.53	0.16	1.73	62.10
240.00	0.41	63.69	239.99	0.85	0.85	1.60	0.46	1.81	62.08
250.00	0.53	64.07	249.99	0.88	0.88	1.67	1.20	1.89	62.16
260.00	0.47	65.28	259.99	0.92	0.92	1.75	0.63	1.98	62.27
270.00	0.43	64.67	269.99	0.95	0.95	1.82	0.35	2.06	62.37
280.00	0.46	63.95	279.99	0.99	0.99	1.89	0.22	2.13	62.44
290.00	0.45	65.05	289.99	1.02	1.02	1.96	0.11	2.21	62.51
300.00	0.54	62.77	299.99	1.06	1.06	2.04	0.91	2.30	62.56
310.00	0.49	67.69	309.99	1.10	1.10	2.12	0.66	2.39	62.66
320.00	0.49	62.00	319.99	1.13	1.13	2.20	0.48	2.47	62.73
330.00	0.47	51.77	329.99	1.18	1.18	2.27	0.87	2.55	62.55
340.00	0.66	61.69	339.99	1.23	1.23	2.35	2.15	2.65	62.36
350.00	0.74	61.79	349.99	1.29	1.29	2.46	0.73	2.77	62.33
360.00	0.65	68.34	359.99	1.34	1.34	2.57	1.15	2.90	62.44
370.00	0.74	69.81	369.99	1.38	1.38	2.68	0.93	3.02	62.71
380.00	0.81	68.65	379.99	1.43	1.43	2.81	0.72	3.15	62.99



# Survey Report

Well Name: R #48  
 Survey: Computed from R#48-2.BIN's HighSpeed: InRun  
 Survey Date: 2009/06/03

MD ft	Inc deg	Azim deg	TVD ft	VS ft	Northing ft	Easting ft	DLS deg/100ft	Closure Distance ft	Closure Angle deg
390.00	0.81	72.82	389.99	1.48	1.48	2.94	0.59	3.29	63.32
400.00	0.88	60.03	399.98	1.54	1.54	3.07	2.03	3.44	63.44
410.00	0.84	60.22	409.98	1.61	1.61	3.20	0.45	3.59	63.30
420.00	0.88	65.18	419.98	1.68	1.68	3.34	0.84	3.74	63.28
430.00	0.90	70.86	429.98	1.74	1.74	3.48	0.90	3.89	63.47
440.00	0.88	68.41	439.98	1.79	1.79	3.63	0.40	4.05	63.70
450.00	0.89	66.65	449.98	1.85	1.85	3.77	0.29	4.20	63.85
460.00	0.89	64.02	459.98	1.92	1.92	3.91	0.41	4.36	63.90
470.00	0.85	62.46	469.98	1.98	1.98	4.05	0.49	4.51	63.88
480.00	0.94	72.79	479.97	2.04	2.04	4.19	1.87	4.66	64.01
490.00	1.02	73.30	489.97	2.09	2.09	4.36	0.79	4.83	64.33
500.00	0.93	69.09	499.97	2.15	2.15	4.52	1.20	5.00	64.57
510.00	0.89	69.37	509.97	2.20	2.20	4.67	0.35	5.16	64.71
520.00	0.87	70.61	519.97	2.26	2.26	4.81	0.29	5.31	64.86
530.00	0.97	73.09	529.97	2.31	2.31	4.96	1.09	5.47	65.07
540.00	0.91	75.87	539.97	2.35	2.35	5.12	0.78	5.63	65.34
550.00	0.88	75.73	549.97	2.39	2.39	5.27	0.26	5.79	65.62
560.00	0.89	68.36	559.96	2.44	2.44	5.42	1.15	5.94	65.79
570.00	0.96	75.68	569.96	2.49	2.49	5.57	1.36	6.10	65.96
580.00	1.04	64.49	579.96	2.55	2.55	5.74	2.10	6.28	66.06
590.00	1.02	67.48	589.96	2.62	2.62	5.90	0.57	6.46	66.06
600.00	1.02	70.16	599.96	2.68	2.68	6.07	0.48	6.63	66.14
610.00	1.12	71.62	609.96	2.74	2.74	6.24	1.00	6.82	66.27
620.00	1.00	74.14	619.95	2.80	2.80	6.42	1.27	7.00	66.44
630.00	1.04	73.05	629.95	2.85	2.85	6.59	0.47	7.18	66.62
640.00	1.04	72.78	639.95	2.90	2.90	6.76	0.06	7.36	66.77
650.00	1.12	71.76	649.95	2.96	2.96	6.94	0.85	7.55	66.91
660.00	1.03	71.15	659.95	3.02	3.02	7.12	0.91	7.74	67.02
670.00	1.01	71.49	669.95	3.08	3.08	7.29	0.27	7.91	67.12
680.00	0.98	74.04	679.94	3.13	3.13	7.46	0.52	8.09	67.24
690.00	0.90	75.72	689.94	3.17	3.17	7.61	0.79	8.25	67.39
700.00	1.04	78.78	699.94	3.21	3.21	7.78	1.45	8.41	67.59
710.00	1.10	81.34	709.94	3.24	3.24	7.96	0.78	8.60	67.86
720.00	1.06	79.77	719.94	3.27	3.27	8.15	0.53	8.78	68.13
730.00	1.04	79.32	729.94	3.30	3.30	8.33	0.16	8.96	68.36
740.00	0.91	80.86	739.94	3.33	3.33	8.50	1.38	9.13	68.57
750.00	0.81	86.03	749.93	3.35	3.35	8.65	1.23	9.27	68.81
760.00	0.89	84.15	759.93	3.36	3.36	8.79	0.79	9.41	69.06



# Survey Report

Well Name: R #48  
 Survey: Computed from R#48-2.BIN's HighSpeed: InRun  
 Survey Date: 2009/06/03

MD ft	Inc deg	Azim deg	TVD ft	VS ft	Northing ft	Easting ft	DLS deg/100ft	Closure Distance ft	Closure Angle deg
770.00	0.89	79.10	769.93	3.39	3.39	8.95	0.78	9.57	69.26
780.00	0.99	73.30	779.93	3.43	3.43	9.10	1.42	9.73	69.38
790.00	0.92	80.76	789.93	3.46	3.46	9.27	1.44	9.89	69.50
800.00	0.80	85.43	799.93	3.48	3.48	9.42	1.40	10.04	69.70
810.00	0.84	89.27	809.93	3.49	3.49	9.56	0.72	10.18	69.95
820.00	0.84	87.61	819.93	3.49	3.49	9.71	0.25	10.31	70.21
830.00	0.85	87.14	829.93	3.50	3.50	9.85	0.11	10.45	70.44
840.00	0.91	76.91	839.92	3.52	3.52	10.00	1.70	10.60	70.61
850.00	0.88	80.43	849.92	3.55	3.55	10.16	0.65	10.76	70.72
860.00	0.84	87.71	859.92	3.57	3.57	10.30	1.16	10.90	70.90
870.00	0.91	89.27	869.92	3.57	3.57	10.46	0.81	11.05	71.14
880.00	0.88	75.66	879.92	3.59	3.59	10.61	2.15	11.20	71.30
890.00	0.87	79.57	889.92	3.62	3.62	10.76	0.61	11.35	71.38
900.00	0.76	94.35	899.92	3.63	3.63	10.90	2.36	11.49	71.57
910.00	0.69	90.87	909.92	3.63	3.63	11.03	0.80	11.61	71.79
920.00	0.61	100.93	919.92	3.62	3.62	11.14	1.42	11.71	72.02
930.00	0.46	98.96	929.92	3.60	3.60	11.23	1.49	11.79	72.23
940.00	0.39	100.15	939.91	3.59	3.59	11.30	0.71	11.86	72.39
950.00	0.38	91.83	949.91	3.58	3.58	11.37	0.57	11.92	72.52
960.00	0.17	120.86	959.91	3.57	3.57	11.42	2.46	11.96	72.63
970.00	0.29	149.49	969.91	3.54	3.54	11.44	1.66	11.98	72.80
980.00	0.26	121.49	979.91	3.51	3.51	11.47	1.37	12.00	73.00
990.00	0.32	169.65	989.91	3.47	3.47	11.50	2.42	12.01	73.21
1000.00	0.29	151.48	999.91	3.42	3.42	11.52	1.00	12.01	73.46
1010.00	0.37	161.46	1009.91	3.37	3.37	11.54	0.93	12.02	73.73
1020.00	0.41	195.91	1019.91	3.30	3.30	11.54	2.35	12.00	74.03
1030.00	0.48	204.98	1029.91	3.23	3.23	11.51	0.97	11.96	74.33
1040.00	0.46	182.80	1039.91	3.15	3.15	11.49	1.82	11.92	74.66
1050.00	0.41	189.98	1049.91	3.08	3.08	11.48	0.76	11.89	75.00
1060.00	0.38	230.02	1059.91	3.02	3.02	11.45	2.70	11.84	75.22
1070.00	0.28	249.44	1069.91	2.99	2.99	11.40	1.46	11.79	75.30
1080.00	0.31	284.13	1079.91	2.99	2.99	11.35	1.79	11.74	75.25
1090.00	0.47	300.64	1089.91	3.02	3.02	11.29	1.90	11.69	75.05
1100.00	0.71	303.01	1099.91	3.07	3.07	11.21	2.43	11.62	74.68
1110.00	0.78	302.67	1109.91	3.14	3.14	11.10	0.75	11.53	74.19
1120.00	0.98	313.21	1119.91	3.24	3.24	10.98	2.50	11.44	73.57
1130.00	1.05	308.20	1129.91	3.35	3.35	10.84	1.18	11.35	72.82
1140.00	1.06	304.65	1139.91	3.46	3.46	10.69	0.65	11.24	72.07



# Survey Report

Well Name: R #48  
 Survey: Computed from R#48-2.BIN's HighSpeed: InRun  
 Survey Date: 2009/06/03

MD ft	Inc deg	Azim deg	TVD ft	VS ft	Northing ft	Easting ft	DLS deg/100ft	Closure Distance ft	Closure Angle deg
1150.00	1.10	298.19	1149.90	3.56	3.56	10.53	1.31	11.12	71.33
1160.00	1.23	282.19	1159.90	3.63	3.63	10.34	3.48	10.96	70.68
1170.00	1.26	280.37	1169.90	3.67	3.67	10.13	0.48	10.78	70.09
1180.00	1.22	279.01	1179.90	3.71	3.71	9.92	0.51	10.59	69.51
1190.00	1.17	280.33	1189.90	3.74	3.74	9.71	0.56	10.41	68.94
1200.00	1.22	285.52	1199.89	3.79	3.79	9.51	1.21	10.24	68.28
1210.00	1.20	284.89	1209.89	3.84	3.84	9.31	0.22	10.07	67.56
1220.00	1.37	274.48	1219.89	3.88	3.88	9.09	2.84	9.88	66.88
1230.00	1.50	273.92	1229.89	3.90	3.90	8.84	1.34	9.66	66.20
1240.00	1.62	271.44	1239.88	3.91	3.91	8.56	1.41	9.41	65.46
1250.00	1.71	266.89	1249.88	3.91	3.91	8.27	1.56	9.15	64.73
1260.00	2.04	264.77	1259.87	3.88	3.88	7.95	3.38	8.84	63.97
1270.00	2.26	265.36	1269.87	3.85	3.85	7.57	2.25	8.50	63.06
1280.00	2.28	265.21	1279.86	3.82	3.82	7.18	0.16	8.13	62.00
1290.00	2.57	264.09	1289.85	3.78	3.78	6.76	2.95	7.74	60.80
1300.00	2.79	264.82	1299.84	3.73	3.73	6.29	2.21	7.32	59.33
1310.00	2.94	263.27	1309.82	3.68	3.68	5.80	1.72	6.87	57.59
1320.00	3.12	261.56	1319.81	3.61	3.61	5.27	2.02	6.39	55.60
1330.00	3.06	261.81	1329.80	3.53	3.53	4.74	0.59	5.91	53.30
1340.00	2.99	259.85	1339.78	3.45	3.45	4.22	1.26	5.45	50.73
1350.00	2.84	260.76	1349.77	3.36	3.36	3.72	1.55	5.01	47.86
1360.00	2.90	255.55	1359.76	3.26	3.26	3.23	2.67	4.59	44.71
1370.00	2.97	255.82	1369.74	3.13	3.13	2.73	0.71	4.16	41.07
1380.00	2.65	257.52	1379.73	3.02	3.02	2.25	3.33	3.77	36.73